ABSTRACT

Title of dissertation: PHENOMENOLOGY OF
WARPED EXTRA DIMENSIONS
Lijun Zhu, Doctor of Philosophy, 2010

Dissertation directed by: Professor Kaustubh Agashe
Department of Physics

Warped extra dimensions provide a very interesting and attractive framework that solves the hierarchy problem of the Standard Model (SM) of particle physics through the curvature along an extra dimension. In this thesis I will discuss various aspects of collider phenomenology of warped extra dimensions. First, I will discuss a class of models within this framework that are very attractive due to their naturalness, which are called warped/composite Pseudo-Goldstone Boson (PGB) Higgs models. A generic prediction of these models is the existence of extra gauge bosons (called coset gauge bosons), which give rise to distinctive signatures at the Large Hadron Collider (LHC). However, due to the large masses (beyond 3 Teraelectronvolt (TeV)) of the coset gauge bosons and their small couplings to standard model states, their discovery would be very challenging at the LHC, and an upgrade of the LHC is needed.

My second topic is about the phenomenology of the Higgs boson in warped extra dimensions. In models where fermions propagate in the extra dimension, there exist heavy excitations of SM fermions, which are called the Kaluza-Klein (KK)

fermions. These KK states give sizable new contributions to the production and decay channels of the Higgs boson. I will give a detailed analysis of the Higgs boson couplings to massless vector bosons (gluons and photons) in warped extra dimensions. I will show that KK fermions of all generations contribute to these couplings, leading to significant deviation from the prediction of the SM. Therefore, precision measurement of the properties of the Higgs boson can shed light on the structure of warped extra dimensions even if KK particles cannot be directly produced at the LHC due to their heavy masses.

PHENOMENOLOGY OF WARPED EXTRA DIMENSIONS

by

Lijun Zhu

Dissertation submitted to the Faculty of the Graduate School of the
University of Maryland, College Park in partial fulfillment
of the requirements for the degree of
Doctor of Philosophy
2010

Advisory Committee:
Professor Kaustubh Agashe, Chair/Advisor
Professor Zackaria Chacko
Professor Nicholas Hadley
Professor Paulo Bedaque
Professor Jaydev P. Desai

© Copyright by
Lijun Zhu
2010

Acknowledgments

The five years of graduate school in Maryland has become the most memorable period of time in my life. I want to thank all people who have brought fun and joy into this cherishable memory.

First and foremost, I would like to thank my advisor Prof. Kaustubh Agashe, whose immense knowledge and passion for physics has guided me through many abstract physics theories. His encouragement and great patience has helped me go through numerous critical points of my research. I will always remember that during countless afternoons, he tried tirelessly to explain some subtle ideas to me over and over again. It is my honor and great pleasure to have worked with such an extraordinary physicist.

I owe my thanks to Prof. Zackaria Chacko, Prof. Nicholas Hadley, Prof. Paulo Bedaque and Prof. Jaydev Desai for reading my thesis and providing helpful comments. I want to thank Prof. Rabindra Mohapatra for his great class on quantum field theory, which intrigued me to study elementary particle physics. I also want to thank Prof. Zackaria Chacko, Prof. Oscar Greenberg, Prof. Bei-Lok Hu and Prof. S. James Gates for enlightening classes that gave me a glimpse of the beauty of physics. I would like to thank Prof. Markus Luty for his guidance during the early phase of my graduate research. I want to thank faculty members of Maryland Center for Fundamental Physics: Prof. Ted Jacobson, Prof. Kevork Abazajian and Prof. Raman Sundrum, and postdoc fellows: Andrey Katz, Steve Blanchet, Takemichi Okui and Shaolong Chen for providing a stimulating and dynamic environment for

me to discuss and learn physics.

I am grateful to my collaborators: Aleksandr Azatov, Manuel Toharia and Yingchuan Li. It was great fun to work with them. And the result of our collaboration provides much of the basis for this thesis. I have learned a lot from my friends Ryan Behunin, Haipeng An and Yue Zhang through interesting discussions and occasionally heated debate. Their passion for physics give me motivation to move forward in the quest for secrets of nature. I want to thank my fellow students and friends Haibo Yu, Yi Cai, Ken Hsieh, Prateek Agrawal, Christopher Krenke, Michael Buchoff, Minho Son, Daniel Chapman, Konstantinos Koutrolikos, Bhupal Dev and Doojin Kim, for the joy and laughter they brought to me.

I owe my deepest thanks to my family. I thank my dear wife Shu Zhang for her love and support. Meeting and marrying her is the most important thing I have done during my graduate life. I thank my parents, who, despite being half a world away, have never been reluctant to show me their support and encouragement.

Table of Contents

List of Tables

List of Figures

List of Abbreviations

LHC	Large Hadron Collider
SM	Standard Model
BSM	Beyond Standard Model
RS	Randall Sundrum
4D	four-dimensional
5D	five-dimensional
UV	Ultraviolet
IR	Infrared
TeV	Teraelectronvolt
GeV	Gigaelectronvolt
NGB	Nambu-Goldstone Boson
PGB	Pseudo-Goldstone Boson
PNGB	Pseudo-Nambu-Goldstone Boson
VEV	Vacuum Expectation Value
EW	Electroweak
EWSB	Electroweak Symmetry Breaking
CMB	Cosmic Microwave Background
CFT	Conformal Field Theory
AdS	Anti -deSitter
CKM	Cabibbo Kobayashi Maskawa
GIM	Glashow Illiopoulos Maiani
FCNC	Flavor Changing Neutral Currents
GK	Georgi-Kaplan
GHU	Gauge Higgs Unification
EWPT	Electroweak Precision Test
CW	Coleman-Weinberg

Chapter 1

Introduction and Outline

At the dawn of the LHC era, there is great anticipation and excitement among many particle physicists around the world. Looking back at the history, we can only marvel at the success in our understanding of the basic laws of nature. The Standard Model (SM) of particle physics is one of the great treasures we found during this endeavor. It describes the three fundamental interactions (electromagnetic, strong nuclear and weak nuclear forces, leaving out gravity) in the unifying and elegant framework of gauge theories. Within this model, the most fundamental building blocks of nature are divided into two classes: the matter particles and the force carriers. The matter particles are fermions (spin 1/2), which include electrons and the quarks that make up protons and neutrons. The force carriers are vector bosons (spin 1). Exchange of force carriers between matter particles give rise to the fundamental interactions. The form of interactions between matter particles and force carriers and between force carriers themselves are dictated by the gauge symmetry, which provides a very beautiful and predictive mathematical structure for the model (see section 2.1 for a more detailed discussion on gauge symmetry). The phenomenal success of the standard model lies in the fact that it has undergone experimental tests of remarkable precision during the past decades. With simple yet profound mathematical structure, which at the same time provides accurate

experimental predictions, the standard model has been set as the classic theory of particle physics.

Despite its glorious success, there is still an important missing piece of the standard model - the Higgs boson, which is a scalar boson (spin 0) that has escaped experimental detection until now. The Higgs boson is responsible for giving masses to force carriers of weak nuclear interaction ($\sim$ 100 Gigaelectronvolt (GeV)), which in turn set the strength of this force. On the other hand, the Planck scale ($\sim 10^{19}$ GeV) sets the mass scale of gravitational interaction. The largeness of the Planck scale explains why gravity is so weak compared to other forces. However, due to the lack of symmetry that protects the Higgs boson mass, the large quantum corrections tend to drive its mass and thus the weak scale up to the Planck scale [1]. So we are left to explain why there is this 17 orders of magnitude hierarchy between the Planck scale and the weak scale. The quest for a solution to this problem has generated various Beyond the Standard Model (BSM) theories, including supersymmetry, extra dimensions, little Higgs and technicolor.

In this thesis, I will discuss models of warped extra dimensions *à la* Randall-Sundrum (RS) model [2]. These models try to solve the hierarchy problem by invoking an extra dimension with curved geometry. Due to the curvature, the effective mass scale depends exponentially on the location along the 5th dimension. At one end of the extra dimension, where gravity resides, the effective mass scale is of order of the Planck scale, thus explaining the weakness of gravitational interaction. The Higgs boson lives at the other end of the extra dimension, where the effective mass scale gets exponentially suppressed to $\sim 100 - 1000$ GeV. Therefore,

the Higgs boson mass gets protected from large quantum corrections, and the hierarchy between the Planck scale and the weak scale is "stabilized". This way of solving the hierarchy problem using geometry has attracted a lot of attention within the particle physics community, and a large number of realistic models have been built in this framework. In addition, in models where fermions propagate inside the extra dimension (called the bulk), and different types (called flavor) of fermions are localized differently, the hierarchy of fermion masses can be explained as well.

The collider phenomenology for some of these models is the main topic of this thesis. One of the most important prediction of RS models is the existence of Kaluza-Klein (KK) partners of SM states, i.e. heavier excitations in the extra dimension. So a lot of work has been done in studying the collider signature of these KK states, including KK gluon [3] and KK electroweak gauge bosons [4]. A class of models in warped extra dimensions that is attractive due to its naturalness is the warped/composite Pseudo-Goldstone boson (PGB) Higgs model [5, 6]. Previous collider studies on these models have focused on the signature of light KK fermions (see [7, 8]). However, there exist extra KK gauge bosons (beyond SM KK gauge bosons) in this framework, which are called coset gauge bosons. Their quantum numbers are the same as that of the Higgs boson and they exhibit a distinctive structure in their couplings. Their collider signatures can serve as model-independent prediction for this generic framework (see [9]).

The properties of the Higgs boson in the RS models are modified with respect to that of SM due to the mixing of SM and KK fermions. It was shown that in RS models the Higgs boson can mediate interactions that convert one flavor

of fermion into another [9, 10, 11, 12, 13], also known as Flavor Changing Neutral Currents (FCNC), unlike in the SM. This leads to interesting bounds from low energy experiments and exotic signals at the LHC. The Higgs boson coupling to gluons are also modified in RS models due to the existence of KK fermions [13, 14, 15, 16], which changes the production rate of the Higgs boson at the LHC significantly.

The outline for my thesis is as follows: in chapter 2, I will give a brief review of the standard model and then point out its features and problems. In chapter 3, I will review the basic formulation of theories of warped extra dimensions, focusing on its geometric aspects and the way it solves the hierarchy problem. The solution to fermion mass hierarchy problem is also discussed, together with its implications. In chapter 4, I will discuss the warped/composite PGB Higgs models and their phenomenology. I will give a detailed discussion of the properties of the coset gauge bosons, and the prospect of their discovery at the LHC. In chapter 5, I will discuss the phenomenology of the Higgs boson in warped extra dimensions. The discussion will be focused on the new physics contributions to the Higgs boson couplings with massless vector gauge bosons such as gluon and photon, which are the relevant couplings for Higgs boson production and decay at the LHC. I will show that these couplings get modified in the RS models significantly and can be used to obtain signals for the warped extra dimension framework even if the KK excitations are too heavy to be produced directly at the LHC. These collider signals will give us a more transparent picture of the underlying structure of the warped extra dimension. The conclusion and outlook will be presented in chapter 6. Various technical details and calculations are presented in the appendices.

Chapter 2

Review of the Standard Model

In this chapter, I will give a brief review of the standard model of particle physics. The gauge structure will be discussed first, together with an explanation of the Higgs mechanism and how the masses of gauge bosons arise from it. Then the fermion content is introduced, followed by the discussion of the Yukawa interactions and how they give masses to fermions. This leads to the complete Lagrangian for the standard model. The implications and problems of the standard model will be mentioned. A more complete discussion of the standard model can be found in [17, 18, 19].

2.1 Gauge Theories and the Higgs Mechanism

The beauty of the standard model lies in its gauge structure. The power of gauge theories is due to the fact that the dynamics of the theory is dictated by its symmetry alone. This makes the standard model a very predictive theory.

To illustrate the essential features of gauge theories, we consider here a simple model with $SU(2)$ symmetry. Specifically, we consider a fermion pair transforming in the doublet representation of $SU(2)$:

$$\Psi(x) = \begin{pmatrix} \psi(x) \\ \\ \chi(x) \end{pmatrix}. \tag{2.1}$$

The Lagrangian is given by

$$\mathcal{L} = \bar{\Psi} i \partial\!\!\!/ \Psi - m \bar{\Psi} \Psi. \tag{2.2}$$

It is easy to see that this Lagrangian is invariant under global $SU(2)$ transformation:

$$\Psi(x) \to e^{i \frac{\theta^a \sigma^a}{2}} \Psi(x), \tag{2.3}$$

where σ^a are Pauli matrices, and θ^a are constants. This theory is rather trivial since it is a free theory. An interesting fact is that interactions will arise once we require gauge invariance, i.e. we demand the theory to be invariant under the local transformation:

$$\Psi(x) \to e^{i \frac{\theta^a(x) \sigma^a}{2}} \Psi(x) \equiv V(x) \Psi(x), \tag{2.4}$$

where we have defined the transformation matrix $V(x)$. Now the Lagrangian is not invariant anymore. In fact, an extra term in the transformed Lagrangian arises due to the kinetic term in the original Lagrangian:

$$\mathcal{L} \to \mathcal{L} + i \bar{\Psi}(x) \left[V(x)^\dagger \partial\!\!\!/ V(x) \right] \Psi(x). \tag{2.5}$$

To cancel the extra term in the above equation, we can introduce a vector field (called the gauge field) that couples to fermions with the following Lagrangian:

$$\mathcal{L} = \bar{\Psi} \gamma^\mu \left(i \partial_\mu + g A^a_\mu \frac{\sigma^a}{2} \right) \Psi - m \bar{\Psi} \Psi. \tag{2.6}$$

In addition, we let the gauge field transform in the following way

$$A^a_\mu \frac{\sigma^a}{2} \to V(x) A^a_\mu \frac{\sigma^a}{2} V(x)^\dagger + \frac{i}{g} V(x) \partial_\mu V(x)^\dagger. \tag{2.7}$$

It can be easily verified that the Lagrangian Eq. (2.6) is indeed invariant under the transformations Eq. (2.4) and (2.7). We can define a covariant derivative

$$D_\mu \equiv \partial_\mu - igA^a_\mu \frac{\sigma^a}{2}. \tag{2.8}$$

Then the Lagrangian Eq. (2.6) can be simplified to

$$\mathcal{L} = \bar{\Psi} i \not{D} \Psi - m\bar{\Psi}\Psi. \tag{2.9}$$

We can also write down another gauge-invariant term involving just the gauge fields as follows. Notice that

$$[D_\mu, D_\nu] = -igF^a_{\mu\nu}\frac{\sigma^a}{2}, \tag{2.10}$$

with

$$F^a_{\mu\nu}\frac{\sigma^a}{2} = \partial_\mu A^a_\nu \frac{\sigma^a}{2} - \partial_\nu A^a_\mu \frac{\sigma^a}{2} - ig[A^b_\mu \frac{\sigma^b}{2}, A^c_\nu \frac{\sigma^c}{2}]. \tag{2.11}$$

From Eq. 2.10, we can see that the field strength $F^a_{\mu\nu}$ transforms in a simple way under the local transformation:

$$F^a_{\mu\nu}\frac{\sigma^a}{2} \to V(x)F^a_{\mu\nu}\frac{\sigma^a}{2}V(x)^\dagger. \tag{2.12}$$

Therefore, we can add a term, namely, $-\frac{1}{4}F^a_{\mu\nu}F^{a,\mu\nu}$ involving just the gauge field into the Lagrangian. The full Lagrangian becomes

$$\mathcal{L} = -\frac{1}{4}F^a_{\mu\nu}F^{a,\mu\nu} + \bar{\Psi} i \not{D} \Psi - m\bar{\Psi}\Psi. \tag{2.13}$$

Some comments are in order here. First, we note that the requirement that the Lagrangian be invariant under local transformation leads to the introduction of

gauge fields. Second, the structure of the interaction is fixed by gauge invariance (note that this is a non-trivial statement, since the gauge coupling between fermions and gauge fields and the coupling between gauge fields themselves are required to be equal). In fact, the full Lagrangian in Eq. (2.13) is the most general Lagrangian with terms that have dimension less or equal to 4, i.e. renormalizable. Therefore, gauge invariance and renormalizability together completely restrict the form of the interactions. This makes the principle of gauge invariance a very powerful tool.

The gauge group of the SM is $SU(3)_c \times SU(2)_L \times U(1)_Y$. The $SU(3)_c$ group give rise to strong interaction, and the $SU(2)_L \times U(1)_Y$ group give rise to electroweak couplings. However, the gauge theory we constructed above has only massless gauge fields, while the charged and neutral weak gauge bosons ($W^{\pm}/Z$) are massive. To accommodate heavy gauge bosons, one might naively add a mass term for the gauge fields $\frac{1}{2}m_A^2 A_\mu^a A^{a,\mu}$. However, this mass term spoils the gauge symmetry. The physical embodiment of this problem is that the longitudinal W boson scattering amplitude would grow with energy, leading to a violation of unitary at high energy. So to have massive gauge bosons while at the same time preserve gauge invariance, we need new ingredients in the theory. This new ingredient is the Higgs mechanism, which we discuss below.

In order to give gauge bosons masses, we can introduce a scalar field which transforms under the gauge group. For simplicity, we still consider the $SU(2)$ gauge theory we discussed before. Let us introduce a scalar field transforming as a doublet

under $SU(2)$

$$H = \begin{pmatrix} H_1 \\ \\ H_2 \end{pmatrix}, \qquad H \to e^{i\frac{\theta^a(x)\sigma^a}{2}} H \tag{2.14}$$

As before, in order to write down a gauge invariant Lagrangian, we need to replace derivative with covariant derivative. We arrive at the following Lagrangian

$$\mathcal{L} = -\frac{1}{4} F^a_{\mu\nu} F^{a,\mu\nu} + (D_\mu H)^\dagger (D^\mu H) - V(H^\dagger H), \tag{2.15}$$

with a gauge invariant potential

$$V(H^\dagger H) = -\mu^2 H^\dagger H + \frac{\lambda}{2}(H^\dagger H)^2. \tag{2.16}$$

In order to ensure gauge invariance, the covariant derivative should be the same as the one defined in Eq. (2.8). The quartic coupling λ in the scalar potential (Eq. (2.16)) should be positive so that the potential is bounded from below. But the coefficient of the quadratic term μ^2 can be both positive and negative. We pick it to be positive here. Then we can easily see that the minimum of the potential is not achieved at $\langle H \rangle = 0$. We can always do a gauge transformation such that $\langle H \rangle = \begin{pmatrix} 0 \\ \\ v \end{pmatrix}$. Then the potential turns out to be

$$V(v) = -\mu^2 v^2 + \frac{\lambda}{2} v^4, \tag{2.17}$$

and it is easy to see that the minimum of the potential is achieved at $v = \sqrt{\frac{\mu^2}{\lambda}}$. The fact that $v \neq 0$ tells us that the vacuum of the theory spontaneously breaks the gauge invariance. It is useful to note that if there is only a global symmetry, then

this spontaneous symmetry breaking will lead to three massless scalar bosons - the Nambu-Goldstone bosons (NGB).

To see how the masses of gauge bosons arise after this spontaneous symmetry breaking, we expand the covariant derivatives in the kinetic term of the scalar field

$$\begin{aligned}(D_\mu H)^\dagger (D^\mu H) &\supset g^2(0,\ v) A^a_\mu \frac{\sigma^a}{2} A^{b,\mu} \frac{\sigma^b}{2} \begin{pmatrix} 0 \\ \\ v \end{pmatrix} \\ &= \frac{g^2 v^2}{4} A^a_\mu A^{a,\mu}.\end{aligned} \tag{2.18}$$

Therefore, the gauge bosons obtain masses $m_A^2 = \frac{g^2 v^2}{2}$. A counting of degree of freedom is in order here. Before the breaking of gauge invariance, we have three massless gauge fields. We know that in four dimensions, massless vector fields have two degree of freedom. Now, after the spontaneous breaking of gauge symmetry, we are left with three massive gauge bosons, but massive vector fields in four dimensions have three degree of freedom. Therefore, we conclude that the massive gauge bosons "eat" three degrees of freedom from the scalar multiplet. These three "eaten" degree of freedom are the would-be NGBs mentioned above. We can choose the unitary gauge such that these would-be NGBs do not appear in the theory. A detailed discussion on this procedure called gauge fixing in spontaneously broken gauge theories can be found in [17].

In the scalar sector of the theory, we are left with one massive degree of freedom. To find its mass, we can substitute $H = \begin{pmatrix} 0 \\ \\ v + \frac{1}{\sqrt{2}} h \end{pmatrix}$ into the potential (Eq. 2.16):

$$V \supset \mu^2 h^2, \tag{2.19}$$

i.e. the mass for this massive scalar excitation is $m_h = \sqrt{2}\mu = \sqrt{2\lambda}v$.

The Higgs mechanism can be applied to the standard model gauge group in a straightforward way. The gauge group now is $SU(3)_c \times SU(2)_L \times U(1)_Y$. We let the Higgs scalar field transform in doublet representation of $SU(2)_L$ and carry $U(1)_Y$ charge 1/2. The Lagrangian for the gauge and Higgs sector of the standard model is:

$$\mathcal{L}_g = -\frac{1}{4}G^a_{\mu\nu}G^{a,\mu\nu} - \frac{1}{4}W^i_{\mu\nu}W^{i,\mu\nu} - \frac{1}{4}B_{\mu\nu}B^{\mu\nu} + (D_\mu H)^\dagger(D^\mu H) - V(H^\dagger H), \quad (2.20)$$

where G, W, B are gauge fields for the $SU(3)_c, SU(2)_L, U(1)_Y$ gauge group respectively, and the potential for Higgs field is the same as Eq. (2.16). The covariant derivative for Higgs is $D_\mu H = \left(\partial_\mu - igW^a_\mu \frac{\sigma^a}{2} - \frac{ig'}{2}B_\mu\right) H$. The potential of the Higgs field drives its Vacuum Expectation Value (VEV) to be $\langle H \rangle = \frac{1}{\sqrt{2}} \begin{pmatrix} 0 \\ v \end{pmatrix}$. Three degrees of freedom in the Higgs doublet get eaten by the gauge bosons, leaving one massive scalar excitation: the physical Higgs boson. The masses of the gauge bosons can be found by similar method as we did before. The charged gauge bosons ($W^\pm$) get masses $m_W = \frac{gv}{2}$. The massive neutral gauge boson is $Z_\mu = \frac{1}{\sqrt{g^2+g'^2}}(gW^3_\mu - g'B_\mu)$ with mass $m_Z = \sqrt{g^2+g'^2}\frac{v}{2}$. The experimentally measured W/Z boson masses and coupling constants g and g' fix the Higgs VEV to be $v = 246$ GeV. There is also a massless neutral gauge boson $A_\mu = \frac{1}{\sqrt{g^2+g'^2}}(g'W^3_\mu + gB_\mu)$, and it is identified as the photon.

2.2 The Fermion Content

There are three generations of fermions in the standard model. The left-handed fermions live in doublet representation of $SU(2)_L$ and the right-handed fermions live in the singlet representation. We list the representation of one generation as follows

$$q_L\ (3,2,1/6); \quad u_R\,(3,1,2/3); \quad d_R\ (3,1,-1/3); \tag{2.21}$$
$$l_L\ (1,2,-1/2); \quad e_R\ (1,1,-1),$$

where the numbers in the parentheses give its represention/charge under $SU(3)_c$, $SU(2)_L$, $U(1)_Y$ respectively. Due to the different representations for left-handed and right-handed fermions, we cannot write down a bare mass term for the fermions. The fermion masses are generated after Electro-Weak Symmetry Breaking (EWSB) through the Yukawa couplings

$$\mathcal{L}_Y = -Y_l \bar{l}_L H e_R - Y_d \bar{q}_L H d_R - Y_u \bar{q}_L \tilde{H} u_R + h.c., \tag{2.22}$$

where $\tilde{H} = \epsilon \cdot H^\dagger$, and we ignored the generation indices here. After Higgs gets a VEV, the fermions would acquire a mass proportional to their Yukawa couplings.

There is one important feature that arises when we consider three generations (flavors) of fermions. The Yukawa matrices in flavor space are generally not diagonal. So we need to do unitary transformations $u_L \to V_L^u u_L$, $u_R \to V_R^u u_R$, $d_L \to V_L^d d_L$, $d_R \to V_R^d d_R$ etc. to diagonalize the mass matrices of fermions. The transformations for right-handed fermions are immaterial since it can be absorbed into a redefinition of fields. But the left-handed fermion transformation leads to physical effect in their

couplings to W boson. The W boson coupling is now flavor violating:

$$\mathcal{L}_w \supset \frac{g}{2} W_\mu^+ \bar{u}_L \gamma^\mu V_L^{u,\dagger} V_L^d d_L. \tag{2.23}$$

The combination of the transformation matrices $V_{CKM} \equiv V_L^{u,\dagger} V_L^d$ is called the Cabibbo-Kobayashi-Maskawa (CKM) matrix. It is the only source of flavor violation in the standard model.

Now we have a complete picture of the standard model, we can layout some of the important implications of it.

- The mass of W and Z bosons satisfy the relation

$$\frac{m_W}{m_Z} = \cos\theta_w = \frac{g}{\sqrt{g^2 + g'^2}}. \tag{2.24}$$

  This relation is an important prediction of the SM and it receives small quantum corrections through loop diagrams. We will see that in warped extra dimensions, we need to introduce extended gauge group in the bulk such that the quantum corrections of the new physics states do not spoil this relation.

- As mentioned before, the only flavor violation in the SM is due to the CKM matrix. Moreover, after field redefinition, there is only one physical phase in the CKM matrix, which is the only source of CP violation in the SM. Until now, the CKM picture of flavor and CP violation explains all related experimental data [1]. We will see later that in warped extra dimensions, there are more flavor and CP violation sources, leading to interesting constraints and flavor violating signals at the LHC.

[1] Recently, there is experimental indication for 3.2σ deviation from the SM prediction for CP violation in the B_s system [20].

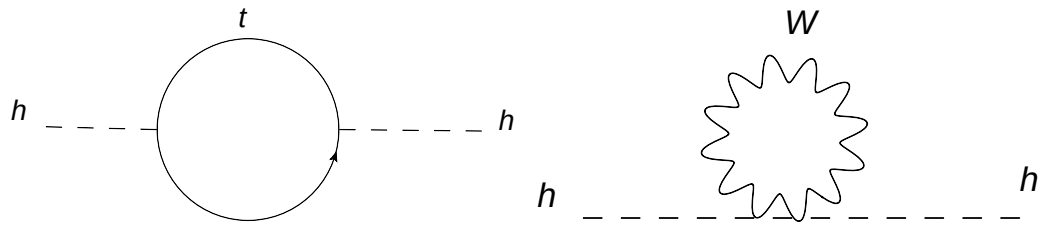

(A) (B)

Figure 2.1: One loop corrections to the Higgs mass in the SM coming from top quark (A) and W boson (B).

- Since the fermion masses come only from the Higgs VEV after EWSB, the Yukawa coupling matrix and the mass matrix of the fermions are proportional to each other. So they can be simultaneously diagonalized. This means that the Higgs boson cannot have flavor violating couplings in the SM. We will see later that this is not true in warped extra dimensions.

2.3 Problems of the Standard Model

Despite its success in explaining data, the SM suffers from some problems. First of all, there is the famous hierarchy problem. The Higgs doublet is a scalar field in the SM. The mass of the Higgs boson gets quantum corrections from loop diagrams such as the ones shown in Fig. 2.1. Let us consider the main contributions coming from the top and W boson in the loop:

$$\Delta m_H^2 \sim \frac{1}{16\pi^2}\left(g^2\Lambda_{UV}^2 - \lambda_t^2\Lambda_{UV}^2\right), \tag{2.25}$$

where Λ_{UV} is the UV cutoff scale, g is the $SU(2)_L$ gauge coupling and λ_t is the top quark Yukawa coupling. If we consider the SM to be a complete theory of strong and electroweak interactions all the way up to the Planck scale, then the UV cutoff

of the theory should be around the Planck scale. So we get two very large terms in Eq. (2.25), and these two terms should cancel against tree level/bare mass term to give us a mass of the Higgs boson around the weak scale. This extreme fine-tuning required to obtain the electroweak scale is the hierarchy problem [1]. The heart of the hierarchy problem lies in the fact the Higgs boson is a fundamental scalar in the SM. While the masses of fermions and gauge bosons get protected by chiral and gauge symmetry respectively, there is no built-in protection mechanism for the mass of a fundamental scalar. We will see that this observation is the starting point for many BSM models.

The second problem we discuss here is the fermion mass hierarchy problem. This problem comes from the fact that in the SM, the fermion masses range from 174 GeV (top quark) to 0.5 MeV (electron), a hierarchy of $5-6$ orders of magnitude. What is giving this large hierarchy of fermion masses? Note that in the SM, the hierarchy in fermion masses can be translated into a hierarchy of the Yukawa couplings, which is stable against quantum corrections (unlike the Higgs mass), but it is a rather unappealing feature of the SM. It is hard to believe that nature's most fundamental interactions would give rise to such large and rather arbitrary mass hierarchy. The third problem is related to CP violation in the SM. Even though the CKM mechanism of the SM has been very successful in explaining experimental phenomena in colliders, the single phase in the CKM matrix gives too small CP violation in order to give rise to the baryon anti-baryon asymmetry observed in the universe. This means that there should be additional source of CP violation beyond the SM, which could arise in various BSM models.

Last but not least, there is the problem of the dark matter. The existence of the dark matter has been firmly established based on various astrophysical observations, ranging from the rotation curve of galaxies to the Cosmic Microwave Background (CMB) spectrum. However, there is no particle in the SM that can serve as a dark matter candidate.

Various BSM models have been built during the past decades, mainly focusing on solving the hierarchy problem. Supersymmetry tries to protect the Higgs mass by invoking a symmetry relating fermions and bosons (see [21] for a review). Technicolor theories replace the fundamental Higgs scalar with a condensate of a new strongly interacting gauge theory (see [22] for a review). Little Higgs propose that the Higgs boson comes from a Pseudo-Nambu-Goldstone boson (PNGB) of some approximate global symmetry of the new sector that is spontaneously broken (see [23] for a review). Warped extra dimensions, which is the main focus of this thesis, tries to solve the hierarchy problem by geometry (see [24] for review).

2.4 Summary

In this chapter, I gave an introductory review of the standard model, focusing on the gauge theoretical structure of the model and the Higgs mechanism. The fermion content and the fermion mass generation mechanism was introduced. I then pointed out some important implications of the standard model, such as the ratio of W and Z boson masses, the CKM picture and its implication for CP violation, and the flavor structure of Higgs boson interactions. The last topic of this chapter

was on the problems of the standard model, mainly the hierarchy problem. The discussion of the standard model and its problems can be contrasted with that of warped extra dimension theories, which I will discuss in later chapters.

Chapter 3

Warped Extra Dimensions (Randall-Sundrum Model)

The Randall-Sundrum (RS) model was proposed by Lisa Randall and Raman Sundrum in 1999 [2]. It is a novel approach to solve the hierarchy problem with the introduction of a warped extra dimension. In this chapter, we first give an overview of the Randall-Sundrum model, focusing on its geometrical aspects. We then move on to discuss gauge bosons and fermions in the bulk. These discussions naturally leads to the introduction of a very attractive mechanism to generate fermion mass and mixing angle hierarchy. And it is shown that this framework does not introduce excessive new flavor violation.

3.1 Overview of the Randall-Sundrum Model

In Randall-Sundrum model, the spacetime is a slice of 5D AdS space with the following metric [2]:

$$\begin{aligned} ds^2 &= \frac{1}{(kz)^2}(\eta_{\mu\nu}dx^\mu dx^\nu - dz^2), \quad z \in [R, R'] \\ &= e^{-2ky}\eta_{\mu\nu}dx^\mu dx^\nu - dy^2, \quad y \in [0, \pi r_c], \end{aligned} \tag{3.1}$$

where $k = 1/R$ is the curvature scale of the warped extra dimension. We have expressed the metric in two different coordinate systems, which are related by $z = Re^{ky}$. The AdS spacetime is cutoff by two branes, one at $z = R$ and another one at $z = R'$ (see Fig. 3.1 for an illustration of the spacetime structure). This spacetime

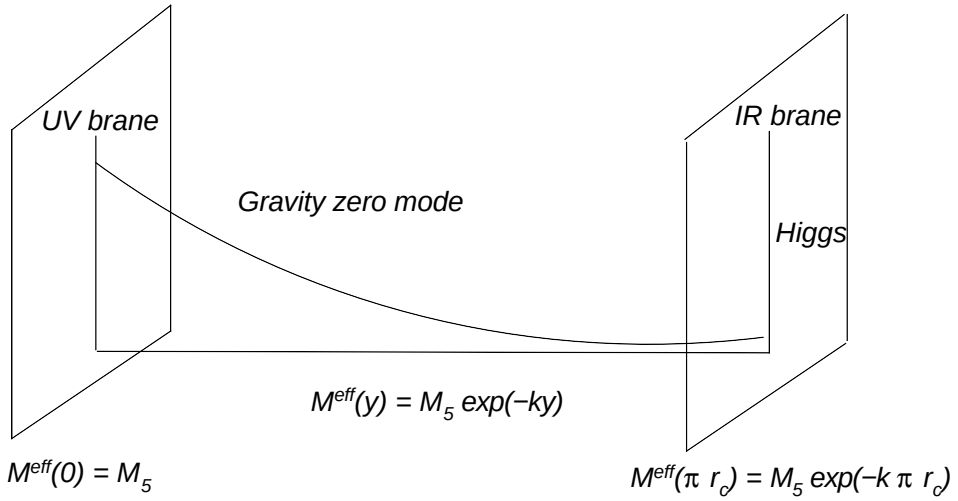

Figure 3.1: The spacetime structure of Randall-Sundrum model. The bulk is a 5D AdS space, with UV brane at $z = R$ and IR brane at $z = R'$. The effective cutoff scale along the extra dimension gets warped down by an exponential factor e^{-ky}. The gravity zero mode is localized near the UV brane, and the Higgs boson is localized around the IR brane.

is a solution to 5D Einstein equation with a large cosmological constant in the bulk and localized cosmological constants on the branes. The slices of 4D spacetime are flat, which accounts for the flatness of our observable universe.

Due to the AdS nature of the bulk spacetime, the effective cutoff mass scale depends on the location along the 5th dimension $M^{eff} = M_5 \frac{R}{z} = M_5 e^{-ky}$ (see Fig. 3.1). To study the 4D effective theory, we can do KK decomposition of all 5D fields. For 5D gravitational field, the wavefunction of the zero mode is localized near the brane at $z = R$ (see Fig. 3.1), where the effective mass scale is $\sim M_5$ (hence called the UV brane). By choosing $M_5 \sim M_{pl}$, we can get ordinary 4D gravity with the correct interaction strength. In addition, by choosing $k \sim M_5$, we get a

theory without any hierarchy in the fundamental parameters. On the other hand, the Higgs boson lives near the brane at $z = R'$, where the effective mass scale is exponentially suppressed $M_{IR}^{eff} = M_5 e^{-k\pi r_c}$ (hence called the IR brane). We can see that if the size of the extra dimension πr_c is moderately larger than k^{-1} (i.e., by a factor of ~ 35), then $M_{IR}^{eff} \sim$ TeV, and the hierarchy between the Planck and weak scale is explained. This size of extra dimension is proven to be natural based on the Goldberger-Wise stabilization mechanism [25].

In the original RS model, all the SM fields live on the IR brane. It was then realized that this scenario leads to problems such as too large new physics contributions to FCNC. A natural extension of the model seems to be placing some of the SM fields in the bulk. In fact, this leads to very interesting new phenomenology, which we will discuss below.

3.2 Gauge Bosons in the Bulk

The gauge field placed in the bulk has 5 components: A_M with $M = \mu, 5$. The action is [26]

$$\begin{aligned} S_{gauge} &= \int d^4x dz \sqrt{G} \left(-\frac{1}{4g_5^2} \right) F_{MN} F^{MN} \\ &= \int d^4x dz \Big\{ -\frac{1}{4g_5^2} \frac{1}{kz} F_{\mu\nu} F^{\mu\nu} + \frac{1}{2g_5^2} \frac{1}{kz} (\partial_\mu A_5)^2 \\ &\quad -\frac{1}{g_5^2} \partial^\mu A_\mu \partial_z \left(\frac{A_5}{kz} \right) + \frac{1}{2g_5^2} \frac{1}{kz} (\partial_z A_\mu)^2 \Big\}, \end{aligned} \tag{3.2}$$

where we used integration by part to get the third term. Note that this is a cross term between A_5 and A_μ, which we need to get rid of by choosing a gauge-fixing

term [27]. After that we can do the KK decomposition of gauge fields

$$A_\mu(x,z) = A_\mu^{(n)}(x) f_A^{(n)}(z). \tag{3.3}$$

The gauge fixing procedure and details of KK decomposition is presented in appendix A. For gauge fields with $(+,+)$ boundary conditions [1], the zero mode wavefunction is flat, while the KK wavefunctions are given by [28]

$$f_A^{(n)}(z) = \sqrt{\frac{1}{R}} \frac{z}{N_n^g} [J_1(m_n z) + b_n Y_1(m_n z)], \tag{3.4}$$

where the normalization factor is given by

$$N_n^{g,2} = \frac{1}{2} \left[R'^2 [J_1(m_n R') + b_n Y_1(m_n R')]^2 - R^2 [J_1(m_n R) + b_n Y_1(m_n R)]^2 \right]. \tag{3.5}$$

The mass eigenvalues and parameter b_n are given by

$$\frac{J_0(m_n R)}{Y_0(m_n R)} = \frac{J_0(m_n R')}{Y_0(m_n R')} = -b_n. \tag{3.6}$$

These wavefunctions are obtained by imposing IR boundary conditions on the suitable basis functions found in Eq. (A.13) and then normalizing them. Solving Eq. 3.6, we find that the mass of the first KK mode is $m_1 \approx 2.45 R'^{-1}$. Note that $R'^{-1} = R^{-1} e^{-k\pi r_c} \approx$ TeV. Therefore, the KK gauge bosons have masses around the TeV scale.

For completeness, we give the KK decomposition for gauge bosons with $(-,+)$ boundary conditions. There is no zero mode for this boundary condition. The KK wavefunction is given by the same form as Eq. (3.4). The mass eigenvalues and b_n

[1] The notation (+,+) gives the boundary conditions on UV and IR branes respectively, where +/− means Neumann/Dirichlet.

parameter is given by

$$\frac{J_1(m_n R)}{Y_1(m_n R)} = \frac{J_0(m_n R')}{Y_0(m_n R')} = -b_n. \tag{3.7}$$

We lay out here some important features of gauge bosons in the bulk:

- The zero mode of the gauge field has a flat profile. Therefore, any field that lives in the bulk would have the same coupling with the gauge zero mode. This is a consequence of gauge invariance since the zero mode is massless. The zero mode gauge coupling is given by

$$g = \frac{g_5}{\sqrt{\pi r_c}}. \tag{3.8}$$

- The KK modes of gauge fields (both (+,+) and (-,+) boundary conditions) have masses starting at the TeV scale. In addition, the wavefunctions for these KK modes are localized near the IR brane. Therefore, they couple strongly with fields near the IR brane and weakly with fields localized near UV brane.

In RS models with gauge fields in the bulk, the SM gauge groups have $(+,+)$ boundary conditions, whose zero modes give rise to usual SM gauge bosons. In addition, we need another gauge group $SU(2)_R$ in the bulk, with boundary condition $(-,+)$ [29]. The purpose of this extra bulk gauge group is to ensure that the theory passes the Electro-Weak Precision Test (EWPT).

3.3 Fermions in the Bulk

The action for fermions in the bulk is given by [26]

$$S_{fermion} = \int d^4x\, dz\, \sqrt{G}[i\bar{\Psi}\Gamma^M D_M \Psi + ck\bar{\Psi}\Psi], \tag{3.9}$$

where c is the dimensionless bulk mass parameter, $\Gamma^M = \Gamma^A e_A^M$, with $\Gamma^A = (\gamma^\mu, -i\gamma^5)$ and $e_A^M = \frac{R}{z}\delta^{AM}$. The covariant derivative is given by

$$D_\mu = \partial_\mu - \frac{i}{2}\gamma_5\gamma_\mu\frac{R}{z}. \tag{3.10}$$

The 5D bulk fermion field Ψ contains two 4D chiral fields (ψ_L, ψ_R). The boundary conditions for these two chirality are opposite to each other. For concreteness, we consider the boundary condition $\psi_L(+,+), \psi_R(-,-)$. Similar to the case with gauge bosons, we can proceed to do KK decomposition:

$$\psi_L(x,z) = \sum_n \psi_L^{(n)}(x) f_F^{(n)}(c,z). \tag{3.11}$$

The normalization for the profile is

$$\int dz \left(\frac{R}{z}\right)^4 \left(f_F^{(n)}(c,z)\right)^2 = 1. \tag{3.12}$$

We have a fermion zero mode with profile

$$f_F^{(0)}(c,z) = f(c)\left(\frac{z}{R}\right)^{2-c}\frac{1}{\sqrt{R}}\left(\frac{R}{R'}\right)^{1/2-c}, \tag{3.13}$$

with

$$f(c) = \sqrt{\frac{1-2c}{1-(R'/R)^{2c-1}}}. \tag{3.14}$$

The KK fermion profiles for the same chirality as the zero modes are given by [28]

$$f_F^{(n)}(c,z) = \left(\frac{z}{R}\right)^{5/2}\frac{1}{N_n^f\sqrt{\pi r_c}}[J_\alpha(m_n z) + b_\alpha(m_n)Y_\alpha(m_n z)] \tag{3.15}$$

with $\alpha = |c+1/2|$, m_n and b_α are given by

$$\frac{J_{\alpha\mp1}(m_n R)}{Y_{\alpha\mp1}(m_n R)} = \frac{J_{\alpha\mp1}(m_n R')}{Y_{\alpha\mp1}(m_n R')} = -b_\alpha(m_n), \tag{3.16}$$

with upper (lower) signs for $c > -1/2$ ($c < -1/2$) and the normalization condition gives

$$|N_n^f|^2 = \frac{1}{2\pi r_c R}\Big[R'^{,2}[J_\alpha(m_n R') + b_\alpha(m_n)Y_\alpha(m_n R')]^2 \\ -z_h^2[J_\alpha(m_n R) + b_\alpha(m_n)Y_\alpha(m_n R)]^2\Big]. \tag{3.17}$$

It is useful to note that the ratio of zero and KK fermion profile at TeV brane is

$$\frac{f_F^{(0)}(c, R')}{f_F^{(n)}(c, R')} \approx \frac{f(c)}{\sqrt{2}}. \tag{3.18}$$

The bulk fermions couple to Higgs field on the brane through Yukawa couplings

$$\mathcal{L}_Y = \int d^x\, dz \sqrt{G}\frac{\delta(z - R')}{kz} Y_{u,d}^{5D}\bar{\Psi}^q H(\Psi^u, \Psi^d). \tag{3.19}$$

where Ψ^q is $SU(2)_L$ doublet and $\Psi^{u,d}$ are $SU(2)_L$ singlet. We choose the boundary conditions such that $\Psi_L^q, \Psi_R^{u,d}$ has $(+,+)$ boundary conditions. The zero modes of these chiralities give rise to SM fermion fields. These zero modes acquire mass through the Yukawa coupling. The SM fermion mass is given by

$$m_f^{SM} = (Y_{u,d}^{5D} k) v f(c_q) f(c_{u,d}). \tag{3.20}$$

We list here some important points about fermions in the bulk:

- The fermion zero mode profile is not flat along the extra dimension. In fact, for $c > 1/2$, the zero mode profile is localized towards the UV brane, and is exponentially suppressed on the IR brane. On the other hand, for $c < 1/2$, the zero mode profile is localized towards the IR brane.

- The fermionic KK modes are all localized towards the IR brane, and the sizes of their wavefunctions on the IR brane are approximately equal. The masses of these KK modes are of the order of TeV.

Based on Eqs. (3.20) and (3.14), we can see that the hierarchy in SM fermion masses can be generated by order one difference in the c's, namely, we can choose $c > 1/2$ for the light generations and $c < 1/2$ for the top quark (even if the 5D Yukawa couplings are not hierarchical). In this sense, bulk fermions in warped extra dimension provide a very attractive mechanism that addresses fermion mass hierarchy.

3.4 Flavor Anarchy and RS-GIM Mechanism

The discussion of last section leads to the proposal of flavor anarchy[28]. The basic assumption of flavor anarchy is that the fermion mass hierarchy arises *solely* due to zero mode fermion wavefunctions. The 5D Yukawa couplings are "anarchic", i.e. they are all of the same order with no specific structure. For simplicity, we consider only up-type quarks here. We define the dimensionless 5D Yukawa coupling by $Y_* = Y_u^{5D} k$. Then the fermion mass matrix is given by

$$m_u^{ij} = f(c_{q_i}) Y_*^{ij} f(c_{u_j}) v. \tag{3.21}$$

By choosing $c_{q_1} > c_{q_2} > c_{q_3}$ and similarly for c_{u_j}, we can have hierarchical wavefunctions

$$f(c_{q_1}) \ll f(c_{q_2}) \ll f(c_{q_3}), \quad f(c_{u_1}) \ll f(c_{u_2}) \ll f(c_{u_3}). \tag{3.22}$$

So the fermion mass matrix has the following rough structure

$$m_u \sim \begin{pmatrix} f_{q_1} f_{u_1} & f_{q_1} f_{u_2} & f_{q_1} f_{u_3} \\ f_{q_2} f_{u_1} & f_{q_2} f_{u_2} & f_{q_2} f_{u_3} \\ f_{q_3} f_{u_1} & f_{q_3} f_{u_2} & f_{q_3} f_{u_3} \end{pmatrix} \bar{Y} v, \tag{3.23}$$

where $\bar{Y}$ is the typical size of Y_*^{ij}. We need to do bi-unitary transformation to diagonalize this matrix. The transformation matrices have the following structure

$$U_L \sim \begin{pmatrix} 1 & f_{q_1}/f_{q_2} & f_{q_1}/f_{q_3} \\ f_{q_1}/f_{q_2} & 1 & f_{q_2}/f_{q_3} \\ f_{q_1}/f_{q_3} & f_{q_2}/f_{q_3} & 1 \end{pmatrix}, \tag{3.24}$$

$$U_R \sim \begin{pmatrix} 1 & f_{u_1}/f_{u_2} & f_{u_1}/f_{u_3} \\ f_{u_1}/f_{u_2} & 1 & f_{u_2}/f_{u_3} \\ f_{u_1}/f_{u_3} & f_{u_2}/f_{u_3} & 1 \end{pmatrix}. \tag{3.25}$$

The transformation matrices for down-type quarks have similar structure. The mass eigenvalues have hierarchical structure as well

$$m_u^{\text{diag}} \sim \text{diag}(f_{q_1} f_{u_1},\, f_{q_2} f_{u_2},\, f_{q_3} f_{u_3}) \bar{Y} v. \tag{3.26}$$

The hierarchical quark masses are then easily generated due to the hierarchical wavefunctions (see Eq. (**??**)). The CKM matrix is given by $V^{CKM} = U_L^\dagger D_L$ and it has the same structure as that of U_L, i.e. $V_{ij}^{CKM} \sim f_{q_i}/f_{q_j}$ for $i < j$. From experiment, we know that the CKM matrix has the following hierarchical structure

$$V_{CKM} \sim \begin{pmatrix} 1-\lambda^2/2 & \lambda & \lambda^3 \\ \lambda & 1-\lambda^2/2 & \lambda^2 \\ \lambda^3 & \lambda^2 & 1 \end{pmatrix}, \tag{3.27}$$

where $\lambda \approx 0.2$. Therefore, if we pick $f_{q_1}/f_{q_2} \sim \lambda$ and $f_{q_2}/f_{q_3} \sim \lambda^2$, we can account for the hierarchical structure of the CKM matrix.

The flavor anarchy framework gives a very attractive and natural picture for the origin of fermion mass hierarchy. On the other hand, it has a richer flavor

structure, in particular there are new flavor violating sources in this framework. So we need to make sure that these new contributions to flavor violating processes do not contradict low energy experiments. Surprisingly, the power of hierarchical wavefunctions shows up here again. Recall from the previous two sections that the KK modes are all localized near the IR brane, so their couplings to zero mode fermions are determined by the fermionic wavefunctions near the IR brane. The zero mode wavefunctions at the IR brane for the $1^{\text{st}}/2^{\text{nd}}$ generation quarks are exponentially suppressed in the flavor anarchy scenario, in order to account for their small masses. Therefore, the couplings of heavy KK states with that of light quarks are suppressed, which in turn leads to suppression in FCNC from exchange of KK states. In a sense, the lightness of quarks guarantees small flavor violation. This reminds us of the Glashow-Iliopoulos-Maiani (GIM) mechanism in the SM. Therefore, this way of suppressing the new sources of flavor violation is called the RS-GIM mechanism [28, 30, 31].

3.5 Summary

In this chapter, I gave a brief review of the warped extra dimensions. I first discussed the geometrical aspect of the Randall-Sundrum model, focusing on how it solves the hierarchy problem of the SM. I then described the scenarios with gauge bosons and fermions in the bulk. I reviewed the KK decomposition for gauge bosons and fermions in warped extra dimension, and pointed out the relevant features of the zero and KK modes. Based on this, I discussed the flavor anarchy framework and

explained how it manages to explain the fermion mass and mixing angle hierarchy. The RS-GIM mechanism, which provides protection against flavor violation coming from exchange of KK modes, was then illustrated.

Chapter 4

Warped/Composite PGB Higgs Models and Their Phenomenology

4.1 Introduction

In the previous chapters, we have discussed the basic idea of warped extra dimensions and how it solves the hierarchy problem through geometry. We also argued that the models with SM fields propagating in the bulk give a very attractive framework that addresses the fermion mass hierarchy problem while at the same time protecting $1^{\text{st}}/2^{\text{nd}}$ generation quarks from receiving large FCNC. However, with the 5D electroweak (EW) gauge symmetry being $SU(2)_L \times SU(2)_R$,[1] and a Higgs transforming as a bi-doublet (henceforth called "minimal Higgs sector"), the framework still suffers from an incarnation of the little hierarchy problem. Namely, the Higgs mass is still sensitive to the $5D$ cut-off, albeit warped-down (compared to the fundamental $5D$ scale which is Planckian) at the TeV brane. The problem is that the mass scale of the Kaluza-Klein (KK) excitations of the SM particles is constrained to be at least a few TeV by various precision tests (see reference [32] for a review) and the (warped-down) $5D$ cut-off should be larger than the KK scale by (roughly) an order-of-magnitude in order for the $5D$ effective field theory description to be valid.

[1] Here, we include a $SU(2)_R$ factor, which is motivated by suppressing contributions to the T parameter [29], as part of the "SM" EW gauge symmetry.

This naturalness problem motivates incorporating more structure in (i.e., a non-minimal) Higgs/EW sector. The idea is to suitably extend the $5D$ EW gauge symmetry beyond the SM – the additional $5D$ EW gauge fields are called coset gauge bosons – and break it down to the SM by a scalar vev localized near TeV brane [5]. It can be shown that in this process, a massless (at tree-level) scalar mode (localized near the TeV brane) with SM Higgs quantum numbers can emerge. Moreover, the quantum corrections to the Higgs mass in this case has a reduced sensitivity to the $5D$ cut-off.

In this chapter, we study the signals for coset gauge bosons in this framework at the LHC [9]. We find that the 3σ reach of the LHC for the coset gauge bosons is ~ 2.6 TeV with ~ 1000 fb^{-1} of integrated luminosity, under certain well-motivated assumptions which we discuss. However, we also argue that the (indirect) lower bound on masses of coset gauge boson masses is expected to be (at least) ~ 3 TeV [33] (for review see reference [32]). So, our results provide a strong motivation for LHC luminosity and/or energy upgrade.

An outline of this chapter is as follows. We begin with an overview of the above framework which we call (in its full generality) "warped/composite PGB Higgs" for reasons which we explain there. Then, in section 4.3 we present a discussion of this framework using the convenient "two-site" approach [34] in order to get a *general* idea of spectrum and couplings of coset gauge bosons. In section 4.4, we review specific warped extra dimensional models, namely, minimal "gauge-Higgs unification" (GHU) models, and the mechanism of radiative generation of Higgs potential. In particular, in section 4.4.4, we focus on the couplings of coset gauge

boson in the GHU framework, showing in section 4.4.4.1 that the couplings of coset gauge bosons follow a general pattern which is independent of the details of this $5D$ model, and then in section 4.4.4.2 presenting the *exact* formulae for them in the specific model within this framework by Medina et. al. [35]. In Section 4.4.5, we show our numerical results for the particle spectrum and couplings from a scan of parameter space in the model (in the process backing-up our *estimates* for the couplings of the coset gauge bosons from section 4.4.4.1), and present sample points for collider study. Section 4.5 focuses on the collider phenomenology, where we study the production and decay of coset gauge bosons, and the prospect of their discovery at LHC. We summarize in Section 4.6. Technical details of the $5D$ model are relegated to appendices.

4.2 Overview

As discussed in the introduction, we study the warped extra dimensional models where the SM Higgs arises from the breaking of an extended EW gauge symmetry down to the SM gauge symmetry near the TeV brane. A particular limit of this framework is where the scalar vev involved in this breaking of EW gauge symmetry is much larger than the AdS curvature scale such that the above breaking of $5D$ EW gauge symmetry is effectively the result of Dirichlet boundary condition on the TeV brane. The massless scalar mode can then be thought of as the extra polarization (A_z) of the coset gauge fields. Hence, this model is dubbed "gauge-Higgs unification (GHU)": see, for example, reference [36] for a review of and more references for this

idea. Quantum corrections do generate a potential (including a mass term) for it – this is the Hosotani mechanism for symmetry breaking [37]. However, such effects are saturated at the typical KK scale rather than at the warped-down $5D$ cut-off [5, 6, 38].

By the AdS/CFT correspondence [39], the general $5D$ framework mentioned above [i.e., whether vev breaking $SO(5) \to SO(4)$ is infinite as in GHU or not] is conjectured to be a dual description of ($4D$) Georgi-Kaplan (GK) models [40]. In GK models, the SM Higgs is a composite of purely $4D$ strong dynamics which is also a pseudo-Goldstone boson (PGB) of a spontaneously broken global symmetry and hence naturally lighter than the compositeness scale (dual to the typical KK scale) [5, 41]. This aspect of the $5D$ models motivates using the terminology warped/composite PGB Higgs for this *general* framework, i.e., including various $5D$ models [i.e., both the infinite scalar vev for $SO(5) \to SO(4)$ breaking, i.e. the GHU models, and the finite scalar vev] and $4D$ models based on strong dynamics.

Our goal is to study how to distinguish the possibility of such a framework from the minimal Higgs sector framework by directly producing the extra particles (i.e., those arising as a result of the extension of the $5D$ EW gauge symmetry) at the LHC[2]. Clearly, the $5D$ fermions – whose zero-modes are identified with the SM

[2]Alternatively, one can probe the extra states indirectly, for example, via their virtual effects on lower-energy observables or how the properties of the *usual* states are modified in warped/composite PGB Higgs framework relative to minimal Higgs sector framework. However, such indirect effects might not be able to provide robust distinction between the two frameworks. The reason is that the minimal Higgs sector framework has a large number of free parameters and hence, for some choice of these, can mimic effects of extra particles of warped/composite PGB Higgs framework.

fermions – must also now be in representations of the extended $5D$ EW gauge symmetry, i.e., they are larger than in the case of minimal Higgs sector, with the extra components not having zero-modes (just like the coset gauge bosons). In particular, in some $5D$ Warped/composite PGB Higgs models, some of these fermionic KK states (associated with top/bottom quarks) are lighter than SM gauge KK modes [7] (and hence, as discussed below, lighter than the coset gauge boson), whereas KK fermions have same mass as gauge KK modes in minimal Higgs sector framework. Hence these fermionic KK modes might be easier to detect at the LHC [8] than the SM (or coset) gauge KK modes and their discovery would be suggestive of warped/composite PGB Higgs models rather than the models with minimal Higgs sector. However, in the models constructed so far, most of these light fermionic states have the same quantum numbers under SM EW symmetry as those of SM fermions[3] so that they could be mistaken for similar states in *other* extensions of the SM[4] . Thus, it is crucial to consider *additional* signals for the warped/composite PGB Higgs framework.

Such a test can be provided by detection of

- the coset gauge bosons which, being doublets of $SU(2)_L$, have novel (i.e., non-adjoint) representations under the SM EW gauge symmetry

[3]The exception is a 5/3-charged light KK fermion, but its existence might have more to do with the need for Zbb protection rather than PGB Higgs.

[4]KK fermionic states in the minimal Higgs sector framework also have the same quantum numbers, although these states are expected to be as heavy as SM gauge KK modes. So, there is less possibility of confusion between minimal Higgs sector models and warped/composite PGB Higgs framework based on these states.

(such quantum numbers for gauge bosons are obviously absent in the minimal Higgs sector framework). Thus these coset gauge bosons can result in distinctive LHC signals as compared to EW gauge KK modes in minimal Higgs sector models. Similarly, we discuss how coset gauge bosons can also be differentiated from new gauge bosons in *other* extensions of the SM. This feature of coset gauge bosons motivates our study of signals from their direct production at the LHC.[5]

Our study suggests that

- the LHC 3 σ reach for (charged) coset gauge bosons masses is $\sim 2(2.6)$ TeV with $\sim 100(1000)$ fb^{-1} luminosity, using their associated production with (light) KK top and decay into KK top and bottom quarks.

For this analysis, we use values of couplings which are motivated by the ($5D$) *minimal* (i.e., with no brane-localized kinetic terms for bulk fields and with AdS$_5$ metric: see later) GHU model. A note on the allowed mass scale is in order here. In the minimal GHU model, it turns out that the coset gauge boson mass is $\approx 5/3$ larger than SM gauge KK modes [6]. And, the lower bound on the latter gauge boson masses is ~ 3 TeV from EW precision tests [33] (for a review see reference [32]), assuming custodial symmetries are implemented [29, 43] (and, depending on details of flavor structure, the bound can be somewhat stronger from flavor violation [28, 44, 45][6] although these constraints can be ameliorated by addition of $5D$ fla-

[5]Very recently, in reference [42], a different signal (than what we study) for coset gauge bosons was suggested based (again) on the distinctive quantum numbers, but it was not studied in the context of a complete framework, for example, one that explains the flavor hierarchy.

[6]See references [46] and [47] for "latest" constraints from lepton and quark flavor violation,

vor symmetries [48]). Thus, the coset gauge boson mass is constrained to be at least 5 TeV which is well beyond reach of even 1000 fb^{-1} luminosity at the LHC.[7] This situation then motivates upgrade of the energy of the LHC or building another higher-energy collider.

However, in *non*-minimal $5D$ models – for example, with brane-localized kinetic terms for bulk fields [49] or with the metric near the TeV brane being modified from pure AdS [50] *within* the GHU models or with the scalar vev giving masses to coset gauge bosons being finite (instead of infinite as in GHU models), the indirect bound on coset mass scale might be relaxed because the ratio of coset to SM gauge KK masses is closer to 1. In fact, inspired by deconstruction/latticization and the AdS/CFT correspondence, a purely $4D$, two-site approach [34] – keeping only SM and 1st KK excitations – has been proposed in order to efficiently/economically capture the phenomenology of similar variations of $5D$ models with a *minimal* Higgs sector. Such a two-site approach can be extended to PGB Higgs models as well [51].

Using a two-site approach for the general warped/composite PGB Higgs, we argue that

- coset gauge bosons are expected to be at most be as light as (i.e., cannot be

respectively, i.e.,including variations of the minimal framework.

[7]The bound on mass scale of coset gauge bosons from precision tests involving exchange of coset gauge bosons themselves is rather weak since there is no coupling of single coset gauge boson to purely SM particles at leading order (simply due to quantum numbers) so that coset gauge boson exchange at *tree*-level does not contribute to purely SM operators (and hence precision tests). The flip side of this feature is that resonant production of coset gauge bosons is suppressed, which is in part responsible for the poor LHC reach.

lighter than) SM gauge KK (or composite) modes.

Moreover, using the same approach, it can be shown that the bound on SM gauge KK (or composite) modes is unlikely to be reduced below ~ 3 TeV even in the non-minimal models, i.e., in the general framework[8]. Thus, coset gauge bosons are expected to have mass $\gtrsim 3$ TeV in general. We argue based on the two-site approach that couplings of coset gauge bosons in the general framework will still be similar to those in minimal $5D$ GHU models which we used for the study of LHC signals. This feature implies that the LHC reach for coset gauge bosons that we find based on couplings in minimal $5D$ GHU model is expected to apply in general to the framework of warped/composite PGB Higgs. Thus, even optimistically, i.e., assuming that in some models within this framework the coset gauge bosons can be as light as SM gauge KK modes *and* using the 1000 fb^{-1} luminosity, we see that the LHC can barely be sensitive to the lower (indirect) limit of ~ 3 TeV on coset gauge boson masses.

4.3 Model-independent Analysis Using Two-site Approach

In this section, we provide a *rough* description of masses and couplings of the coset gauge bosons of the *general* warped/composite PGB Higgs framework, i.e., the analysis presented here is applicable to both $5D$ and $4D$ models in this framework. The detailed description of a *specific* (5D) model, namely minimal GHU, will be

[8]It has been claimed that in soft-wall models, this bound can be lower than 3 TeV. However, such models have not been developed fully as yet.

given in the next section.

Here we use the two-site model [34] which is a convenient parametrization for this framework. It can be shown that this effective 4D description is the deconstructed version of warped extra dimension models with SM fields propagating in the bulk, including the zero and only the 1st KK modes. In the original setup presented in reference [34], Higgs was *not* a PGB. So first we will briefly review this model (for more details, the reader is referred to this paper), and then we will show what changes we have to make to account for the PGB origin of the Higgs.

The original two-site model consists of two sectors: "elementary" and "composite" (this nomenclature is inspired by the AdS/CFT correspondence). The elementary sector is a copy of all SM states except for the Higgs field. The composite sector consists of massive gauge bosons, massive vector-like fermions and the Higgs field. The composite sector states live in complete representation of the *global* symmetry $SU(3)_c \times SU(2)_L \times SU(2)_R \times U(1)_X$, where the additional custodial $SU(2)_R$ is introduced to suppress new physics contribution for T parameter. The massive gauge bosons live in adjoint representation while part of massive fermions live in the same representation as that of SM fermion.

These two sectors mix with each other, leading to massless fermion and gauge boson eigenstates which correspond to SM fermions ($\psi_{L,R}$) and gauge bosons (A_μ) before Electro-Weak Symmetry Breaking (EWSB). The heavy eigenstates are denoted by ρ_μ for gauge bosons and $\chi_{L,R}$ for fermions.[9] The SM states (except for the

[9]The SM states and heavy eigenstates further mix with each other after EWSB, but this effect is not relevant here.

Higgs) are mixtures of elementary and composite states:

$$|\text{SM}\rangle = \cos\theta \ |\text{elementary}\rangle + \sin\theta \ |\text{composite}\rangle \ , \tag{4.1}$$

where all SM states (except for the top) are mostly made of the elementary sector ones (i.e., $\sin\theta \ll 1$), while the heavy states are mostly the composite sector ones and finally the SM Higgs is fully a composite sector state. The composite sector states are assumed to have strong couplings to each other, in order to match the 5D description (or equivalently, inspired by AdS/CFT correspondence). We use g_* and Y_* to denote the composite gauge and Yukawa couplings (and will take them to be roughly of order a few). In the flavor anarchy models, Y_* for different flavors are of the same order and have no structure, which we assume for the following discussion. Clearly the SM states couple to heavy states through the mixing (Eq. (4.1)). For example the Yukawa couplings between SM fermions and Higgs is given schematically by

$$Y_{SM} \sim \sin\theta_{\psi_L} Y_* \sin\theta_{\psi_R} \ . \tag{4.2}$$

The fermionic mixing angles $\theta_{\psi_{L,R}}$ are assumed to be hierarchical, which explains the SM fermion mass hierarchy. In warped extra dimension picture, $\sin\theta_\psi$ is related to the fermion zero mode wavefunction evaluated at the TeV brane (see $f(c)$ in Eq. (3.14), with an exponential dependence on 5D mass parameter, c), thus the hierarchical mixing angles $\sin\theta_\psi$ can be naturally generated in the warped extra dimension picture. The mixing angles for gauge bosons are given by $\sin\theta_G = \frac{g_{el}}{g_*}$, where g_{el} is the elementary gauge coupling, while the SM gauge coupling is given by $g_{SM} = g_{el} g_* / \sqrt{g_{el}^2 + g_*^2}$. We will choose $g_* \sim$ a few such that $g_* \gg g_{SM}$ and thus g_{el} can be approximated by the SM gauge couplings. Specifically, in order

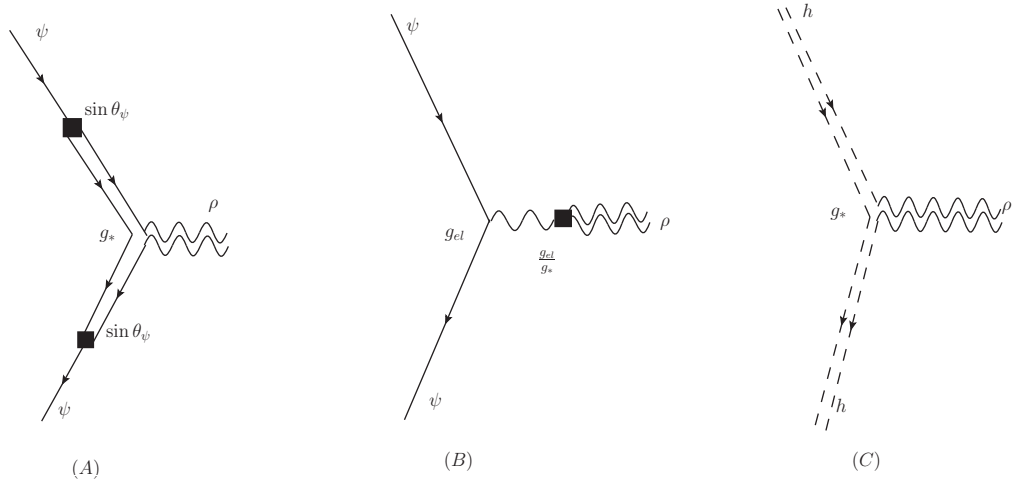

Figure 4.1: Couplings of heavy gauge bosons with SM states. Fig. (A),(B) give the couplings between heavy gauge bosons and SM fermions coming from fermionic and gauge boson mixings, respectively. Fig. (C) gives the coupling between heavy gauge bosons and Higgs field, which after EWSB give rise to the coupling to physical Higgs and longitudinal W/Z.

to match 5D theories $\sin\theta_G$ should be $\sim 1/\sqrt{\text{logarithm of UV-IR hierarchy}}$, i.e., $\sim 1/6$ for the case of Planck-weak hierarchy. Here we review the couplings of heavy gauge bosons ρ_μ to SM states, which we use to compare with the couplings of coset gauge bosons later. The SM fermion coupling to heavy gauge bosons are generated both through fermionic and gauge boson mixings. This is illustrated using insertion approximation in Fig. 4.1 (A)(B) . This gives the coupling

$$g_{\rho\psi\psi} \approx \sin\theta_\psi g_* \sin\theta_\psi + \frac{g_{el}^2}{g_*} \ . \tag{4.3}$$

Note that there is a flavor dependent contribution (first term in the above equation) that comes from elementary composite mixing of fermions, which is suppressed by the fermionic mixing angles $\sin\theta_{\psi_{L,R}}$, and there is a flavor universal contribution

(second term in the above equation) that comes from elementary/composite mixing of gauge bosons, which is suppressed by $\frac{g_{el}}{g_*}$ relative to SM gauge couplings. For light fermions, the flavor universal term dominates. Moreover, this coupling is only mildly (i.e., $\sim 1/6$) suppressed relative to the SM one. The heavy gauge bosons couple strongly to Higgs field since they are both mostly composite states (See Fig. 4.1(C)):

$$g_{\rho hh} \approx g_* \ . \tag{4.4}$$

Using Goldstone boson equivalence theorem, we can see that after EWSB, the heavy gauge bosons acquire strong coupling $\approx g_*$ with physical Higgs boson and *longitudinal* component of W/Z.

We now turn to the two-site description of warped/composite *PGB* Higgs. First let us ignore $SU(3)_c \times U(1)_X$ part of the composite sector global symmetry because it is irrelevant for the Higgs part of the model. We want composite sector of the model to have a global symmetry H which includes $SU(2)_L \times SU(2)_R$ [latter group is isomorphic to SO(4)]. At the same time, Higgs should be a PGB. One can see that in order to achieve this setup, the composite sector should have larger global symmetry G, which later should be spontaneously broken down to its subgroup H, and Higgs is PGB of this symmetry breaking pattern $G \to H$ in the composite sector. The simplest example which we will study here corresponds to the $G = SO(5)$ and $H = SO(4)$, i.e., the *full* global symmetry of the composite sector is extended from $SU(3)_c \times SU(2)_L \times SU(2)_R \times U(1)_X$ of the original model to $SU(3)_c \times SO(5) \times U(1)_X$. One can see that due to the larger symmetry G of the composite sector there will be

additional heavy gauge bosons which belong to the group G/H (i.e., the coset), and they correspond to the coset gauge bosons of the general warped/composite PGB Higgs framework.

We can learn some important properties of the coset gauge bosons based on this simple setup. First, we argue that coset gauge bosons are generally heavier than the usual composite gauge bosons (i.e. the gauge bosons of the gauge group H). The argument is the following. Before the symmetry breaking $G \to H$, the gauge bosons of H (ρ^μ) and G/H (ρ_c^μ) of the composite sector should have the same mass (due to the global symmetry, G). After the symmetry breaking, the masses of the gauge bosons of H remain the same, while the coset gauge bosons in G/H get extra mass contribution coming from the breaking. For example, for the case that we consider, i.e., with $G = SO(5)$ and $H = SO(4)$, the breaking $G \to H$ can be achieved by the vev of a scalar ϕ transforming in fundamental representation of $SO(5)$. We can parameterize ϕ by

$$\phi = e^{-iT_c^a h^a} \begin{pmatrix} 0 \\ 0 \\ 0 \\ 0 \\ f_\phi + \eta \end{pmatrix} , \tag{4.5}$$

where f_ϕ is the magnitude of ϕ vev, T_c^a are the generators of G/H, h^a are the pseudo-Goldstone bosons which are also the Higgs, η is a massive scalar excitation. The covariant derivative of ϕ gives rise to extra contribution to the masses of coset

gauge bosons

$$(D_\mu \phi)^\dagger (D^\mu \phi) \supset g_*^2 f_\phi^2 \rho_{c,\mu} \rho_c^\mu \ . \tag{4.6}$$

This extra contribution is always positive, thus ρ_c^μ are generally heavier than ρ^μ[10]. We conclude that

- there is an indirect bound of $\gtrsim 3$ TeV for the coset gauge boson masses, which comes from the bound (from precision tests) of ~ 3 TeV on the ordinary composite gauge bosons (as mentioned earlier).

On the other hand, since it is the coset gauge bosons that cancel the quadratic divergence in Higgs mass from W/Z loops, it is clear that naturalness favors the coset gauge bosons to not be heavier than several TeV. We can also study the structure of coset gauge boson *couplings* based on the two-site language. Note that the discussion here is independent of the scale f_ϕ (see Eq. (4.6)) that controls the masses of coset gauge bosons (relative to the other gauge bosons)[11]. We will see that the quantum numbers of coset gauge bosons give important restrictions on their couplings. First, we study their couplings with two SM gauge bosons. For this purpose, we consider the SM gauge bosons before EWSB: W_μ^a transform in adjoint representation of $SU(2)_L$ and B_μ transform as a singlet. The SM quantum numbers of coset gauge bosons are the same as that of Higgs, i.e., they are $SU(2)_L$ doublet. Just based on quantum numbers, we can see that

[10] assuming only the minimal couplings of ϕ to coset gauge bosons as above.

[11] f_ϕ is also (roughly) related to the size of the scalar vev breaking $SO(5) \to SO(4)$ in the 5D model.

- there is no coupling between one coset gauge boson and two SM gauge bosons or two Higgs bosons at lowest order (i.e., without EWSB),

which is independent of the elementary/composite nature of SM/coset gauge bosons. This is to be contrasted with Eq. (4.4) and Fig. 4.1(C), where we see that the usual heavy gauge bosons have large couplings to Higgs bosons and longitudinal W/Z.

We turn to the couplings between coset gauge bosons and SM fermions. We denote the SM fermions by q_L ($SU(2)_L$ doublet) and u_R ($SU(2)_L$ singlet) respectively, where L, R subscripts stand for the 4D chirality.[12] Based on quantum numbers, we cannot write down dimension 4 coupling between SM fermions and coset gauge bosons. The only allowed dimension 4 couplings are

$$g_{qU}\bar{q}_L\gamma_\mu\rho_c^\mu U_L + g_{uQ}\bar{u}_R\gamma_\mu\rho_c^\mu Q_R + h.c.\ , \tag{4.7}$$

where Q_R, U_L are heavy (purely composite) fermionic states transforming under $SU(2)_L$ as doublet and singlet, respectively, i.e., opposite chirality to the SM fermions. Recall that the composite sector fermions are in vector-like and complete representations of $SO(5)$ (in particular, the SM gauge group), while the elementary sector fermions are only in complete, chiral representation of SM gauge group.

There could be higher dimensional operators that couple coset gauge bosons

[12] Couplings of coset gauge bosons to right-handed down-type quarks and leptons can be similarly studied, but these states are not relevant here since the associated elementary-composite mixings (even for bottom quark and τ, i.e., the heaviest fermions) are small and, as we will discuss later, these sectors also do not result in light KK states.

with just SM fermions. These couplings can be schematically written as:

$$\frac{\tilde{g}_q}{\Lambda}\bar{q}_L\gamma_\mu\rho_c^\mu h q_L + \frac{\tilde{g}_u}{\Lambda}\bar{u}_R\gamma_\mu\rho_c^\mu h u_R \ , \tag{4.8}$$

where Λ is some mass scale which depends on the specific model. There could also be magnetic dipole moment type operators involving just SM fermions and coset gauge bosons:

$$\frac{g_{\rm dipole}}{\Lambda}\bar{q}_L\sigma^{\mu\nu}D_{[\mu}\rho^c_{\nu]}u_R + \text{h.c.}, \tag{4.9}$$

where D_μ is the covariant derivative operator with respect to $SU(2)_L \times U(1)_Y$.

So far we have been analyzing the couplings of the coset gauge bosons based only on their quantum numbers without implementing any specific property of the model. Let us now first estimate the size of the couplings $g_{qU,uQ}$ in Eq. (4.7) based on our two-site description of the general warped/composite PGB Higgs framework, i.e., utilizing the elementary or composite sector nature of the various particles. Since the SM fermions are mostly elementary, the above couplings must arise due to elementary/composite fermionic mixing. In the insertion approximation the couplings in Eq. (4.7) will be generated (dominantly) from the diagram shown in Fig.4.2(A) and thus can be estimated to be:

$$g_{qU} \sim g_* \sin\theta_{q_L}, \quad g_{uQ} \sim g_* \sin\theta_{u_R}, \tag{4.10}$$

For the third generation quarks (especially top quark), it is possible that $\sin\theta_{t_{L,R}}, \sin\theta_{b_L} \sim O(1)$. Therefore,

- coset gauge boson should couple strongly with $t_{L,R}, b_L$ and composite fermions.

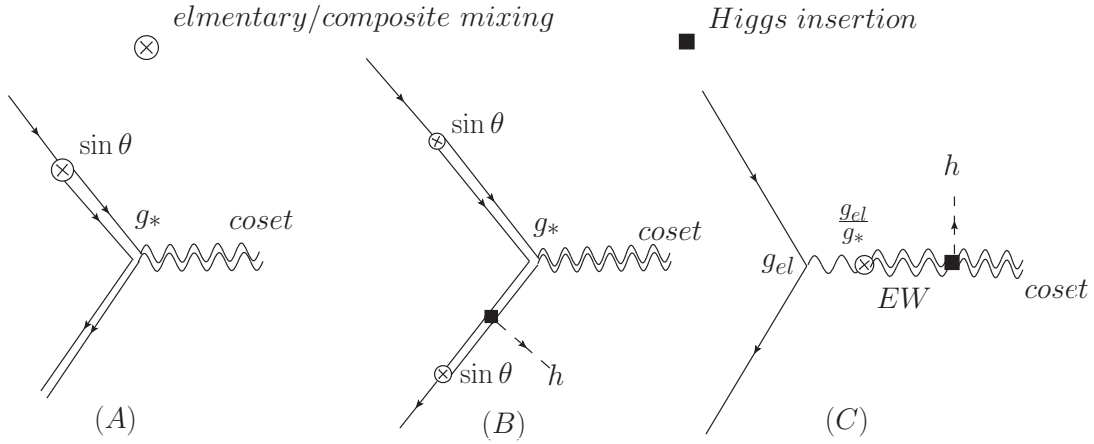

Figure 4.2: Couplings between coset gauge bosons and fermions using insertion approximation. Fig. (A) shows the couplings between coset gauge boson, SM fermion and composite fermion. Estimates of these couplings are given in Eq. (4.10). Fig. (B) shows the couplings between coset gauge boson and two SM fermions coming from elementary/composite mixing of fermions. A Higgs insertion is needed since otherwise the composite fermion cannot mix with elementary fermion due to quantum numbers, namely, this composite fermion has opposite-to-SM chirality. Estimates of these couplings are given in Eq. (4.11). Fig. (C) shows the couplings between coset gauge boson and two SM fermions coming from the mixing of elementary and composite gauge bosons of the SM-type (denoted by "EW") followed by their mixing with coset gauge bosons induced by the Higgs vev. Estimates of these couplings are given in Eq. (4.12).

Turning now to the couplings in Eq. (4.8), they can be generated via elementary-composite fermion mixing, as shown in Fig.4.2(B) in insertion approximation. Thus the mass scale Λ of Eq. (4.8) in the two-site description of PGB Higgs becomes equal to the mass of composite sector fermions (denoted by M_*) and the order of the coupling factor $\tilde{g}$ can be estimated to be $g_* \sin\theta_\psi^2$. Once Higgs gets vev, the couplings between coset gauge bosons and SM fermions can then be generated:

$$g_{qq}^{f.d.} \sim \frac{v}{M_*} g_*^2 (\sin\theta_{q_L})^2, \quad g_{uu}^{f.d.} \sim \frac{v}{M_*} g_*^2 (\sin\theta_{u_R})^2, \tag{4.11}$$

where "f.d." denotes flavor-dependent couplings.

Another contribution to these couplings comes from elementary-composite *SM*-type gauge boson mixing – recall that there is no elementary coset gauge boson, followed by composite SM-coset mixing via Higgs vev, as shown in Fig. 4.2(C) with

$$g_{qq,\,uu}^{f.i.} \sim \frac{g_{el}^2}{g_*} \frac{g_* v}{M_*} \tag{4.12}$$

Clearly, these couplings are flavor-independent (hence denoted by "f.i.") and dominate the ones in Eq. (4.11) for light SM fermions, whereas those in Eq. (4.11) dominate for third generation quarks. The magnetic dipole moment type operator (Eq. (4.9)) is recently discussed in [42]. In our framework, this operator is only generated through loop processes, and it is further suppressed by the fermion mixing angle $(\sin\theta_\psi)^2$. Therefore, it is not phenomenologically important here, even for top/bottom quarks.

We can now study the phenomenological implications of these couplings of coset gauge bosons. As studied in [4], the dominant *production* channel for the "usual" (i.e., transforming as adjoint of SM gauge group) heavy gauge bosons is

through the (flavor-universal) coupling between light quarks and heavy gauge bosons (see second term of Eq. (4.3) and Fig. 4.1(B)). However, as argued above, the coupling of coset gauge bosons to two light quarks is suppressed by $\sim g_* v/M_*$ compared to similar couplings of usual heavy gauge bosons. Since for realistic models one usually finds $g_* v/M_* \lesssim 0.4$, the resonant production of coset gauge bosons via light quarks is expected to be suppressed by at least an order of magnitude compared to that of usual heavy gauge bosons (for the same mass).

On the other hand, the dominant discovery channel for usual heavy gauge boson is via *decay* into two Higgs or two (longitudinal) W/Z gauge bosons or into two third generation quarks due to the composite sector nature of all these particles. However, the main decay channels for coset gauge bosons are into one third generation SM quark and one *heavy* quark based on above analysis; of course, for this decay to be kinematically allowed, the heavy quark must be lighter than coset gauge bosons – we find that such a scenario does indeed occur in part of the parameter space[13]. Again, even if $\sin\theta_{t_{L,R},b_L} \sim O(1)$, the decay into two third generation SM quarks is suppressed compared to the decay into one third generation quark and one heavy quark due to suppression of the former coupling by $\sim g_* v/M_*$ relative to the latter. And, couplings of coset gauge bosons to light quarks are even smaller.

We can see that the phenomenology of coset gauge bosons is very distinct from that of usual heavy gauge bosons so that the two types of gauge bosons can

[13]The coupling of coset gauge bosons to *two* heavy (mostly composite) fermions is also large, but we find that (typically) such a decay is not kinematically possible and hence this coupling is not relevant for our analysis.

be distinguished based on their signals at the LHC. Note that the conclusion here is general in the sense that it is the result of the quantum numbers of coset gauge bosons and their (purely) composite sector nature. This renders our collider study to be robust and not dependent on specific models.

4.3.1 "Pollution" from the usual heavy gauge bosons in the signal from the resonant production of coset gauge bosons

Finally, we would like to emphasize that a study of channels other than resonant production (via light quarks) for coset gauge bosons is motivated for the following reasons. The point is that for resonant production of coset gauge bosons, even though the coset gauge bosons have distinctive decays (as discussed above), it turns out in the end that there is a larger contribution from resonant production of the usual heavy gauge bosons (i.e., composite sector W/Z's) to the same final states. Given that coset gauge boson is a doublet of $SU(2)_L$, it is clear that the dominant fermionic decay (i.e., not requiring EWSB) of coset gauge bosons is to a doublet and singlet (whether SM or heavy) – we will focus here on final state with SM top/bottom and composite (heavy, i.e., non-SM) fermion. Whereas, the usual heavy gauge bosons are triplets/singlets and so cannot decay without EWSB into this final fermionic state, but instead decay into two doublets or two singlets. However, after EWSB, the usual heavy gauge bosons can decay into the same final state as the coset gauge boson. One possibility is EWSB mixing on *gauge boson* line, i.e., the usual heavy gauge bosons do have an admixture of coset gauge bosons

[again, resulting from the Higgs vev as shown in Fig. 4.2(C)]. Hence, via this coset gauge boson component, the usual heavy gauge bosons will decay into the same final state as that of the coset. Of course, this effect does not really constitute a "pollution" since it does require presence of the coset gauge boson, i.e., in this case, the top/bottom and composite fermion final state can still be taken as "evidence" for coset gauge boson.

However, another possibility is EWSB mixing on *fermion* line: the composite sector W/Z's decay into two doublets or two singlet fermions, followed by doublet mixing with a singlet (or vice versa) via EWSB, i.e., the fermionic mass eigenstates are also admixtures of doublet and singlet. The crucial point is that this decay of usual heavy gauge boson to the same final state as that of coset gauge boson can occur even in the *absence* of the coset gauge boson and hence is a genuine pollution. Of course, such decays of usual heavy gauge bosons will be suppressed by this EWSB mixing, i.e., factors of $g_* v/M_*$ (or $Y_* v/M_*$), compared to other final states such as WW/WZ and $t\bar{t}/t\bar{b}$ to which the usual heavy gauge bosons couple strongly. However, it is clear that the above suppression in the decay of usual heavy gauge bosons to the same final state as for coset gauge boson simply serves to compensate (in the total amplitude) the larger coupling (as mentioned above) of the usual heavy gauge bosons to the initial state light quarks. Moreover, given that the coset gauge bosons are heavier than usual gauge bosons (they cannot be lighter as suggested by the two-site description), the PDF's will then result in the contribution to the top/bottom and composite fermion final state from the production/decay of usual heavy gauge bosons actually *dominating* that from coset gauge bosons.

Thus, in this case, the pollution from usual heavy gauge bosons might make it difficult to extract a signal for the coset gauge bosons from their resonant production via light quark annihilation. Of course, we could undertake the difficult task of reconstruction of the invariant mass of the final state of top/bottom and composite fermion in order to separate the two contributions (again, coset gauge bosons are generically heavier than the usual heavy gauge bosons). Thus, a very careful study (i.e., including production of usual heavy gauge bosons), would be required to ascertain whether resonant production via light quarks is actually a useful channel. Therefore, in section 4.5, we will pursue another channel (namely associated production of W_C) which has comparable cross-section to resonant production via light quarks and furthermore has no significant pollution from production of the usual heavy gauge bosons.

4.4 Gauge-Higgs Unification in Warped Extra Dimension

4.4.1 Gauge Bosons and Higgs Fields

Having discussed general two-site description of the general warped/composite PGB Higgs framework, we now turn to a specific 5D model. In this section, we review models of (minimal) GHU in a warped extra dimension: for more details, see reference [35]. The spacetime metric is given by Eq. (3.1). The Standard Model (SM) gauge group $SU(3)_C \times SU(2)_L \times U(1)_Y$ is a subgroup of the bulk gauge symmetry. To be specific, we take the bulk gauge symmetry to be $SU(3)_C \times SO(5) \times U(1)_X$ in the following analysis (the group algebra of $SO(5)$ can be found

in Appendix B). We will drop the color group $SU(3)_C$ in the following analysis since it does not affect our result. The gauge boson action is given by

$$S_g = \int d^5x\sqrt{-G}\left[-\frac{1}{2g_5^2}\mathrm{Tr}(F^{(A)MN}F^{(A)}_{MN}) - \frac{1}{4g_X^2}F^{(X)MN}F^{(X)}_{MN}\right], \tag{4.13}$$

with

$$A_M = \sum_{a=1}^{3} A_M^{a_L}T_L^a + \sum_{a=1}^{3} A_M^{a_R}T_R^a + \sum_{\hat{a}=1}^{3} A_M^{\hat{a}}T^{\hat{a}} + A_M^{\hat{4}}T^{\hat{4}}, \tag{4.14}$$

where $T^a_{L,R}$ are the generators of $SU(2)_L \times SU(2)_R \cong SO(4) \subset SO(5)$, and $T^{\hat{a},\hat{4}}$ are the generators of the coset $SO(5)/SO(4)$. X_M is the gauge boson of $U(1)_X$. The boundary conditions are chosen such that only the subgroup $SU(2)_L \times U(1)_Y$ is unbroken at UV brane ($z = R$) and $SU(2)_L \times SU(2)_R \times U(1)_X \cong SO(4) \times U(1)_X$ is unbroken at IR brane ($z = R'$), where the hypercharge Y is defined as $\frac{Y}{2} = T_R^3 + Q_X$. Specifically, we choose the $A_\mu\,(\mu = 0, 1, 2, 3)$ components of $SU(2)_L \times U(1)_Y$ and $SO(4) \times U(1)_Y$ to have Neumann boundary condition ("+") on the UV brane and IR brane respectively, and all the other $A_\mu\,(\mu = 0, 1, 2, 3)$ have Dirichlet boundary condition ("−") on both branes. To reproduce hypercharge in Standard Model, we do the following rotation of fields [35]

$$\begin{pmatrix} A_M'^{3_R} \\ B_M^Y \end{pmatrix} = \begin{pmatrix} c_\phi & -s_\phi \\ s_\phi & c_\phi \end{pmatrix} \begin{pmatrix} A_M^{3_R} \\ X_M \end{pmatrix}, \tag{4.15}$$

$$c_\phi = \frac{g_5}{\sqrt{g_5^2 + g_X^2}}, \qquad s_\phi = \frac{g_X}{\sqrt{g_5^2 + g_X^2}}, \tag{4.16}$$

where we need $s_\phi^2 \approx \tan^2\theta_W \approx 0.30$ to get the correct Weinberg angle. Based on this definition, we set B_μ^Y to have "+" boundary condition on both branes, and A'^{3_R} to have "−" boundary condition on UV brane and "+"boundary condition on IR brane. With this set of assignment of boundary conditions, we can reproduce

SM gauge group at low energy, while at the same time preserve $SU(2)_L \times SU(2)_R$ custodial symmetry [29].

An important observation here is that for gauge fields A_M, its A_μ and A_z components should have opposite boundary conditions on the branes. This means that $A_z^{\hat{a},\hat{4}}$ have "+" boundary conditions on both branes, thus there are zero modes associated with them. We identify these zero modes of $A_z^{\hat{a},\hat{4}}$ as the Higgs fields $H^{a,4}$. They transform as a doublet under $SU(2)_L$, thus have the same gauge quantum numbers of SM Higgs. Due to 5D gauge invariance, these Higgs fields are massless at tree level, and their potential is generated by the breaking of $SO(5)$ on UV and IR branes. Therefore, the Higgs potential will be generated through loop effects. Since from 5D point of view, this is a non-local effect, the generated Higgs potential will be finite. We will discuss the mechanism of radiative generation of Higgs potential later in this section.

4.4.2 Fermions

The fermions also propagate in the bulk, with the following action

$$S_f = \int d^5x\sqrt{-G}\sum_i \bar{\Psi}_i(i\Gamma^M D_M - c_i k)\Psi_i, \tag{4.17}$$

where $D_M = \partial_M - iA_M - iX_M$ and c_i are the bulk masses of the 5D fermions in units of k, which control the localization of fermion zero modes. To be specific, the zero modes for left-handed (right-handed) fermions are localized near UV brane if $c > 1/2$ ($c < -1/2$), and they are localized near IR brane if $c < 1/2$ ($c > -1/2$).

For convenience, we recite here the definition of $f(c)$ from Eq. (3.14)

$$f(c) = \sqrt{\frac{1/2 - c}{1 - e^{-(1-2c)kL}}} \ , \tag{4.18}$$

which is the size of zero mode fermion wavefunction at IR brane in units of $\sqrt{2k}$. There are various scenarios to embed SM fermions into representations of $SO(5)$[6, 35, 45]. For the following discussion, we just consider the third generation fermions, since the first two generation fermions are not important for EWSB and collider phenomenology. For concreteness, we follow [35] and choose the fermion representation to be $5 \oplus 5 \oplus 10$ for one generation. The generators of $SO(5)$ for **5** representation can be found in Appendix B. The fermions in **5** of $SO(5)$ have the following charge assignment under $SU(2)_L \times SU(2)_R$:

$$\mathbf{5} = \frac{1}{\sqrt{2}} \begin{pmatrix} iq_{++} + iq_{--} \\ q_{--} - q_{++} \\ iq_{-+} - iq_{+-} \\ q_{-+} + q_{+-} \\ \sqrt{2} q^c \end{pmatrix} , \tag{4.19}$$

where $\pm$ means $\pm 1/2$ under $SU(2)_L$ and $SU(2)_R$ respectively, and q^c means singlet. A more convenient basis is

$$\xi_5 = \begin{pmatrix} q_{++} \\ q_{-+} \\ q_{+-} \\ q_{--} \\ q^c \end{pmatrix} \equiv \begin{pmatrix} \chi \\ \tilde{t} \\ t \\ b \\ \hat{t} \end{pmatrix} , \tag{4.20}$$

where χ, t, b denote fermions with charge $+5/3, +2/3, -1/3$ respectively. The transformation between the two basis is

$$\xi_5 = A \times \mathbf{5} \quad \text{with} \quad A = \frac{1}{\sqrt{2}} \begin{pmatrix} -i & -1 & 0 & 0 & 0 \\ 0 & 0 & -i & 1 & 0 \\ 0 & 0 & i & 1 & 0 \\ -i & 1 & 0 & 0 & 0 \\ 0 & 0 & 0 & 0 & \sqrt{2} \end{pmatrix}. \tag{4.21}$$

The fermions are embedded in **10** of $SO(5)$ as follows

$$\mathbf{10} = \begin{pmatrix} \chi & \tilde{t} & t & b & \Xi' & T' & B' & \Xi & T & B \end{pmatrix}^T, \tag{4.22}$$

where $\begin{pmatrix} \chi & t \\ \tilde{t} & b \end{pmatrix}$ form an $SU(2)_L \times SU(2)_R$ bidoublet, (Ξ, T, B) form $SU(2)_R$ triplet, and (Ξ', T', B') form $SU(2)_L$ triplet. We can also write down the **10** representation in the form of 5×5 matrix

$$\xi_{10} = \frac{1}{2} \begin{pmatrix} 0 & T'+T & i\frac{B'-\Xi'}{\sqrt{2}}+i\frac{B-\Xi}{\sqrt{2}} & \frac{B'+\Xi'}{\sqrt{2}}-\frac{B+\Xi}{\sqrt{2}} & b+\chi \\ -T'-T & 0 & \frac{B'+\Xi'}{\sqrt{2}}+\frac{B+\Xi}{\sqrt{2}} & -i\frac{B'-\Xi'}{\sqrt{2}}+i\frac{B-\Xi}{\sqrt{2}} & i(b-\chi) \\ -i\frac{B'-\Xi'}{\sqrt{2}}-i\frac{B-\Xi}{\sqrt{2}} & -\frac{B'+\Xi'}{\sqrt{2}}-\frac{B+\Xi}{\sqrt{2}} & 0 & T'-T & t+\tilde{t} \\ -\frac{B'+\Xi'}{\sqrt{2}}+\frac{B+\Xi}{\sqrt{2}} & i\frac{B'-\Xi'}{\sqrt{2}}-i\frac{B-\Xi}{\sqrt{2}} & -T'+T & 0 & -i(t-\tilde{t}) \\ -b-\chi & -i(b-\chi) & -t-\tilde{t} & i(t-\tilde{t}) & 0 \end{pmatrix}. \tag{4.23}$$

The fermion content and the boundary condition assignment can be summarized as follows

$$\Psi_{1L} = \begin{pmatrix} \chi_{1L}(-,+) \\ \tilde{t}_{1L}(-,+) \\ t_{1L}(+,+) \\ b_{1L}(+,+) \\ \hat{t}_{1L}(-,+) \end{pmatrix}, \Psi_{2R} = \begin{pmatrix} \chi_{2R}(-,+) \\ \tilde{t}_{2R}(-,+) \\ t_{2R}(-,+) \\ b_{2R}(-,+) \\ \hat{t}_{2R}(+,+) \end{pmatrix}, \Psi_{3R} = \begin{pmatrix} \chi_{3R}(-,+) \\ \tilde{t}_{3R}(-,+) \\ t_{3R}(-,+) \\ b_{3R}(-,+) \\ \Xi'_{3R}(-,+) \\ T'_{3R}(-,+) \\ B'_{3R}(-,+) \\ \Xi_{3R}(-,+) \\ T_{3R}(-,+) \\ B_{3R}(+,+) \end{pmatrix}, \quad (4.24)$$

while the opposite chirality fields have the opposite boundary conditions. From this set of boundary conditions, we can see that there are fermion zero modes for one $SU(2)_L$ doublet and two $SU(2)_L$ singlets, which reproduce the SM fermion gauge representations at low energy. To get SM fermion masses, we need the following boundary mass terms

$$\begin{aligned} S_b &= \int d^5x\sqrt{-G}\; 2(kz)\delta(z-R')\Big[M_{B_1}\bar{\hat{t}}_{1L}\hat{t}_{2R} \\ &+ M_{B_2}(\bar{\chi}_{1L},\bar{\tilde{t}}_{1L},\bar{t}_{1L},\bar{b}_{1L})\begin{pmatrix}\chi_{3R}\\ \tilde{t}_{3R}\\ t_{3R}\\ b_{3R}\end{pmatrix} + \text{h.c.}\Big]. \end{aligned} \quad (4.25)$$

We have to choose the parameters $c_1, c_2, c_3, M_{B_1}, M_{B_2}$ to reproduce the top and bottom masses.

4.4.3 Higgs Potential and KK Decomposition

We have identified Higgs fields as the 5th components of the gauge fields of coset $SO(5)/SO(4)$. Here, we briefly review the KK decomposition of bulk fields with a background Higgs fields and how the potential of Higgs is radiatively generated . For more details, see [35].

We denote A_μ^a as the gauge bosons of $SU(2)_L \times SU(2)_R$ and $A_\mu^{\hat{a}}$ ($\hat{a} = 1...4$) as the gauge bosons of $SO(5)/SO(4)$. The zero mode of $A_z^{\hat{a}}$ gives the Higgs. We can do the following KK decomposition

$$\begin{aligned} A_\mu^a(x,z) &= \sum_n f_n^a(z,v) A_{\mu,n}(x), \\ A_5^a(x,z) &= \sum_n \frac{\partial_z f_n^a(z,v)}{m_n(v)} h_n(x), \\ A_\mu^{\hat{a}}(x,z) &= \sum_n f_n^{\hat{a}}(z,v) A_{\mu,n}(x), \\ A_5^{\hat{a}}(x,z) &= C_h h^{\hat{a}}(x) kz + \sum_n \frac{\partial_z f_n^{\hat{a}}(z,v)}{m_n(v)} h_n(x). \end{aligned} \tag{4.26}$$

We need $C_h = \sqrt{\frac{2k}{(e^{2kL}-1)}} g_5$ to make the Higgs field canonically normalized. Note that all the wavefunctions depend on the vev of Higgs ($\langle h^{\hat{4}} \rangle = v$). The boundary conditions for these wavefunctions are complicated. However, the wavefunctions with non-vanishing Higgs vev are related to the wavefunctions with vanishing Higgs vev by a gauge transformation [52]

$$f^\alpha(z,v) T^\alpha = \Omega^{-1}(z,v) f^\alpha(z,0) T^\alpha \Omega(z,v), \tag{4.27}$$

with

$$\begin{aligned}\Omega(z,v) &= e^{-iC_h v T^{\hat{4}} \int_R^z dz' k z'} = exp\left[-iC_h v T^{\hat{4}} k(z^2-R^2)/2\right] \\ &\equiv exp\left[-i\frac{v(z^2-R^2)}{f_h(R'^2-R^2)}T^{\hat{4}}\right],\end{aligned} \tag{4.28}$$

where we defined the "Higgs decay constant" $f_h \equiv \frac{\sqrt{2k}}{g_5\sqrt{e^{2kL}-1}}$. Therefore, to simplify the task, we can just calculate the wavefunctions with vanishing Higgs vev, and do a transformation $\Omega(z,v)$ to find the wavefunctions with non-vanishing Higgs vev. We then apply boundary conditions for the wavefunctions $f^{a,\hat{a}}(z,v)$ on the IR brane to get the mass spectrum of gauge KK modes. The details of the calculation are shown in Appendix C. In the end, we get two spectral functions $\rho_{W,Z}(m,v)$ for W,Z bosons (Eqs. (C.15) and (C.25)), whose roots give us the mass spectra $m^n_{W,Z}$ for W,Z bosons.

Similarly, the wavefunctions for fermions with non-vanishing Higgs vev $F^{\Psi}_{1,2,3}(z,v)$ are also related to the wavefunctions for fermions with vanishing Higgs vev $F^{\Psi}_{1,2,3}(z,0)$ by the gauge transformation $\Omega(z,v)$:

$$\begin{aligned}F^{\Psi}_{1,2}(z,v) &= A\Omega(z,v)^{-1}A^{-1}F^{\Psi}_{1,2}(z,0) \\ F^{\Psi}_{3}(z,v) &= \Omega(z,v)^{-1}F^{\Psi}_{3}(z,0)\Omega(z,v)\end{aligned} \tag{4.29}$$

where we have written $F^{\Psi}_{1,2}$ in the basis specified in Eq. (4.20) and F^{Ψ}_3 in the form of 5×5 matrix (see Eq. (4.23)), and matrix A is defined in Eq. (4.21). Similarly to the gauge boson case, we can get spectral functions for top and bottom quarks $\rho_{t,b}(m,v)$ (Eqs. (C.41) and (C.42)), whose roots give us the mass spectra $m^n_{t,b}$ for t,b fermions. We can calculate the Coleman-Weinberg potential for Higgs once we

know all the spectral functions [52]

$$V_{CW}^{W}(v) = \frac{1}{(4\pi)^2}\int_0^\infty dp\ p^3\Big\{6\ln[\rho_W(ip,v)] + 3\ln[\rho_Z(ip,v)] - 12\ln[\rho_t(ip,v)] - 12\ln[\rho_b(ip,v)]\Big\}. \tag{4.30}$$

This integral can be done numerically. We can minimize this potential to find the Higgs vev v. Then we can find the mass spectra of the model through the spectral functions $\rho_{W,Z,t,b}(m,v)$.

4.4.4 Couplings of Coset Gauge Bosons

4.4.4.1 Estimates and General Patterns

The exact couplings for coset gauge bosons involve overlap integrals of wavefunctions, which has to be done numerically and hence are not very illuminating. We defer showing the formulae for exact couplings to section 4.4.4.2 and a discussion of the numerical analysis to section 4.4.5. In order to gain some insights into the structure of coset gauge boson couplings, we concentrate here on estimating the sizes of the couplings between both charged (W_C) and neutral (Z_C) coset gauge bosons and fermions based on 5D profiles, and we will show that the results here match the ones coming from two-site description shown earlier in section 4.3.[14] In the following analysis, we focus on the parametric dependence of these couplings on $\theta_H \equiv \frac{h}{\sqrt{2}f_h}$ and wavefunctions of fermion zero modes, both of which give rise to more

[14]The coupling between coset gauge bosons and two SM gauge bosons are not studied here since they vanish at leading order in Higgs vev due to quantum number (as argued in Section 4.3) and thus are not relevant for collider study.

than an order-of-magnitude effect on the couplings. There are also effects coming from fermion boundary mixing terms (Eq. (4.25)), which will introduce only order one uncertainty in our estimates. However, the dependence of the couplings on the parameters θ_H and wavefunctions of fermion zero modes should be robust against the effects from these mixing terms.

A comment is in order here about the region of parameter space we are considering. As pointed out in [7, 35], a light $t^{(1)}$ (first KK mode of top quark) is a promising signature for GHU. We will see later that a light $t^{(1)}$ is also desirable for the collider study of the coset gauge bosons. We generically get *two* light $t^{(1)}$ states in the regions of parameter space when $c_1 < 0$. In this case, the SM $(t, b)_L$ profile is highly peaked near the TeV brane and thus the SM t_R is less so (in order to obtain the correct top quark mass). We find that one of the light $t^{(1)}$ states is mostly $SU(2)_L$ *singlet* in this case. Thus, the coupling of SM bottom (doublet) and this light $t^{(1)}$ to the coset gauge boson (doublet) is large since it is allowed by the quantum numbers (i.e., no need for EWSB) and is not suppressed by profiles either. This coupling can then give a significant contribution to the production of the coset gauge boson. Therefore, we focus on this region of parameter space. We will often denote this singlet light $t^{(1)}$ as "*the* light $t^{(1)}$" in what follows. To simplify notation, we will also use t, b to denote SM top and bottom fermions when there is no confusion.

References [33] showed that the one loop contributions of such light $t^{(1)}$ states to the T parameter and to the shift in $Zb\bar{b}$ coupling can be consistent with the data. Another potential constraint comes from the shift in the Wtb coupling. We have

numerically studied the shift in the tbW coupling induced by mixing of zero and KK modes of both W and top (including the effect of the light $t^{(1)}$ state). We find that this shift is smaller than $\sim 10\%$, as required by the recent measurements at Tevatron [53].

Alternatively, the SM t_R can be highly peaked near the TeV brane [and the SM $(t,b)_L$ less so], which results in the light $t^{(1)}$ being a doublet [7] and a large coset-t_R-$t^{(1)}$ coupling. However, the top quark content of the proton is negligible (cf. bottom quark content which is larger) so that this coupling will not be that useful for production of coset gauge bosons.

- Charged Coset Gauge Bosons (W_C)

- $g_{W_C tb}$: coupling between coset W_C, SM top and SM bottom. We first discuss the coupling for left-handed fermions. Once the Higgs boson gets a vev, there will be mixing between W_L and W_C and between t_{1L} and $\hat{t}_{1L}$. From another point of view, this mixing comes from the gauge transformation (Eqs. (4.27) and (4.29)) that link the wavefunctions with vanishing Higgs vev and wavefunctions with non-vanishing Higgs vev. For example, from Eq. (C.6) we can see the wavefunction of W_L with non-vanishing Higgs vev contains some part of W_C wavefunction with vanishing Higgs vev, and the amount is $\frac{\sin\theta_H}{\sqrt{2}}$. Therefore the dominant contribution to the coupling comes from the following overlap integral of wavefunctions

$$g_{W_C t_L b_L} \approx -\frac{g_5}{\sqrt{2}} \int \frac{dz}{z^4} \left[f_{W_L} F_{t_1} F_{b_1} + f_{W_C} F_{\hat{t}_1} F_{b_1} \right] \tag{4.31}$$

The first term comes from the mixing between W_L and W_C, and the second

term comes from the mixing between t_{1L} and $\hat{t}_{1L}$. Here we have assumed that the zero mode t_L, b_L lives mainly in the first fermion multiplet Ψ_1. This happens when $c_1 < 0$. To estimate this coupling, we need to know the wavefunctions of t_L, b_L and W_C. The wavefunctions of W_C are peaked near the IR brane (i.e., their size at the IR brane is $\sim O(1)$ in units of $\sqrt{k}$) since they are KK modes, and *each* of the wavefunctions of t_L and b_L at the IR brane is $f(c_1) \approx \sqrt{\frac{1}{2} - c_1}$ (in units of $\sqrt{k}$). Finally, the overlap integral will be dominated by a region of size $\sim \frac{1}{k}$ near the IR brane. This gives us an estimate

$$|g_{W_C t_L b_L}| \sim \frac{g_5\sqrt{k}}{\sqrt{2}} \left(\frac{1}{2} - c_1\right) \frac{\sin\theta_H}{\sqrt{2}}, \tag{4.32}$$

where $\frac{\sin\theta_H}{\sqrt{2}}$ comes from mixing induced by Higgs vev. From Eq. (4.32) we can see that it is possible to get order one coupling between W_C and SM top and bottom quarks.[15] The right-handed coupling $g_{W_C t_R b_R}$ should be much smaller than the left-handed coupling $g_{W_C t_L b_L}$ since the wavefunction of b_R is much smaller than that of b_L near the IR brane. Therefore, it is irrelevant for collider study.

- $g_{W_C t^{(1)} b}$: coupling between coset W_C, first top KK mode, SM bottom quark. We first study the left-handed coupling. Note that the $t^{(1)}$ is mostly $SU(2)_L$

[15] Clearly, the coupling analogous to Eq. (4.32) is negligible for light left/right-handed SM fermions which have $c > (<) 1/2 (-1/2)$ and hence $f(c) \ll 1$. In particular, the coset gauge boson wavefunctions vanish near the Planck brane so that the wavefunction overlap comes only from near the TeV brane, unlike for KK W/Z where the flavor-universal part of the coupling to two SM fermions comes from overlap near the Planck brane.

singlet and its wavefunction is also peaked near the IR brane (i.e., its size at the IR brane is $\sim O(1)$ in units of $\sqrt{k}$), just like W_C. Thus the size of this coupling should be controlled simply by the single b wavefunction near the IR brane (i.e., no factor of EWSB). Therefore the coupling should be of order $\frac{g_5\sqrt{k}}{\sqrt{2}} f(c_1) \approx \frac{g_5\sqrt{k}}{\sqrt{2}} \sqrt{\frac{1}{2} - c_1}$ in the $\theta_H \to 0$ limit. Including the effect of nonzero Higgs vev will only give a small correction to this coupling, thus the estimate remains the same. The coupling for right-handed fermions should be much smaller due to the same reason that the wavefunction of b_R near the IR brane is small.

- $g_{W_C t^{(1)} b^{(1)}}$: coupling between coset W_C, first top KK mode and first bottom KK mode. Since the KK modes of fermions are localized near the IR brane, the coupling for both left-handed and right-handed fermions should be of order $\frac{g_5\sqrt{k}}{\sqrt{2}}$ (i.e., no suppression due to profiles or EWSB), up to order one coefficients coming from boundary mixing terms.

- Neutral Coset Gauge Boson (Z_C)

- $g_{Z_C tt}$: coupling between neutral coset gauge boson Z_C and SM top quark. For left-handed coupling, the estimate is similar to that of $g_{W_C t_L b_L}$:

$$g_{Z_C t_L t_L} \sim g_5\sqrt{k}\left(\frac{1}{2} - c_1\right)\frac{\sin(\theta_H)}{\sqrt{2}} \tag{4.33}$$

For right-handed coupling, the estimate is also similar

$$g_{Z_C t_R t_R} \sim g_5\sqrt{k}\left(\frac{1}{2} + c_2\right)\frac{\sin(\theta_H)}{\sqrt{2}} \tag{4.34}$$

- $g_{Z_C t^{(1)} t}$: coupling between coset Z_C, KK top and SM top quark. For left-handed coupling the estimate is

$$g_{Z_C t_L^{(1)} t_L} \sim g_5 \sqrt{k} \sqrt{\frac{1}{2} - c_1} \tag{4.35}$$

and for right-handed coupling

$$g_{Z_C t_R^{(1)} t_R} \sim g_5 \sqrt{k} \sqrt{\frac{1}{2} + c_2} \tag{4.36}$$

- $g_{Z_C t^{(1)} t^{(1)}}$: coupling between coset Z_C and KK top quark. Since Z_C always couples to two fermions transforming in different representation of $SU(2)_L$, this coupling will not be generated in the $\theta_H \to 0$ limit. Therefore, a rough estimate of this coupling is

$$g_{Z_C t^{(1)} t^{(1)}} \sim g_5 \sqrt{k} \frac{\sin \theta_H}{\sqrt{2}} \tag{4.37}$$

This estimate holds for both left-handed and right-handed couplings since the wavefunctions for $t_L^{(1)}$ and $t_R^{(1)}$ are both IR localized.

- $g_{Z_C b b}$: coupling between neutral coset gauge boson Z_C and SM bottom quark. For the left-handed coupling, naive estimate will give us

$$g^{\text{naive}}_{Z_C b_L b_L} \sim g_5 \sqrt{k} \left(\frac{1}{2} - c_1 \right) \frac{\sin \theta_H}{\sqrt{2}} \tag{4.38}$$

However, this coupling is very small (i.e., not relevant for collider signals) due to custodial symmetry. To be specific, the two contributions to this coupling coming from Z_C mixing with $W^3_{L,R}$ cancel each other. Similarly, the contributions to this coupling coming from $(2,2)$ fermion mixing with $(1,3)$ and $(3,1)$

fermion cancel each other. This cancelation is related to the build-in custodial symmetry of the model that protects the $g_{Zb_Lb_L}$ coupling (see Appendix D for more detailed discussion). Note that this cancelation does not happen for top quark since its W_L^3 and W_R^3 charges are different. The right-handed coupling is small due to the small b_R wavefunction near IR brane.

- $g_{Z_C b b^{(1)}}$: coupling between coset Z_C, SM bottom and KK bottom quark. The left-handed coupling is small due to similar cancelation that suppress $g_{Z_C b_L b_L}$ coupling. The right-handed coupling is also small because of the small b_R wavefunction near IR brane.

There is an additional coset gauge boson $A_\mu^{\hat{4}}$ (gauge boson of the generator $T^{\hat{4}}$) which is the vector partner of physical Higgs boson. We do not consider it here because its coupling with two SM fermions vanishes.[16] Even though it has nonzero coupling with $bb^{(1)}$ and $tt^{(1)}$, its production at the LHC is still suppressed. The reason is that the $b^{(1)}$ is not light (in the case of associated production with $b^{(1)}$ using the coupling to $bb^{(1)}$) and the top quark content of the proton is negligible, even though $t^{(1)}$ is light (in the case of associated production with $t^{(1)}$ using the coupling to $tt^{(1)}$).

We can compare the pattern of couplings estimated here with our conclusion using the two-site approach. In fact, there is a one-to-one correspondence/dictionary

[16]The reason for this is that Higgs vev does not induce an effect on $A_\mu^{\hat{4}}$ coupling since the gauge transformation (Eq. (4.28)) commutes with $T^{\hat{4}}$.

between two-site language and warped extra dimension models (see [34, 54]):

$$\begin{aligned} \text{SM states} &\leftrightarrow \text{zero modes} , \\ \text{heavy states} &\leftrightarrow \text{KK modes} , \\ \sin\theta_{\psi_{L,R}} &\leftrightarrow f(c_{L,R}) , \\ \sin\theta_G &\leftrightarrow \frac{1}{\sqrt{kL}} , \\ g_* &\leftrightarrow g_5\sqrt{k} . \end{aligned} \tag{4.39}$$

Based on this identification, we can see that the estimates for specific 5D model agree with those obtained using two-site description, the latter estimates being applicable to the general warped/composite PGB Higgs framework. Namely, the coset gauge boson generally couple strongly with SM fermions (zero modes) and heavy fermions (KK modes). We emphasize again that the conclusions above for the 5D model are rough, but are quite general, for example, they do not depend on whether the bulk gauge symmetry breaking $[SO(5) \to SO(4)]$ vev is infinite (as in GHU models) or finite[17]. We will further validate these estimates by computing them numerically for the specific 5D GHU model in section 4.4.5.

[17]This insensitivity is related to a similar one in the two-site description in section 4.3, in the latter case to f_ϕ, the scalar vev breaking the global symmetry $[SO(5) \to SO(4)]$ in the composite sector.

4.4.4.2 Exact Couplings

The exact couplings of coset gauge bosons can be obtained by overlap integrals of wavefunctions. We define gauge boson wavefunction matrix

$$G(z,v) \equiv f^{a_L}(z,v)T^{a_L} + f^{a_R}(z,v)T^{a_R} + f^{\hat{a}}(z,v)T^{\hat{a}} + f^{\hat{4}}(z,v)T^{\hat{4}} \ . \tag{4.40}$$

And we just use $F^{\Psi}_{1,2,3}(z,v)$ (see Eq. (4.29)) to denote the wavefunctions of the three fermionic multiplets. Then we can get the coupling between fermions and coset gauge bosons:

$$\begin{aligned} g_{GFF} &= \int \frac{dz}{(kz)^4} \left\{ g_5 \left[F^{\Psi\dagger}_{1,2} A G A^\dagger F^{\Psi}_{1,2} + \mathrm{Tr}\left(F^{\Psi\dagger}_{3} [G, F^{\Psi}_{3}] \right) \right] \right. \\ &+ \left. g_X \left[f^X \left(F^{\Psi\dagger}_{1,2} F^{\Psi}_{1,2} + \mathrm{Tr}\left[F^{\Psi\dagger}_{3} F^{\Psi}_{3} \right] \right) \right] \right\}. \end{aligned} \tag{4.41}$$

where matrix A is defined in Eq. (4.21). We use this formula to do numerical analysis in the next section.

4.4.5 Numerical Results

The purpose of our numerical scan is to find some points in the parameter space of the GHU model, in particular, specific values of the coset gauge boson couplings, which can then be used as benchmarks for our collider study. Therefore, we pick a specific model of GHU introduced in [35] to do our numerical scan. However, we should *not* treat the results as being model dependent for the following reason. As we argued in previous sections, the masses of coset gauge bosons in non-minimal models can be different from minimal GHU models. However, the couplings of coset gauge bosons are not sensitive to this non-minimal structure since

their pattern is determined by the quantum numbers and the fact that coset gauge boson wavefunctions are peaked near the IR brane.

In our numerical scan, we fix $k = 10^{18}$ GeV and we scanned over the input parameters $g_5\sqrt{k}, kL, c_{1,2,3}, M_{B1,B2}$. Even though for minimal model we have $g_5\sqrt{k} \approx g\sqrt{kL}$, this relationship between 5D coupling and 4D gauge coupling is modified once we include brane kinetic terms for gauge fields. Therefore, we choose to scan $g_5\sqrt{k}$ over the range $[g\sqrt{kL}, 2g\sqrt{kL}]$. We calculate the Higgs potential (Eq. (4.30)) and minimize it to find the Higgs vev v. We can then calculate the particle spectrum using the spectral functions (Eqs. (C.15), (C.25), (C.41) and (C.42)). We collect points with reasonable top and W/Z masses. Finally, the couplings of coset gauge bosons are calculated using Eq. (4.41). The important couplings are:

(i) for charged coset gauge boson W_C

$$\begin{aligned}\mathcal{L}_{W_C} &= g_{W_C t_L b_L}\bar{t}_L\gamma_\mu b_L W_C^{+\mu} + g_{W_C t_R b_R}\bar{t}_R\gamma_\mu b_R W_C^{+\mu} \\ &+ g_{W_C t_L^{(1)} b_L}\bar{t}_L^{(1)}\gamma_\mu b_L W_C^{+\mu} + g_{W_C t_R^{(1)} b_R}\bar{t}_R^{(1)}\gamma_\mu b_R W_C^{+\mu} + \text{h.c.},\end{aligned} \tag{4.42}$$

(ii) for neutral coset gauge boson Z_C

$$\begin{aligned}\mathcal{L}_{Z_C} &= g_{Z_C t_L t_L}\bar{t}_L\gamma_\mu t_L Z_C^\mu + g_{Z_C t_R t_R}\bar{t}_R\gamma_\mu t_R Z_C^\mu \\ &+ g_{Z_C t_L^{(1)} t_L}\bar{t}_L^{(1)}\gamma_\mu t_L Z_C^\mu + g_{Z_C t_R^{(1)} t_R}\bar{t}_R^{(1)}\gamma_\mu t_R Z_C^\mu \\ &+ g_{Z_C b_L b_L}\bar{b}_L\gamma_\mu b_L Z_C^\mu + g_{Z_C b_R b_R}\bar{b}_R\gamma_\mu b_R Z_C^\mu \\ &+ g_{Z_C b_L^{(1)} b_L}\bar{b}_L^{(1)}\gamma_\mu b_L Z_C^\mu + g_{Z_C b_R^{(1)} b_R}\bar{b}_R^{(1)}\gamma_\mu b_R Z_C^\mu + \text{h.c.},\end{aligned} \tag{4.43}$$

(iii) for first KK top $t^{(1)}$

$$\begin{aligned}\mathcal{L}_{t^{(1)}} &= g_{Wt_L^{(1)}b_L}\bar{t}_L^{(1)}\gamma_\mu b_L W^{+\mu} + g_{Wt_R^{(1)}b_R}\bar{t}_R^{(1)}\gamma_\mu b_R W^{+\mu} \\ &+ g_{Zt_L^{(1)}t_L}\bar{t}_L^{(1)}\gamma_\mu t_L Z^\mu + g_{Zt_R^{(1)}t_R}\bar{t}_R^{(1)}\gamma_\mu t_R Z^\mu \\ &+ g_{Ht_L^{(1)}t_R}\bar{t}_L^{(1)} h t_R + g_{Ht_R^{(1)}t_L}\bar{t}_R^{(1)} h t_L + \text{h.c.},\end{aligned} \tag{4.44}$$

where the subscripts L, R imply the chirality of the fermion. We present here a sample point with the couplings from the scan in Table 4.1 and Table 4.2. This will be served as benchmark point for collider study.

ke^{-kL}	$g_5\sqrt{k}$	c_1	c_2	c_3	M_{B1}	M_{B2}	θ_H
956 GeV	7.16	-0.364	-0.446	-0.559	1.419	-0.139	0.410

Table 4.1: Input parameters for sample points used in our numerical calculation. We fix $k = 10^{18}$ GeV. $c_{1,2,3}$ are the bulk mass parameters for the fermionic multiplets. M_{B1}, M_{B2} are boundary mass parameters needed to get correct SM fermion masses (see Eq. 4.25).

4.5 LHC signals

As discussed in sections 4.3 and 4.4, the most characteristic feature of coset gauge bosons is that they are vector bosons possessing Higgs quantum number. This uniquely fixes the pattern they are coupled to SM particles and other KK modes — they predominantly couple to one SM and one KK fermions as their couplings to a pair of SM particles are only induced by EWSB and are thus subdominant. This further determines how they are produced and decay at the LHC.

$g_{W_C t_L b_L}$	$g_{W_C t_R b_R}$	$g_{W_C t_L^{(1)} b_L}$	$g_{W_C t_R^{(1)} b_R}$
0.712	0.00169	-1.945	0.00207

$g_{Z_C t_L t_L}$	$g_{Z_C t_R t_R}$	$g_{Z_C t_L^{(1)} t_L}$	$g_{Z_C t_R^{(1)} t_R}$	$g_{Z_C b_L b_L}$	$g_{Z_C b_R b_R}$	$g_{Z_C b_L^{(1)} b_L}$	$g_{Z_C b_R^{(1)} b_R}$
-0.930	0.119	1.242	0.177	0.0235	-0.0219	0.0294	0.136

$g_{W t_L^{(1)} b_L}$	$g_{W t_R^{(1)} b_R}$	$g_{Z t_L^{(1)} t_L}$	$g_{Z t_R^{(1)} t_R}$	$g_{H t_L^{(1)} t_R}$	$g_{H t_R^{(1)} t_L}$
-0.170	0.000040	0.121	-0.0888	0.654	-1.06

Table 4.2: Numerical values of the couplings for the sample point choice.

As will be discussed in section 4.5.2, the production rate of neutral coset KK modes at LHC is very low in general. We will thus focus on the LHC signals of charged coset KK modes W_C. Our study is based on a set of points in the parameter space that give reasonable SM particle masses and generate EWSB radiatively as discussed in section 4.4.5. We first discuss the decay of charged coset gauge KK boson in 4.5.1 and its production at the LHC in 4.5.2 using this set of points. We then use couplings corresponding to the representative benchmark point in Table 4.2 and discuss in detail the signal and background at the LHC in 4.5.3.

4.5.1 Decay of W_C

There are following decay channels of W_C[18]

$$W_C \to t b^{(1)},\ t^{(1)} b,\ t b. \tag{4.45}$$

[18]The other decay channels involving light SM fermions are negligible.

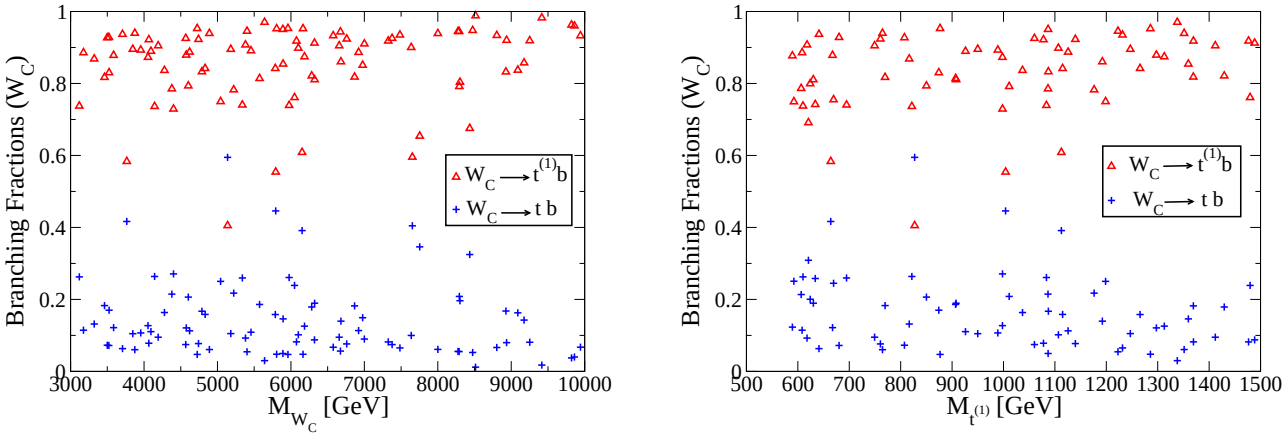

Figure 4.3: Scatter plots for the branching fractions $\mathrm{Br}(W_C \to t^{(1)}b)$ (triangle symbol) and $\mathrm{Br}(W_C \to tb)$ (cross symbol) versus (a) M_{W_C} and (b) $M_{t^{(1)}}$, respectively.

Compared to $W_C \to t^{(1)}b$, the branching fraction of $W_C \to tb^{(1)}$ is substantially suppressed due to kinematical reasons. It is one of the important properties of GHU models that there exists a light KK mode of top quark $t^{(1)}$ [35]. The mass of b-quark KK mode $b^{(1)}$ is, on the other hand, usually much heavier. Thus the decay $W_C \to tb^{(1)}$ is in most cases highly suppressed, if not forbidden. In the following, for simplicity and without losing the general feature, we will assume $b^{(1)}$ is heavier than W_C, forbidding this decay channel completely.

On the other hand, the branching fraction of $W_C \to tb$ is much suppressed compared to $W_C \to t^{(1)}b$ due to dynamical reasons. As discussed in sections 4.3 and 4.4, the quantum number of W_C forbids its coupling to SM quarks like $\bar{t}b$ at leading order. This coupling is only induced by Higgs vev after EWSB and is thus suppressed by v/f_h. This determines the typical trend of branching fractions of $W_C \to t^{(1)}\ b$ and $W_C \to t\ b$ decays, shown in Fig. 4.3.

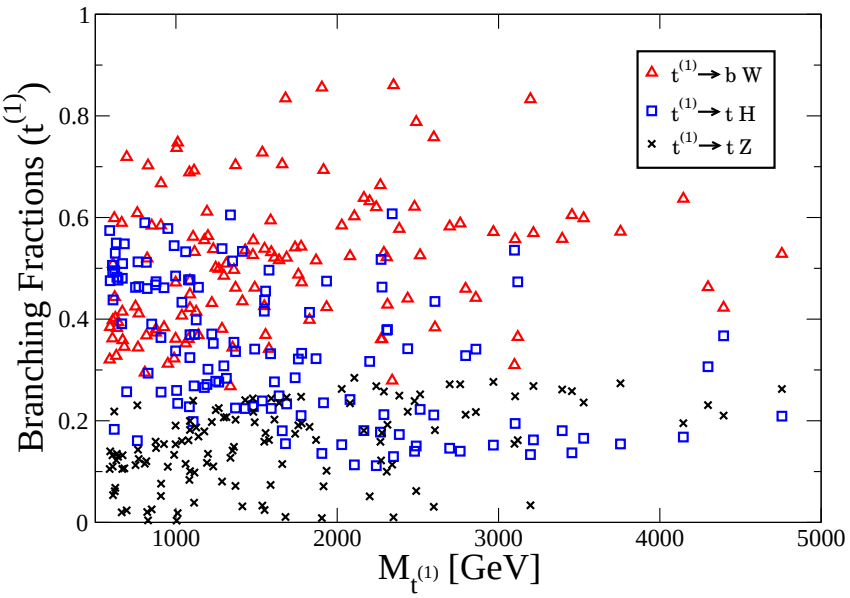

Figure 4.4: Scatter plots for the branching fractions $\mathrm{Br}(t^{(1)} \to Wb)$ (triangle symbol), $\mathrm{Br}(t^{(1)} \to th)$ (square symbol), and $\mathrm{Br}(t^{(1)} \to tZ)$ (cross symbol) versus $M_{t^{(1)}}$.

Since $t^{(1)}$ appears in the most dominant decay channel of W_C, we thus comment on $t^{(1)}$ decay next. There are three decay channels of $t^{(1)}$

$$t^{(1)} \to bW, \quad th, \quad tZ. \tag{4.46}$$

This has been studied in great detail in Ref. [8], where it has been pointed out that, for large $M_{t^{(1)}}$, the branching fractions should follow the relation $2:1:1$, according to the Goldstone Boson Equivalence Theorem, where as for small $M_{t^{(1)}}$, this ratio does not hold. In Ref. [8], the branching fractions are only shown for $M_{t^{(1)}}$ larger than 1 TeV. Since our primary goal is to explore the reach of LHC on discovering W_C, a relatively light $t^{(1)}$ would be more relevant. We thus extend the $t^{(1)}$ decay branching fractions to a wider range of 500 GeV$-$5 TeV, as in Fig. 4.4. The $2:1:1$

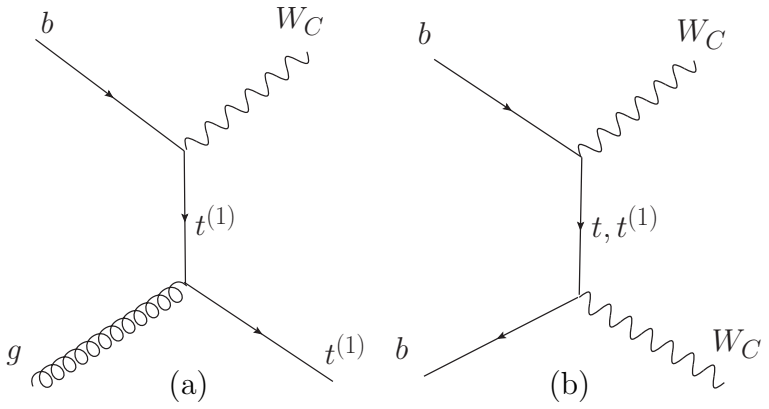

Figure 4.5: Representative Feynman diagrams for (a) $W_C t^{(1)}$ associated production and (b) $W_C W_C$ pair production.

ratios hold for $M_{t^{(1)}}$ >3 TeV. For a light $t^{(1)}$, $M_{t^{(1)}} < 1$ TeV, the branching fractions of $t^{(1)} \to bW$ and $t^{(1)} \to th$ are close and both are significantly larger than that of $t^{(1)} \to tZ$. The LHC search of $t^{(1)}$ has also been discussed in Ref. [8] and positive conclusions were reached. We therefore assume that $t^{(1)}$ has been observed with its mass approximately known a priori to the searches for W_C.

4.5.2 Coset KK modes production at the LHC

The coset gauge bosons, as all the KK modes in general, have profiles with large overlap with the third generation SM fermions ($t,\ b$) and hence couple more strongly to them as compared to the 1st/2nd generation SM quarks. However, the dominant production of KK W/Z is still (typically) via u and d quarks. On the other hand, the coupling to light quarks is smaller for the case of coset gauge bosons than the KK W/Z (as discussed in section 4.3). This feature motivates consideration of coupling of coset gauge bosons to bottom quarks for their production at the LHC.

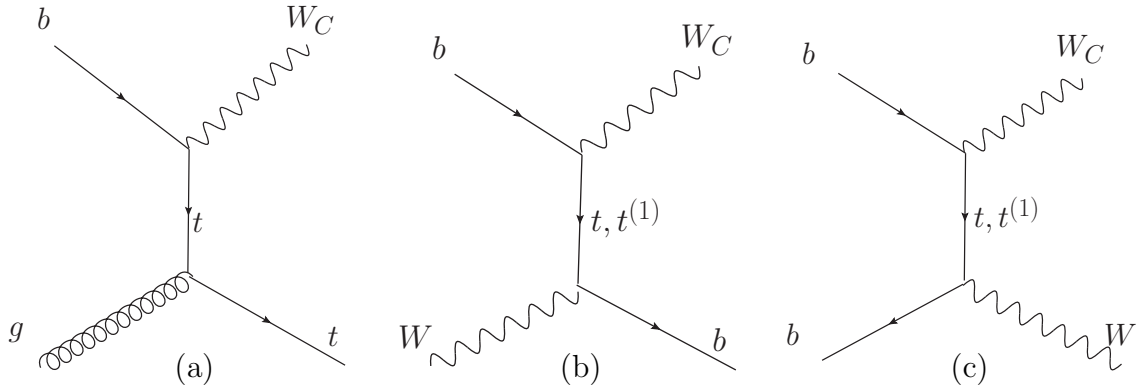

Figure 4.6: Representative Feynman diagrams for associated production (a) $W_C t$, (b) $W_C b$, and (c) $W_C W$, respectively.

From the discussion in section 4.4.4, and as shown explicitly in Table 4.2, the neutral coset KK modes Z_C couple strongly to $t(\bar{t})$, but rather weakly to $b(\bar{b})$, indicating that its production is highly suppressed at the LHC. We will then focus on the production of charged ones $W_C^{\pm}$ in the following. Figures 4.5 and 4.6 show the representative Feynman diagrams for the W_C associated production with a new heavy particle and with a SM particle, respectively. Between the two mechanisms (associated and pair) for production in Fig. 4.5, the production rate $bg(\bar{b}g) \to W_C^{\pm} t^{(1)}$ is clearly higher than that of $b\bar{b} \to W_C^{+} W_C^{-}$, due to its lower kinematical threshold and higher gluon luminosity in the proton. A similar argument also applies in Fig. 4.6 in favor of the production $bg \to W_C^{\pm}\ t$.

In Fig. 4.7, we show the total cross sections for these two processes $bg \to W_C^{\pm} t^{(1)}$, $W_C^{\pm} t$, as a function of their masses (a) M_{W_C} and (b) $M_{t^{(1)}}$. We turn off small couplings $g_{W_C t_R^{(1)} b_R}$ and $g_{W_C t_R b_R}$, fix the relative size of couplings as $g_{W_C t_L^{(1)} b_L} / g_{W_C t_L b_L} = 5$, and factor out the order one coupling $g_{W_C t_L^{(1)} b_L}$. Comparing these two processes, we

see that $W_C^{\pm} t^{(1)}$ production wins due to the stronger coupling as in Fig. 4.7(a); while $W_C^{\pm} t$ production wins for the phase space when $M_{t^{(1)}} > 1$ TeV, as in Fig. 4.7(b). The cross sections can be typically of the order of a fraction of fb in the mass range of our interest. Since our goal is to explore the reach of LHC on discovering W_C, we will focus on the low mass region of $M_{t^{(1)}}$, where the associated production $bg(\bar{b}g) \to W_C^{\pm} t^{(1)}$ dominates among the various non-resonant production channels.

We estimate, based on appropriate rescaling of numbers in Fig. 4 (a) of 1st reference in [4] or Fig. 7 of reference [55] for example, that the resonant production of coset gauge bosons via light quarks might be comparable to the above associated production, but the former channel suffers (as discussed at the end of section 4.3) from a pollution from production of the KK W. On the other hand, it is easy to see that a similar pollution for associated W_C production is negligible: note that (as discussed earlier) KK W does *not* couple to b_L (doublet) and light $t^{(1)}$ (singlet) *before* EWSB, i.e., the pollution from KK W in this channel is suppressed by EWSB.[19]

[19]The coupling of KK W_R^+, i.e., the charged gauge boson of $SU(2)_R$, to $t_L^{(1)}$ and b_L is similarly suppressed compared to that of W_C^+ to $t_L^{(1)}$ and b_L, again since $t^{(1)}$ is mostly singlet of $SU(2)_L \times SU(2)_R$ in the part of parameter space we are considering. Actually, there is another top KK mode living in the bi-doublet representation of $SU(2)_L \times SU(2)_R$, which has a coupling to W_R^+ (but not to KK W_L) and b_L which is similar in size to the coupling of coset gauge bosons to b_L and the singlet $t^{(1)}$. However, its mass is ~ 1.4 times higher than that of the singlet $t^{(1)}$ for the point we are considering, leading to the cross section for associated production of W_R^+ (via exchange of the bi-doublet top KK mode) being suppressed (relative to that for coset gauge boson with singlet top KK mode exchange) for the case when W_R and W_C have the same masses. Again, compare this situation to the pollution encountered in the resonant production of coset gauge bosons mentioned

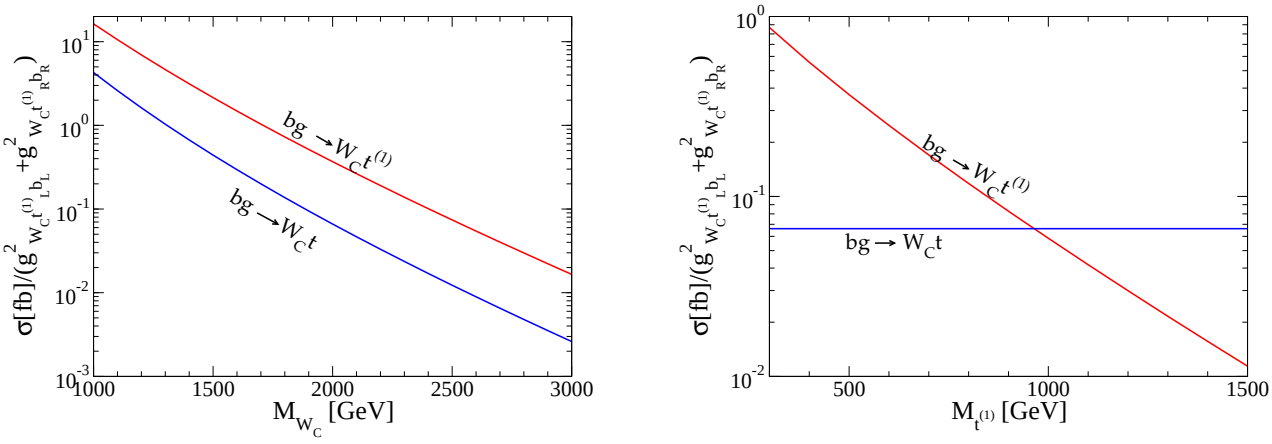

Figure 4.7: Cross section at the LHC (14 TeV) for $pp \to W_C^{\pm} t^{(1)}$, $W_C^{\pm} t$ versus their masses (a) M_{W_C} and (b) $M_{t^{(1)}}$. The coupling ratio $g_{W_C t_L^{(1)} b_L}/g_{W_C t_L b_L} = 5$ is fixed. The small couplings $g_{W_C t_R^{(1)} b_R}$ and $g_{W_C t_R b_R}$ are turned off, and order-one coupling square $g^2_{W_C t_L^{(1)} b_L}$ is factored out.

So, we will consider only associated production of W_C here. For the purpose of illustration, we choose

$$M_{W_C} = 2 \text{ TeV}, \quad M_{t^{(1)}} = 500 \text{ GeV} \tag{4.47}$$

as the reference point, and explore the dependence on the masses later.

4.5.3 Search of W_C at LHC: Signals and Backgrounds

To further quantify the search of W_C at the LHC, we fix to one point in the parameter space and study the signals and background in detail. The couplings corresponding to this parameter point is shown in Table 4.2. We use the M_{W_C} and $M_{t^{(1)}}$ as in Eq. (4.47). The cases with other couplings and masses can be estimated above.

by a proper scaling according to the production cross section shown in Fig. 4.7. We use the CTEQ6.1L parton distribution functions [56]. We concentrate on the dominant channels of production of W_C and its decay

$$bg \to W_C\ t^{(1)} \to bt^{(1)}\ t^{(1)}. \tag{4.48}$$

We consider all the decay channels of $t^{(1)}$ as in Eq. (4.46), which result in different signals, as we will study in detail below.

4.5.3.1 $t^{(1)}t^{(1)} \to bW, bW$

We first consider the case with both $t^{(1)}$'s decaying to $b\ W$:

$$bg \to W_C\ t^{(1)} \to b + 2t^{(1)} \to 3b + 2W, \tag{4.49}$$

whose branching fraction is a product of three factors[20]

$$Br(W_C \to bt^{(1)}) \times Br(t^{(1)} \to bW)^2 \approx 90\% \times (50\%)^2 = 22.5\%. \tag{4.50}$$

We consider the semileptonic decays of 2 W's where one W decays as $W \to l\nu(l = e, \mu)$ while the other as $W \to 2j$ (j denotes a jet from a light quark). The branching fraction for this channel is $\mathrm{Br}(WW) \approx 2/9 \times 6/9 \times 2 = 8/27$ where the factor 2 is from exchanging the leptonic and hadronic decaying W's.

The signal of this channel is therefore $l + 5j$ with large missing transverse momentum carried away by a neutrino. The leading background is

$$pp \to t\bar{t} + j \to l\nu + 5j. \tag{4.51}$$

[20]We take the branching fractions of $\mathrm{Br}(t^{(1)} \to bW)$ as 50% in this estimate. This is a general feature for large $M_{t^{(1)}}$ only. It happens to be approximately true for the parameter point we use for this detailed study, although it corresponds to a small $M_{t^{(1)}}$.

The other background $pp \to W^+W^- + 3j$ is much smaller, not only because W^+W^- cross-section is smaller than $t\bar{t}$ cross-section but also because the two more QCD jets in this background introduce another factor of α_s^2 suppression. We will thus only focus on the background of $t\bar{t}+$ 1 QCD jet.

We adopt the event selection criteria with the basic cuts [57]

$$\begin{aligned} &P_T(l) > 25 \text{ GeV}, \quad |\eta(l)| < 2.5, \\ &P_T(j) > 20 \text{ GeV}, \quad |\eta(j)| < 3, \\ &\not{E}_T > 25 \text{ GeV}, \quad \Delta R_{jj,lj} > 0.4. \end{aligned} \tag{4.52}$$

We smear the lepton and jet energy approximately according to

$$\delta E/E = \frac{a}{\sqrt{E/\text{GeV}}} \oplus b \tag{4.53}$$

where $a_l = 13.4\%$, $b_l = 2\%$ and $a_j = 75\%$, $b_j = 3\%$, and $\oplus$ denotes a sum in quadrature [58]. As shown in Table 4.3, the background is much higher than the signal if only applying the basic acceptance cuts. However, the signal has very unique kinematical features that we will utilize next to suppress the background and to reconstruct the signal.

One of striking features of the signal is that the b jet from W_C decay is very energetic due to the heavy mass of W_C. Among all the jets, this b jet has the highest P_T in most cases. Therefore, one can select the highest jet P_T and impose cut on it

$$P_T^{\text{highest}} > 500 \text{ GeV}. \tag{4.54}$$

Since the effective c.m. energy is quite large in signal for the heavy particle production, which are in general higher than those in background, we further impose cut

Table 4.3: The cross sections (in fb) for the signal process $pp \to W_C\, t^{(1)} \to l\nu{+}5j$ and SM background $pp \to t\bar{t}+j \to l\nu+5j$, with the cuts and veto applied consecutively. Basic cuts refer to those in Eq. (4.52). The "$M_{3j,l\nu j}$ cuts" refers to the cut condition in Eqs. (4.56) and (4.57), and "M_{3j} veto" refers to the veto condition in Eq. (4.58).

	basic cuts	P_T^{highest}	E_T^{vis}	$M_{3j,l\nu j}$ cuts	M_{3j} veto
Signal	0.045	0.040	0.037	0.025	0.025
Background	2.4×10^4	76	8.7	1.7	$< 10^{-4}$

on the scalar sum of the visible transverse energies of all the jets and l

$$E_T^{vis} > 1.5 \text{ TeV}. \tag{4.55}$$

With the jet of highest P_T identified as the b jet from W_C decay, there are 4 jets remaining. One can identify which three of them are from $t^{(1)}$ hadronic decay by selecting 3 jets which give the invariant mass closest to $t^{(1)}$, and require it to satisfy

$$|M_{3j} - M_{t^{(1)}}| < 50 \text{ GeV}, \tag{4.56}$$

where, as discussed earlier, we have assumed that the mass of $t^{(1)}$ is known from the early search. Furthermore, the neutrino momentum can be fully reconstructed using W mass condition $M_W^2 = (p_l + p_\nu)^2$ with a two-fold uncertainty [21]. We select

[21] In doing this, the neutrino P_T is fixed to balance the P_T of l and jets, which have uncertainties due to smearing. To accommodate this uncertainty, we allow the M_W to be as large as 120 GeV. It turns out that, with this range of M_W, there are still cases where there exist no solution for neutrino momentum, and we lose about 1/3 of events in solving for the neutrino momentum.

the solution which, in combination with the momenta of l and the other remaining jet, gives the mass closer to $M_{t^{(1)}}$, and further require it to satisfy[22]

$$|M_{l\nu j} - M_{t^{(1)}}| < 100 \text{ GeV}. \tag{4.57}$$

With these done, the momenta of two $t^{(1)}$'s are reconstructed. One still do not know which $t^{(1)}$ is from W_C decay, and should try both of them, in combination with the jet with highest P_T, to reconstruct the W_C mass. Since one of the two is expected to be the right one, the collection of the events should point to M_{W_C} in the mass distribution.

Although this reconstruction procedure is highly efficient, with a signal efficiency about 56% and the background rejection of a factor of 10^{-4}, as seen from Table 4.3, it is still not sufficient to remove the background. However, beside identifying the characteristics of the signal, we also notice the features of the background. One of the essential and obvious features of the background is that there are two top quarks in the event, one of which decays to 3 jets. One can thus require that there be no combination of 3 jets with invariant mass within the top mass window

$$|M_{3j} - m_t| > 50 \text{ GeV}. \tag{4.58}$$

This veto condition is highly efficient on removing the background.

We show, in Table 4.3, the cross sections of signal and background, with the cuts and veto applied consecutively. Both signal and background are obtained with

[22]Here we assume $M_{t^{(1)}}$ is known. On the other hand, without assuming this, one can still fix it by requiring there are 3 jets and (l, ν, j) having close heavy masses ($\gg m_t$) and identify this common mass scale as $M_{t^{(1)}}$.

parton-level Monte Carlo simulations, with detector effects accounted for by the geometrical acceptance and the energy smearing as discussed earlier. We see that the background is essentially removed with the veto condition of Eq. (4.58) applied.

In fact, the veto on M_{3j} alone would be sufficient to bring this $t\bar{t}j$ background below the signal. Our signal reconstruction scheme is nevertheless effective to single out the signal from the other potential backgrounds and to obtain the necessary knowledge about the masses of the heavy particle produced.

4.5.3.2 $t^{(1)}t^{(1)} \to bW, th(tZ)$

We now consider the case with one $t^{(1)}$ decaying to $b\,W$ and the other decaying to th or tZ. Since the signals of the final states are rather similar for these two cases, we discuss them together. The signal we are looking for is

$$bg \to W_C\ t^{(1)} \to b + 2t^{(1)} \to bbWth(Z) \to l\nu + 7j, \tag{4.59}$$

whose branching fraction (summing over both $t^{(1)} \to t\ h$ and $t\ Z$) is a product of three factors

$$\begin{aligned} 2 \times Br(W_C \to bt^{(1)}) \times Br(t^{(1)} \to bW) \times Br(t^{(1)} \to th, tZ) \\ \approx 2 \times 90\% \times (50\%)^2 = 45\%, \end{aligned} \tag{4.60}$$

where the factor of 2 is from exchanging the decay mode of two $t^{(1)}$'s. We consider semileptonic decay of two W's, which gives branching fraction 8/27 as discussed earlier.

The dominant SM background for this channel is from the

$$pp \to t\bar{t} + 3j \to l\nu + 7j. \tag{4.61}$$

This can be considered as adding two more QCD jets to the background considered in section 4.5.3.1. Although we expect this analysis directly analogous to that in the previous session, one may not be able to effectively calculate this multiple parton final state. Instead, we will thus simply give an estimate on how this background is suppressed by various cuts based on what we learn from the Monte Carlo simulations in section 4.5.3.1. To assess the signal/background ratio for this channel, we compare both the signal and background with those in the channel $(t^{(1)}t^{(1)} \to bW, bW)$ in the previous section.

For signal, this channel has larger branching fraction than the one considered in section 4.5.3.1. However, since there are two more jets in the final state, there are fewer events surviving the cuts of $\Delta R_{jj,lj} > 0.4$. As shown in Table 4.4, the signal cross-section after basic cuts in this channel is very close to that in the channel $(t^{(1)}t^{(1)} \to bW, bW)$.

The cuts on P_T^{highest} and E_T^{vis} are still applicable to this channel. Again, the jet with the highest P_T is identified as the b jet from W_C decay. Among the remaining 6 jets, one can require that there be at least one pair of jets with invariant mass close to *either* M_h, which we assume it to be 125 GeV, or M_Z

$$|M_{2j} - M_h| < 15 \text{ GeV or } |M_{2j} - M_Z| < 15 \text{ GeV} \tag{4.62}$$

The two jets from h or Z decay can be identified in this way[23]. The rest of the

[23]If there are more than one pair of jets satisfying this, one selects the pair whose invariant mass

procedure in reconstructing two $t^{(1)}$ momenta is similar to that in the $(t^{(1)}t^{(1)} \to bW, bW)$ channel.

Among all the remaining 4 jets, we require there exists at least one combination of 3 jets and (l, ν, j), which satisfy

$$\begin{aligned} & |M_{3j} - m_t| < 50 \text{ GeV and } |M_{l\nu j} - M_{t^{(1)}}| < 100 \text{ GeV} \\ \text{or} \quad & |M_{3j} - M_{t^{(1)}}| < 50 \text{ GeV and } |M_{l\nu j} - m_t| < 100 \text{ GeV}. \end{aligned} \tag{4.63}$$

Then, one can combine 2 jets which falls into the h or Z mass region with the cluster of either 3 jets or (l, ν, j), whichever falls into the M_t region, and require this 5 jets or $(l, \nu, 3j)$ has mass close to $M_{t^{(1)}}$

$$|M_{5j} - M_{t^{(1)}}| < 50 \text{ GeV or } |M_{l\nu 3j} - M_{t^{(1)}}| < 100 \text{ GeV}. \tag{4.64}$$

At this stage, the momenta of two $t^{(1)}$'s are reconstructed, and one can go further to reconstruct W_C mass by trying both $t^{(1)}$'s with the jet with the highest P_T. Again, the correlation among events should point to the correct M_{W_C}.

Since the top quark also appears in the signal of this channel, the simple veto on top mass (used in section 4.5.3.1) is not applicable here. However, the background in this channel is sufficiently reduced to be below the signal with the above cuts applied. This is because there are two more suppressions in this channel. First, the $t\bar{t}+3j$ background is further suppressed by $\alpha_s^2 \approx 10^{-2}$ compared to that of $t\bar{t}+1j$ background of the $(t^{(1)}t^{(1)} \to bW, bW)$ channel due to the appearance of two more QCD jets. Second, the extra cut on M_{2j} in Eq. (4.62) also introduce another factor of suppression, which we estimate it to be a factor of 10^{-1}.

is closer to M_H or M_Z.

Table 4.4: The cross-sections (in fb) for the signal process $pp \to W_C\ t^{(1)} \to l\nu + 7j$ and SM background $pp \to t\bar{t}{+}3j \to l\nu{+}7j$, with the cuts applied successively. Basic cuts refer to those in Eq. (4.52). The cuts on E_T^{vis} and $P_T^{\rm highest}$ refer to Eqs. (4.54) and (4.55). The "M_{2j} cut" refer to Eq. (4.62). The "$M_{3j,l\nu j}$, $M_{5j,l\nu 3j}$ cuts" refer to Eqs. (4.74) and (4.75).

	basic cuts	$P_T^{\rm highest}$	E_T^{vis}	M_{2j} cut	$M_{3j,l\nu j}$, $M_{5j,l\nu 3j}$ cuts
Signal	0.041	0.037	0.035	0.033	0.011
Background	2.4×10^2	0.76	0.087	0.0087	< 0.001

The cross-sections of signal and background in this channel, with cuts applied successively, are summarized in Table 4.4. The cross-section of signal is based on our parton-level Monte Carlo simulation, and that of background is obtained from an estimate based on the cross section of the background in the $t^{(1)}t^{(1)} \to bW, bW$ channel in 4.5.3.1.

4.5.3.3 $t^{(1)}t^{(1)} \to th(tZ), th(tZ)$

Finally, we consider the channel with both $t^{(1)}$ decaying to $th(tZ)$

$$bg \to W_C\ t^{(1)} \to b + 2t^{(1)} \to b\ t\ h(Z)\ t\ h(Z) \to l\ \nu + 9j, \tag{4.65}$$

whose branching fraction (summing over both $t^{(1)} \to t\ h$ and $t\ Z$) is a product of three factors

$$Br(W_C \to bt^{(1)}) \times Br(t^{(1)} \to th, tZ)^2 \approx 90\% \times (50\%)^2 = 22.5\%. \tag{4.66}$$

We will again use semileptonic decay of two W's whose branching fraction is 8/27 as discussed earlier.

The dominant SM background for this channel is from the $pp \to t\bar{t} + 5j \to l\nu + 9j$. We will simply give an estimate on how this background is suppressed by various cuts based on what we learned from the study based on Monte Carlo simulations in section 4.5.3.1.

The branching fraction of this channel is similar to the $(t^{(1)}t^{(1)} \to bW, bW)$ channel. However, with four more jets in the signal event, the cross-section is drastically reduced after imposing basic cuts that involve $\Delta R_{jj,lj} > 0.4$.

On the other hand, the background is smaller by a factor of $\alpha_s^4 \approx 10^{-4}$ than in the $(t^{(1)}t^{(1)} \to bW, bW)$ channel. Some of the cuts discussed previously are still applicable in this channel. They include the cuts on E_T^{vis}, P_T^{highest}, and M_{2j} (we require that there are at least two pairs of jets that satisfy Eq. (4.62) in this channel).

Similarly to the other two channels, the two $t^{(1)}$ momenta can be reconstructed and the W_C mass can be obtained from correlations among events. We skip the details of this procedure here since it should be clear from discussion in the previous sections. One should note that the cuts on 3 jets and (l, ν, j) invariant mass in Eq. (4.74) should be replaced by

$$|M_{3j} - m_t| < 50 \text{ GeV and } |M_{l\nu j} - m_t| < 100 \text{ GeV}, \tag{4.67}$$

since there are two top quarks.

We show, in Table 4.5, the signal and background with the cuts applied successively. Again, the cross-section of signal is based on our parton-level Monte Carlo

Table 4.5: The cross-sections (in fb) for the signal process $pp \to W_C\ t^{(1)} \to l\nu + 9j$ and SM background $pp \to t\bar{t} + 5j \to l\nu + 9j$, with the cuts applied successively. Basic cuts refer to those in Eq. (4.52). The P_T cuts on $P_T^{\rm highest}$ and E_T^{vis} follow Eqs. (4.54) and (4.55), and invariant mass cuts on M_{2j}, $M_{3j,l\nu j}$, and $M_{5j,l\nu 3j}$ follows Eqs. (4.62), (4.67) and (4.75).

	basic cuts	$P_T^{\rm highest}$	E_T^{vis}	two M_{2j} cuts	$M_{3j,l\nu j}$, $M_{5j,l\nu 3j}$ cuts
Signal	0.0081	0.0070	0.0068	0.0064	0.0023
Background	2.4	0.0076	0.00087	$< 8.7 \times 10^{-6}$	$< 1.0 \times 10^{-6}$

simulation, and that of background is based on our estimate built upon section 4.5.3.1.

4.5.3.4 Summarizing all channels

According to the study of each channel presented above, the background in each channel can be sufficiently suppressed after imposing various cut and veto criteria. For reader's convenience, we reiterate and summarize the cuts condition of all three channels here again.

Common cuts for all three channels:

(a) Basic cuts as in Eq. (4.52);

(b) P_T cuts: $P_T^{\rm highest} > 500$ GeV, $E_T^{vis} > 1.5$ TeV;

Specific cuts in each channels:

(i) Channel I ($l + 5j + \not{E}_T$)

(c) $M_{3j,l\nu j}$ cuts: with the jet with highest P_T excluded, requiring there exists such a combination of 3 jets and (l, ν, j) satisfying the invariant mass cut

$$|M_{3j} - M_{t^{(1)}}| < 50 \text{ GeV}, \ |M_{l\nu j} - M_{t^{(1)}}| < 100 \text{ GeV} \tag{4.68}$$

(d) M_{3j} veto: requiring there exist no combination of 3 jets that has invariant mass close to top mass

$$|M_{3j} - m_t| > 50 \text{ GeV} \tag{4.69}$$

(ii) Channel II ($l + 7j + \not{E}_T$)

(c) M_{2j} cut: with the jet with highest P_T excluded, requiring there exists at least one pair of jets with mass close to h or Z

$$|M_{2j} - M_h| < 15 \text{ GeV or } |M_{2j} - M_Z| < 15 \text{ GeV} \tag{4.70}$$

(d) $M_{3j,l\nu j}$ cuts: within the remaining 4 jets, requiring there exists at least one combination of 3 jets and (l, ν, j) that satisfy

$$\begin{aligned} & |M_{3j} - m_t| < 50 \text{ GeV and } |M_{l\nu j} - M_{t^{(1)}}| < 100 \text{ GeV} \\ \text{or} \quad & |M_{3j} - M_{t^{(1)}}| < 50 \text{ GeV and } |M_{l\nu j} - m_t| < 100 \text{ GeV}. \end{aligned} \tag{4.71}$$

(e) $M_{5j,l\nu 3j}$ cuts: combining 2 jets that falls into the h or Z mass region with the cluster of either 3 jets or (l, ν, j), whichever falls into the M_t region, and requiring this 5 jets or $(l, \nu, 3j)$ has mass close to $M_{t^{(1)}}$

$$|M_{5j} - M_{t^{(1)}}| < 50 \text{ GeV or } |M_{l\nu 3j} - M_{t^{(1)}}| < 100 \text{ GeV}. \tag{4.72}$$

(iii) Channel III ($l + 9j + \not{E}_T$)

(c) M_{2j} cut: with the jet with highest P_T excluded, requiring there exists at least two pairs of jets with mass close to h or Z

$$|M_{2j} - M_h| < 15 \text{ GeV or } |M_{2j} - M_Z| < 15 \text{ GeV} \tag{4.73}$$

(d) $M_{3j,l\nu j}$ cuts: within the remaining 4 jets, requiring there exists at least one combination of 3 jets and (l, ν, j) that satisfy

$$|M_{3j} - m_t| < 50 \text{ GeV and } |M_{l\nu j} - m_t| < 100 \text{ GeV}. \tag{4.74}$$

(e) $M_{5j,l\nu 3j}$ cuts: combining 2 pairs of jets which falls into the h or Z mass region with 3 jets and (l, ν, j), and requiring that in one of the two possible combinations, both 5 jets and $(l, \nu, 3j)$ have invariant mass satisfying

$$|M_{5j} - M_{t^{(1)}}| < 50 \text{ GeV and } |M_{l\nu 3j} - M_{t^{(1)}}| < 100 \text{ GeV}. \tag{4.75}$$

To assess the discovery potential, we combine the number of events in all the channels based on the above study of the benchmark point in the parameter space (with $M_{W_C} = 2$ TeV). The luminosity needed at the LHC (14 TeV) for a 95%(2σ), 99.7%(3σ), and 99.9999%(5σ) c.l. discovery of W_C, which implies about 3, 5, and 15 events, respectively (assuming that the background is negligible, as is the case here), can then be determined. For other M_{W_C} masses, we rescale this total number of events from the 2 TeV case, based on the dependence of cross-section on M_{W_C} as in Fig. 4.7. These results are displayed in Fig. 4.8. Conversely, for a luminosity of 1000 fb^{-1}, the reach in M_{W_C} is 2.3 TeV at 5σ, 2.6 TeV at 3σ, and 2.8 TeV at 2σ.

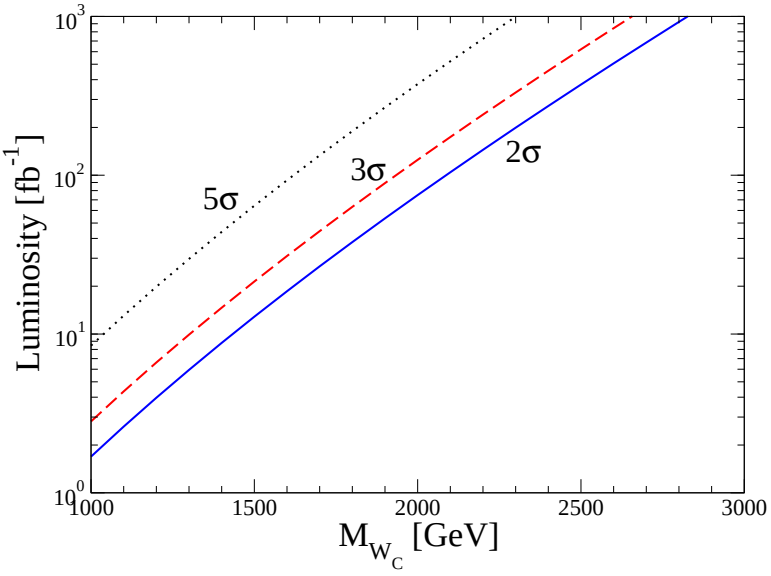

Figure 4.8: The luminosity needed for a 2σ(blue solid line), 3σ(red dashed line), and 5σ(black dotted line) discovery of W_C at LHC (14 TeV) as a function of M_{W_C}.

4.6 Summary and Discussions

In this chapter, we give a full-fledged presentation for the formalism involving the coset gauge bosons in this framework, *i.e.*, the extra (beyond SM-type) EW gauge bosons which are characteristically doublets under $\mathrm{SU}(2)_L$. We have then performed a study of LHC signals for the coset gauge boson W_C. We have developed a judicial and complex set of kinematical cuts to optimize the signal-to-background ratios. We have found that discovery of these gauge bosons at the LHC is very challenging. The primary reason for this is due to their unique gauge quantum numbers, so that the coset gauge bosons do not couple at leading order (in Higgs vev) to two SM particles, whether gauge bosons or fermions. Thus the s-channel resonant production of coset gauge bosons is quite suppressed, making production in

association with KK top an important mechanism (assuming that the KK top can be as light ~ 500 GeV, which does indeed happen quite commonly in this framework) and thus we focused on this channel here. This associated production experiences phase space suppression.

On the other hand, the advantage of this feature of the couplings of coset gauge bosons is that their two-body decays to SM particles are also suppressed. The leading decay for charged coset gauge bosons is to $t^{(1)}b$, and in turn, $t^{(1)} \to bW$ or th, tZ. Thus the final states are richer than just two SM particles, enabling separation from leading SM backgrounds, such as $t\bar{b}$, $t\bar{t}$. Based on such an analysis, we have estimated the 3σ reach for coset gauge bosons to be ~ 2 (2.6) TeV with ~ 100 (1000) fb^{-1} of luminosity. We notice, however, that typical models suggest that the mass scale of these gauge bosons is at least ~ 3 TeV. This expectation is based on an *indirect* limit from precision EW observables (direct bound on coset gauge boson mass being weaker), namely, due to the masses of coset gauge boson and those of the KK excitations of SM gauge bosons being related and the latter being directly constrained by precision EW observables.

The same feature of the coset gauge boson couplings also makes their signals distinct from those of other heavy EW gauge bosons as follows. Consider the signals for the EW KK gauge bosons with the same quantum numbers as the SM gauge bosons within the same framework, *i.e.*, KK Z, W and γ [4]. They couple at leading order to two SM particles, for example, to third generation quarks, WW/WZ[24] and

[24]Note that there are actually more than one neutral and charges states so that one mass eigenstate (i.e., admixture of gauge eigenstates) might have suppressed couplings due to cancelation

even to two light quarks (but typically with suppressed couplings compared to the SM ones), unlike coset gauge bosons which do not couple to WW/WZ or to two SM quarks at leading order in Higgs vev. Thus, the production cross-section is larger for KK $W/Z/\gamma$ than for coset gauge bosons of the same mass, but the decay channels of KK W/Z are not as rich as for coset gauge bosons. We can also compare to signals for Little Higgs models, where Z'/W', without T-parity, generically do couple to (and hence can be produced by or decay into) WW/WZ or to two SM light fermions [59], resulting in distinct signatures from those of the coset gauge bosons. Similarly, $4D$ Left-Right symmetric models have a W_R^+ which does *not* couple to W/Z at leading order but it does couple to two SM right-handed quarks and hence it can be produced by light quark-antiquark annihilation [60] and can decay into $t_R\bar{b}_R$. Finally, we must note that for many of the gauge sector extensions to include Z'/W' (KK W/Z, photon in warped extra dimensional framework being notable exceptions), their leptonic decays are always the gold-plated signatures, which is absent for the coset gauge boson searches.

We envisage the following sequence of events if this framework were realized in Nature: It is likely that a light KK top $t^{(1)}$ will be the first new particles to be discovered, with possibly less than 10 fb^{-1} luminosity. With about 100 fb^{-1} of integrated luminosity, it is the turn of the KK gluon next via its decay to $t\bar{t}$, followed closely by the KK W/Z via both gauge boson WW/WZ and fermion $t\bar{b}/t\bar{t}$ final

between its various components, but then the other (almost degenerate) state does not have such suppressed couplings.

states[25]. Finally with even higher luminosity, the coset gauge bosons can be searched for using final states with top/bottom/W (i.e., like some decays of KK W/Z, but with extra particles), but with no corresponding signal/excess in WW/WZ final states. Although the signatures of the new particles in the warped extra dimensional framework (including those of coset gauge bosons in the more natural versions) are qualitatively distinctive, it is clear that their detailed analysis at the LHC would be required in order to establish this attractive theoretical framework.

[25]although KK gluon decays to $t\bar{t}$ could be a "background" for KK Z in the $t\bar{t}$ channel.

Chapter 5

Higgs Phenomenology in Warped Extra Dimensions

5.1 Introduction

In chapter 3, we introduced the RS model with SM fields propagating in the bulk and explained how it solves the fermion mass hierarchy problem. The KK modes of these SM fields are the main new physics states of this framework, and their couplings to and mixings with SM states should lead to modification of the couplings of these SM states. Specifically, since the Higgs boson is localized near the IR brane in RS models, we should expect its properties to be significantly modified due to its large couplings with various KK states, which are also localized near the IR brane. For example, recently it has been pointed out that models with fermions in the bulk give rise to flavor violation in the couplings of Higgs to SM fermions [10, 11], leading to interesting constraints from $\Delta F = 2$ processes and to flavor violating collider signatures such as $h \to tc$ (see also the most recent analysis of [12, 13] for further details).

In this chapter, we will analyze the Higgs couplings to massless vector bosons such as gluons and photons in RS models where all SM fields are in the bulk [16]. The modification to these couplings arises from integrating out Kaluza-Klein (KK) partners of the SM fields. Previous works on this topic for RS models have been done

in [13, 14, 15, 61, 62][1]. These effects were also studied in models of warped extra dimensions in which the Higgs arises as Pseudo-Nambu-Goldstone boson (PNGB) [63] and within the effective theory formalism [64, 65].

The outline of this chapter is as follows: in section 5.2, we consider the effect of just two vector-like heavy fermions, one singlet under $SU(2)_L$ and one doublet. This simple case helps us to understand in simple terms the effects caused by the full tower of KK fermions in a realistic 5D setup. In section 5.3 we present a calculation of the hgg and $h\gamma\gamma$ couplings for the simple model where all the fermions are in a doublet representation of $SU(2)_L$ or $SU(2)_R$. In this section and in Appendix E we also present a simple way to evaluate the complete KK fermion tower contribution to hgg and $h\gamma\gamma$ couplings. Having explained and derived the new contributions to the Higgs couplings caused by the heavy KK fermions, we proceed in section 5.4 to study quantitatively the main phenomenological effects and summarize in section 5.5.

5.2 Warm-up: New Vector-Like Fermions

We begin by computing the new contribution to the hgg coupling using effective theory with just the zero and first KK modes, where we only consider one family of light quarks (say, up and down quarks) augmented by the presence of two heavy vector-like fermions, one in doublet representation of $SU(2)_L$ and the other in

[1] One of the main differences between our work and previous analysis is that we present analytical results for the contribution of the full KK fermion tower. Other subtle differences are discussed in the main text.

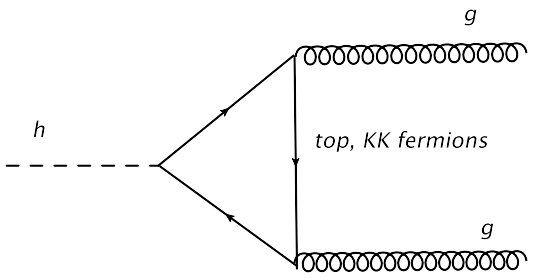

Figure 5.1: hgg coupling induced by fermion loop.

singlet representation. This effective theory description has the advantage of being economical and gives lucid physical intuition of the source of new physics contribution. Therefore, we adopt this approach in this section just to illustrate the essential points of our calculation. Moreover, the calculation is more general is the sense that it applies to any Beyond Standard Model (BSM) model in which there exist extra vector-like fermions which mix with SM fermions (see [66] for a similar discussion). The full calculation of the hgg coupling in the 5D warped extra dimension model will be carried out in the next section.

To start, we review here the Higgs boson production through gluon fusion in SM. The coupling between gluon and Higgs mainly comes from top quark loop (See Fig. 5.1). The partonic cross section for $gg \to h$ is [67]

$$\sigma^{SM}_{gg\to h} = \frac{\alpha_s^2 m_h^2}{576\pi} \left| \sum_Q \frac{y_Q}{m_Q} A_{1/2}(\tau_Q) \right|^2 \delta(\hat{s} - m_h^2), \tag{5.1}$$

where the sum is for all SM fermions, $\hat{s}$ is invariant mass squared of the two incoming gluons, $\tau_Q \equiv m_h^2/4m_Q^2$, y_Q and m_Q are Yukawa couplings and masses of the quarks, and the form factor for fermion in the loop is

$$A_{1/2}(\tau) = \frac{3}{2}[\tau + (\tau - 1)f(\tau)]\tau^{-2}, \tag{5.2}$$

where

$$f(\tau) = [\arcsin\sqrt{\tau}]^2, \quad (\tau \leq 1); \quad -\frac{1}{4}\left[\ln\left(\frac{1+\sqrt{1-\tau^{-1}}}{1-\sqrt{1-\tau^{-1}}}\right) - i\pi\right]^2, \quad (\tau > 1). \tag{5.3}$$

We note that for $\tau_Q \to 0$ i.e. $m_h \ll m_Q$, the form factor tends to be unity, while for $\tau_Q \to \infty$ i.e. $m_h \gg m_Q$, the form factor tends to zero. For reference, we consider a Higgs boson with mass 120 GeV, then for c-quark, we have $A_{1/2}(\tau_c) \approx 0.01$; and for a KK fermion with mass 2000 GeV, we have $A_{1/2}(\tau_{kk}) \approx 1.00021$. Therefore, it is a good approximation to treat the form factors for KK fermions as unity, while for light quarks, we can safely ignore their contributions.

In the effective theory with just one KK mode, we have zero mode fermions (q_L, u_R) and first KK fermions ($Q_L^{(1)}, Q_R^{(1)}, U_L^{(1)}, U_R^{(1)}$), where q, Q denote the up-type quark from $SU(2)_L$ doublet, and u, U denote the up-type quark from $SU(2)_L$ singlet. Then we have the following mass matrix:

$$(\bar{q}_L, \bar{Q}_L^{(1)}, \bar{U}_L^{(1)}) \begin{pmatrix} \frac{Y_{q_L u_R}\tilde{v}}{\sqrt{2}} & 0 & \frac{Y_{q_L U_R}\tilde{v}}{\sqrt{2}} \\ \frac{Y_{Q_L u_R}\tilde{v}}{\sqrt{2}} & M_Q & \frac{Y_{Q_L U_R}\tilde{v}}{\sqrt{2}} \\ 0 & \frac{Y_{U_L Q_R}\tilde{v}}{\sqrt{2}} & M_U \end{pmatrix} \begin{pmatrix} u_R \\ Q_R^{(1)} \\ U_R^{(1)} \end{pmatrix} + \text{h.c}, \tag{5.4}$$

where $Y_{q_L u_R}$ etc. are the Yukawa couplings between the corresponding chiral fermions, and $\tilde{v}$ is the Higgs VEV (note that it is not the same as v_{SM}). The Yukawa couplings matrix is given by

$$(\bar{q}_L, \bar{Q}_L^{(1)}, \bar{U}_L^{(1)}) \begin{pmatrix} \frac{Y_{q_L u_R}}{\sqrt{2}} & 0 & \frac{Y_{q_L U_R}}{\sqrt{2}} \\ \frac{Y_{Q_L u_R}}{\sqrt{2}} & 0 & \frac{Y_{Q_L U_R}}{\sqrt{2}} \\ 0 & \frac{Y_{U_L Q_R}}{\sqrt{2}} & 0 \end{pmatrix} \begin{pmatrix} u_R \\ Q_R^{(1)} \\ U_R^{(1)} \end{pmatrix} h + \text{h.c.} \tag{5.5}$$

To calculate these fermion contributions to the hgg coupling, we assume that the masses of the KK fermions $\gg m_h$, and therefore their form factors are approximately unity. Before proceeding let us classify different effects contributing to the shift of hgg coupling from that of the SM:

- relation between mass and Yukawa coupling of the lightest state (SM fermion) is modified from the SM value $y_{RS}^{\text{light}} \neq \frac{m_f}{v_{SM}}$;
- we have loop of KK fermion running in the triangle diagrams (see Fig. 5.1).

So we should calculate

$$\frac{y_{RS}^{\text{light}}}{m^{\text{light}}} A_{1/2}(\tau_{\text{light}}) + \sum_{\text{heavy}} \frac{Y_i}{M_i} = \text{Tr}(\hat{Y}\hat{M}^{-1}) + \frac{y_{RS}^{\text{light}}}{m^{\text{light}}} \left(A_{1/2}(\tau_{\text{light}}) - 1\right), \tag{5.6}$$

where $\hat{M}$ and $\hat{Y}$ are the fermion mass and Yukawa matrices given in Eq. (5.4) and (5.5)[2]. The first term on the LHS of the above equation gives the contribution from the SM fermion (lightest mass eigenstate), and the second term comes from the contributions of heavy KK fermions. Note that $\hat{Y} = \frac{\partial \hat{M}}{\partial \tilde{v}}$, therefore, we can use the following trick to calculate the trace [68]:

$$\text{Tr}(\hat{Y}\hat{M}^{-1}) = \text{Tr}\left(\frac{\partial \hat{M}}{\partial \tilde{v}}\hat{M}^{-1}\right) = \frac{\partial \ln \text{Det}(\hat{M})}{\partial \tilde{v}}, \tag{5.7}$$

we also have

$$\begin{aligned} \text{Det}(\hat{M}) &= Y_{q_L u_R} M_Q M_U \frac{\tilde{v}}{\sqrt{2}} + Y_{Q_L u_R} Y_{U_L Q_R} Y_{q_L U_R} \left(\frac{\tilde{v}}{\sqrt{2}}\right)^3 \\ &- Y_{q_L u_R} Y_{Q_L U_R} Y_{U_L Q_R} \left(\frac{\tilde{v}}{\sqrt{2}}\right)^3. \end{aligned} \tag{5.8}$$

[2]Note that the real part of the Yukawa coupling will lead to the operator $hG_{\mu\nu}G^{\mu\nu}$, and the imaginary part will lead to the operator $hG_{\mu\nu}\tilde{G}^{\mu\nu}$. For simplicity in this chapter we everywhere will assume that we have only $hG_{\mu\nu}G^{\mu\nu}$ operator.

Now we expand to first order in $\frac{\tilde{v}^2}{M_Q M_U}$:

$$\mathrm{Tr}(\hat{Y}\hat{M}^{-1}) \approx \frac{1}{\tilde{v}}\left[1 + \left(\frac{Y_{Q_L u_R} Y_{U_L Q_R} Y_{q_L U_R}}{Y_{q_L u_R}} - Y_{Q_L U_R} Y_{U_L Q_R}\right)\frac{\tilde{v}^2}{M_Q M_U}\right]. \tag{5.9}$$

Note that the masses and Yukawa couplings of the SM fermions are also modified (see [11] for details),

$$\frac{y_{RS}^{\mathrm{light}}}{m^{\mathrm{light}}} \approx \frac{1}{\tilde{v}}\left(1 + \frac{Y_{Q_L u_R} Y_{U_L Q_R} Y_{q_L U_R}}{Y_{q_L u_R}}\frac{\tilde{v}^2}{M_Q M_U}\right), \tag{5.10}$$

where the last expression was derived using the following assumption ($Y_{q_L u_R} \ll Y_{q_L U_R}, Y_{Q_L u_R} \ll Y_{Q_L U_R}$). This assumption is true the quarks of the first two generations, and the extra contribution which is important for the quarks of the third generation will be presented in the next section. Now Eq. (5.6) reduces to

$$\frac{y_{RS}^{\mathrm{light}}}{m^{\mathrm{light}}} A_{1/2}(\tau_{\mathrm{light}}) - \tilde{v}\frac{Y_{Q_L U_R} Y_{U_L Q_R}}{M_Q M_U}. \tag{5.11}$$

We can see that for the light generation quarks, $A_{1/2}(\tau_{\mathrm{light}}) \approx 0$, we get just the second term in the above equation, which is just the contribution coming from the KK modes. Note that this contribution is proportional to $Y_{Q_L U_R} Y_{U_L Q_R}$, which is the product of Yukawa couplings of the KK fermions of opposite chiralities, this structure of the contribution will become essential in calculating the effects in realistic warped model in the next section. It is interesting to see that even though the light SM quarks give negligible contribution to *hgg* coupling, their KK partners can give sizable new contributions. In addition, there would be an multiplicity enhancement of these KK contributions due to the number of flavors.

The analysis above showed that additional vector-like fermions which mix with SM fermions can alter the *hgg* coupling significantly. In warped extra dimension

models with 5D fermions propagating in the bulk, these extra vector-like fermions naturally come up as the KK towers of fermions. Therefore, we expect generically sizable new physics contributions to hgg coupling in this class of models. We carry out the detailed calculations in warped extra dimension in the next section.

5.3 Minimal Warped Extra Dimension Model with Custodial Protection

In this section, we first calculate the KK fermion contributions to hgg coupling in warped extra dimensions (RS). We then apply similar techniques to calculate both KK fermion and KK gauge boson contributions to $h\gamma\gamma$ coupling. We show that simple analytical formulas can be obtained for these new physics contributions.

5.3.1 hgg coupling in RS

In this subsection, we consider the effect of the full KK fermion tower on hgg coupling. We consider models with bulk gauge group $SU(2)_L \otimes SU(2)_R$, which is motivated to ease the bound from electroweak precision test [29]. We consider here just a single family of quarks for the sake of simplicity. A generalization to 3 generation quarks can be easily applied later. For the quark fields, we consider the simple spinorial representation with the following field contents:

$$\begin{pmatrix} Q^u_L(+,+)\, Q^u_R(-,-) \\ Q^d_L(+,+)\, Q^d_R(-,-) \end{pmatrix}, \begin{pmatrix} U'_R(-,+)\, U'_L(+,-) \\ D_R(+,+)\, D_L(-,-) \end{pmatrix}, \begin{pmatrix} U_R(+,+)\, U_L(-,-) \\ D'_R(-,+)\, D'_L(+,-) \end{pmatrix}. \quad (5.12)$$

The first multiplet is a doublet of $SU(2)_L$ and the last two are doublets of $SU(2)_R$. The boundary conditions are denoted for the corresponding chirality. They have the following Yukawa couplings [3]

$$Y^u\sqrt{R}(\bar{Q}^u_L U_R + \bar{Q}^d_L D'_R)H + Y^d\sqrt{R}(\bar{Q}^u_L U'_R + \bar{Q}^d_L D_R)H + (L \leftrightarrow R) + \text{h.c.} \quad (5.13)$$

Note that Y^u, Y^d are dimensionless and order one, and $1/R = k$ is the curvature scale. After KK decomposition in the basis where Higgs vev is zero, we have zero modes $q^{u,(0)}_L, q^{d,(0)}_L, d^{(0)}_R, u^{(0)}_R$ and the KK modes $Q^{u,(i)}_{L,R}, Q^{d,(i)}_{L,R}, D^{(j)}_{L,R}, U^{(j)}_{L,R}, U'^{(k)}_{L,R}, D'^{(k)}_{L,R}$. For up-type quarks, we have the following infinite dimensional mass matrix

$$(\bar{q}^{u,(0)}_L, \bar{Q}^{u,(i)}_L, \bar{U}^{(j)}_L, \bar{U}'^{(k)}_L) \begin{pmatrix} \frac{Y^u_{qu}\tilde{v}}{\sqrt{2}} & 0 & \frac{Y^u_{qU_b}\tilde{v}}{\sqrt{2}} & \frac{Y^d_{qU'_c}\tilde{v}}{\sqrt{2}} \\ \frac{Y^u_{Q_i u}\tilde{v}}{\sqrt{2}} & M_Q & \frac{Y^u_{Q_i U_b}\tilde{v}}{\sqrt{2}} & \frac{Y^d_{Q_i U'_c}\tilde{v}}{\sqrt{2}} \\ 0 & \frac{Y^{u,*}_{U_j Q_a}\tilde{v}}{\sqrt{2}} & M_U & 0 \\ 0 & \frac{Y^{d,*}_{U'_k Q_a}\tilde{v}}{\sqrt{2}} & 0 & M_{U'} \end{pmatrix} \begin{pmatrix} u^{(0)}_R \\ Q^{u,(a)}_R \\ U^{(b)}_R \\ U'^{(c)}_R \end{pmatrix} + \text{h.c.} \quad (5.14)$$

where i, j, k, a, b, c are KK indices. The Yukawa couplings matrices are defined e.g. by

$$Y^u_{Q_i U_b} = Y^u\sqrt{R}\int dz \left(\frac{R}{z}\right)^5 h(z) q^{u,(i)}_L(z) u^{(b)}_R(z), \quad (5.15)$$

i.e. it is an integral of product of Higgs and fermion wavefunctions, where $h(z)$ is a profile of the Higgs field normalized in the following way

$$1 = \int_R^{R'} dz \left(\frac{R}{z}\right)^3 h(z)^2. \quad (5.16)$$

The KK mass matrices are diagonal, e.g. $M_Q = \text{diag}(M_{Q_1}, M_{Q_2}, \cdots)$. One naively might think that the couplings $Y_{U_j Q_a}$ vanish in the limit of brane Higgs due to

[3] We consider here a general bulk Higgs [69] with vector-like Yukawa coupling for simplicity.

the odd boundary conditions of U_L and Q^u_R, so it is safe to ignore them in this matrix. But these are precisely the Z_2 odd operators described in detail in [11] (detailed analysis without these operators was presented in [14]). These operators as was shown in [11] lead to flavor violation in the Higgs sector, and they are also essential in evaluating the hgg coupling[4]. To avoid subtleties with wave function being discontinuous at IR brane we will assume that the Higgs is 5D bulk field and only at the end we will take a brane Higgs limit.

Now we can use the same determinant trick, the determinant of the mass matrix to the order of $\tilde{v}^3$ is

$$\begin{aligned}\mathrm{Det}(\hat{M}) = &\left(\prod_{i,j,k} M_{Q_i} M_{U_j} M_{U'_k}\right) \times \\ &\left[\frac{Y^u_{qu}\tilde{v}}{\sqrt{2}} - Y^u_{qu}\left(\frac{\tilde{v}}{\sqrt{2}}\right)^3 \sum_{a,b}\left(\frac{Y^d_{Q_a U'_b} Y^{d,*}_{U'_b Q_a}}{M_{Q_a} M_{U'_b}} + \frac{Y^u_{Q_a U_b} Y^{u,*}_{U_b Q_a}}{M_{Q_a} M_{U_b}}\right)\right. \\ &\left. + \left(\frac{\tilde{v}}{\sqrt{2}}\right)^3 \sum_{a,b}\left(\frac{Y^u_{qU_b} Y^{u,*}_{U_b Q_a} Y^u_{Q_a u}}{M_{Q_a} M_{U_b}} + \frac{Y^d_{qU'_b} Y^{d,*}_{U'_b Q_a} Y^u_{Q_a u}}{M_{Q_a} M_{U'_b}}\right)\right]. \end{aligned} \tag{5.17}$$

Now we get

$$\begin{aligned}\mathrm{Tr}(\hat{Y}\hat{M}^{-1}) = \frac{\partial \ln \mathrm{Det}(\hat{M})}{\partial \tilde{v}} = \frac{1}{\tilde{v}}\Bigg[1 - \tilde{v}^2 \sum_{a,b}\left(\frac{Y^d_{Q_a U'_b} Y^{d,*}_{U'_b Q_a}}{M_{Q_a} M_{U'_b}} + \frac{Y^u_{Q_a U_b} Y^{u,*}_{U_b Q_a}}{M_{Q_a} M_{U_b}}\right) \\ + \frac{\tilde{v}^2}{Y^u_{qu}} \sum_{a,b}\left(\frac{Y^u_{qU_b} Y^{u,*}_{U_b Q_a} Y^u_{Q_a u}}{M_{Q_a} M_{U_b}} + \frac{Y^d_{qU'_b} Y^{d,*}_{U'_b Q_a} Y^u_{Q_a u}}{M_{Q_a} M_{U'_b}}\right)\Bigg]. \end{aligned} \tag{5.18}$$

Again, for the light generation quarks there are corrections to the SM fermion masses

[4]These operators can be mimicked by higher dimensional derivative operators [11], which shows UV sensitivity of the effect.

and Yukawa couplings [11]

$$
\begin{aligned}
m^{\text{light}} &= Y^u_{qu}\frac{\tilde{v}}{\sqrt{2}} + \sum_{a,b} Y^u_{qU_b}\frac{1}{M_{U_b}}Y^{u,*}_{U_bQ_a}\frac{1}{M_{Q_a}}Y^u_{Q_au}\left(\frac{\tilde{v}}{\sqrt{2}}\right)^3 \qquad (5.19)\\
&+ \sum_{a,b} Y^d_{qU'_b}\frac{1}{M_{U'_b}}Y^{d,*}_{U'_bQ_a}\frac{1}{M_{Q_a}}Y^u_{Q_au}\left(\frac{\tilde{v}}{\sqrt{2}}\right)^3,\\
y^{\text{light}}_{RS} &= \frac{Y^u_{qu}}{\sqrt{2}} + \frac{3}{\sqrt{2}}\sum_{a,b} Y^u_{qU_b}\frac{1}{M_{U_b}}Y^{u,*}_{U_bQ_a}\frac{1}{M_{Q_a}}Y^u_{Q_au}\left(\frac{\tilde{v}}{\sqrt{2}}\right)^2 \qquad (5.20)\\
&+ \frac{3}{\sqrt{2}}\sum_{a,b} Y^d_{qU'_b}\frac{1}{M_{U'_b}}Y^{d,*}_{U'_bQ_a}\frac{1}{M_{Q_a}}Y^u_{Q_au}\left(\frac{\tilde{v}}{\sqrt{2}}\right)^2.
\end{aligned}
$$

Therefore

$$
\begin{aligned}
\frac{y^{\text{light}}_{RS}}{m^{\text{light}}} &\approx \frac{1}{\tilde{v}}\Big(1 + \sum_{a,b} Y^u_{Q_au}Y^{u,*}_{U_bQ_a}Y^u_{qU_b}\tilde{v}^2\frac{1}{M_{Q_a}M_{U_b}Y^u_{qu}} \qquad (5.21)\\
&+ \sum_{a,b} Y^u_{Q_au}Y^{d,*}_{U'_bQ_a}Y^d_{qU'_b}\tilde{v}^2\frac{1}{M_{Q_a}M_{U'_b}Y^u_{qu}}\Big).
\end{aligned}
$$

So the total contribution to hgg coupling by light generation quarks and their KK partners is (see Eq. 5.6)

$$
-\tilde{v}\sum_{a,b}\left(\frac{Y^d_{Q_aU'_b}Y^{d,*}_{U'_bQ_a}}{M_{Q_a}M_{U'_b}} + \frac{Y^u_{Q_aU_b}Y^{u,*}_{U_bQ_a}}{M_{Q_a}M_{U_b}}\right) + \frac{y^{\text{light}}_{RS}}{m^{\text{light}}}A_{1/2}(\tau_{\text{light}}). \qquad (5.22)
$$

Note that this result is very similar to the one we obtained in the last section (Eq. 5.11), except for an extra term corresponding to the contribution of extra states in the doublet representation of $SU(2)_R$. For light generations, the last term is negligible, and we are left with first two terms. The first two terms can be written as

$$
\begin{aligned}
&-\tilde{v}\sum_{a,b}\Big[Y^uY^{u,*}R\left(\int dzdz'\left(\frac{R^2}{z'z}\right)^5\frac{q^{(a)}_L(z)q^{(a)}_R(z')}{M_{Q_a}}\frac{u^{(b)}_R(z)u^{(b)}_L(z')}{M_{U_b}}h(z)h(z')\right) \qquad (5.23)\\
&+Y^dY^{d,*}R\left(\int dzdz'\left(\frac{R^2}{z'z}\right)^5\frac{q^{(a)}_L(z)q^{(a)}_R(z')}{M_{Q_a}}\frac{u'^{(b)}_R(z)u'^{(b)}_L(z')}{M_{U'_b}}h(z)h(z')\right)\Big].
\end{aligned}
$$

Now we have to evaluate the following sums

$$\sum_{a>0} \frac{q_L^{(a)}(z) q_R^{(a)}(z')}{M_{Q_a}}, \quad \sum_{b>0} \frac{u_R^{(b)}(z) u_L^{(b)}(z')}{M_{U_b}}, \quad \sum_{b>0} \frac{u_R'^{(b)}(z) u_L'^{(b)}(z')}{M_{U_b'}}. \tag{5.24}$$

We can calculate them by using equations of motion for fermion wavefunctions (see discussion in the Appendix E). From the forms of these sums (see Eq. (E.10)), we see that we need to evaluate the integrals of Higgs wavefunction times $\theta(z-z')$ and $\theta(z-z')^2$. This can be done for general bulk Higgs. But for illustration purpose we take the brane Higgs limit of bulk Higgs. Then we get

$$\int dz dz' \theta(z-z')^2 h^{brane}(z) h^{brane}(z') = \frac{1}{2}, \tag{5.25}$$

[5] and Eq. (5.23) now reduces to

$$\frac{1}{2}\left(Y^u Y^{u,*} + Y^d Y^{d,*}\right) \tilde{v} R'^2. \tag{5.26}$$

Therefore, for light generations, the contribution to hgg coupling is given by the above equation, which comes just from KK fermions and is independent of fermion bulk mass parameters.

For the third generation quarks there will be an extra contribution to the formula in (Eq. 5.21) which we parameterize following [11] as $(-\frac{\Delta_2^{t,b}}{m\tilde{v}})$ (see Appendix G for details). This gives us additional contribution relative to (Eq. 5.22)

$$\frac{\Delta_2^t}{m_t \tilde{v}} + \frac{\Delta_2^b}{m_b \tilde{v}}. \tag{5.27}$$

[5] To evaluate this integral we have to somehow regularize the wavefunction of the brane Higgs(δ function), we used bulk Higgs inspired regularization of the delta function $h^{brane}(z) = \lim_{\beta\to\infty} \frac{\beta}{R'}\left(\frac{z}{R'}\right)^\beta$. One can also use a rectangular regularization of brane Higgs wavefunction which will lead to the same result.

Also in this case contributions of the SM bottom and top quarks are no longer negligible, so we have to include them

$$\frac{y_b^{RS}}{m_b}A_{1/2}(\tau_b)+\frac{y_t^{RS}}{m_t}A_{1/2}(\tau_t). \tag{5.28}$$

Note that now Yukawa couplings of the top and bottom quarks are shifted(see discussion in Appendix G).

It is simple to generalize the above result to three generations. The KK towers of the quarks give a contribution proportional to $\mathrm{Tr}(Y_uY_u^\dagger+Y_dY_d^\dagger)$, and we have to combine them with the effect coming from top and bottom quarks. To summarize, compared with SM, the Higgs production cross-section from gluon fusion in RS is

$$\frac{\sigma^{RS}_{gg\to h}}{\sigma^{SM}_{gg\to h}}=\frac{v_{SM}^2}{\tilde{v}^2}\left|\frac{\mathrm{Tr}(Y_uY_u^\dagger+Y_dY_d^\dagger)\tilde{v}^2R'^2+\frac{\Delta_2^t}{m_t}+\frac{\Delta_2^b}{m_b}+x_tA_{1/2}(\tau_t)+x_bA_{1/2}(\tau_b)}{A_{1/2}(\tau_t)+A_{1/2}(\tau_b)}\right|^2 \tag{5.29}$$

where $x_t=\frac{y_t^{RS}\tilde{v}}{m_t}$ and $x_b=\frac{y_b^{RS}\tilde{v}}{m_b}$, with y_t^{RS},y_b^{RS} the shifted top and bottom Yukawa couplings in RS (reference [13] presented numerical results for the analysis of the brane Higgs model including Z_2 odd operators, however, it is hard to compare it with our result due to different particle content of the models). We consider here the ratio $\frac{\sigma^{RS}_{gg\to h}}{\sigma^{SM}_{gg\to h}}$ in order to reduce the uncertainty coming from higher order QCD corrections. It is also important to notice that in the case when the couplings of the $SU(2)_L$ and $SU(2)_R$ are not equal the ratio $\left(\frac{v_{SM}}{\tilde{v}}\right)$ might be quite significant, see discussion and analysis in [14]. In the rest of the chapter we will assume that $SU(2)_L$ and custodial $SU(2)_R$ have the same gauge couplings (see appendix F for discussion of VEV shift in this case).

It is also interesting to point out that the same diagrams that contribute to the gluon fusion will also contribute to the modification of the di-Higgs production.

This might become an interesting option to disentangle new physics contribution (see discussion in the effective field theory approach in [66]).

5.3.2 $h\gamma\gamma$ coupling in RS

The calculation of the $h\gamma\gamma$ coupling comes from similar diagrams as the one for the hgg coupling, the only difference now is that we have to take into account contributions of the towers of charged KK gauge bosons and KK leptons. We will again use the simplest custodial model where leptons are in the doublet representation of $SU(2)_L$ or $SU(2)_R$. We can calculate their contribution in the same way as we did for the quarks. Contribution of the KK tower of the $W_\pm$ was presented in [14], so here we just quote their results and the reader can find more details about the derivation in the Appendix F. The contribution of the tower of the KK $W_\pm$ is given by

$$\sum_{n\geq 0} \frac{C^n_{diag}}{2M_n^2} A_1(\tau_n) = \frac{C_{hww}}{2M_w^2}(A_1(\tau_w)+7) - \frac{7}{\tilde{v}}, \tag{5.30}$$

where C^n_{diag} is coupling between Higgs field and the n-th KK modes (mass eigenstates) of the $W_\pm$, and C_{hww} is coupling between SM W and the Higgs. $A_1(\tau_w)$ is the form-factor for the gauge bosons (see Eq. (F.7)). Including the modification of the coupling between SM W and Higgs, this sum can be expressed in the following way:

$$\begin{aligned}\sum_{n\geq 0} \frac{C^n_{diag}}{2M_n^2} A_1(\tau_n) &= \frac{g^2\tilde{v}}{4M_w^2}\left(1 - \frac{\tilde{v}^2 R'^2(g_{5D}^2+\tilde{g}_{5D}^2)}{4R}\right)(A_1(\tau_w)+7) - \frac{7}{\tilde{v}} \\ &\approx \frac{1}{\tilde{v}}\left[\left(1 - \frac{\tilde{v}^2 R'^2(g_{5D}^2+\tilde{g}_{5D}^2)}{8R}\right)A_1(\tau_w) - \frac{7}{8}\tilde{v}^2 R'^2 \frac{(g_{5D}^2+\tilde{g}_{5D}^2)}{R}\right],\end{aligned} \tag{5.31}$$

where g_{5D} and $\tilde{g}_{5D}$ are the 5D gauge couplings of $SU(2)_L$ and $SU(2)_R$ respectively. Adding both fermion and gauge boson contributions together, now we can present our results for the ratio of $\Gamma(h \to \gamma\gamma)$ between RS and SM:

$$\begin{aligned}
&\frac{\Gamma^{RS}(h \to \gamma\gamma)}{\Gamma^{SM}(h \to \gamma\gamma)} = \left(\frac{v_{SM}}{\tilde{v}}\right)^2 \frac{1}{|A_1(\tau_w) + \frac{16}{9}A_{1/2}(\tau_t) + \frac{4}{9}A_{1/2}(\tau_b)|^2} \\
&\left|\left(1 - \frac{v_{SM}^2 R'^2(g_{5D}^2 + \tilde{g}_{5D}^2)}{8R}\right) A_1(\tau_w) - \frac{7v_{SM}^2 R'^2(g_{5D}^2 + \tilde{g}_{5D}^2)}{8R}\right. \\
&+\frac{16}{9}x_t A_{1/2}(\tau_t) + \frac{4}{9}x_b A_{1/2}(\tau_b) \\
&\left.+\frac{1}{2}v_{SM}^2 R'^2 \mathrm{Tr}\left[\frac{20}{9}\left(Y_u^\dagger Y_u + Y_u^\dagger Y_u\right) + \frac{4}{3}Y_l^\dagger Y_l\right] + \frac{16\Delta_2^t}{9m_t} + \frac{4\Delta_2^b}{9m_b}\right|^2 . \qquad (5.32)
\end{aligned}$$

5.4 Phenomenology

In this section, we discuss the phenomenology of the Higgs boson in warped extra dimensions. We focus our study on the Higgs production through gluon fusion and the branching fraction of $h \to \gamma\gamma$ decay. We will compare our results with that of holographic PNGB Higgs model studied in [63].

To get a handle on the size of new physics contributions, we scan the parameter space of RS with the assumption of flavor anarchy, i.e. the 5D Yukawa matrices are order one and uncorrelated. We find the set of 5D Yukawa couplings and fermion zero mode wavefunctions which give the correct SM quark masses and CKM mixing. We then calculate $\sigma(gg \to h)$ and $\mathrm{Br}(h \to \gamma\gamma)$ using Eq. (5.29) and (5.32), and find the ratio with that of SM. The result of the scan for bulk Higgs is shown in Fig. 5.2.

We can see from the plot in Fig. 5.2 that the new physics contribution to $\sigma(gg \to h)$ tends to be positive and gets larger for lower KK scale. Also the new

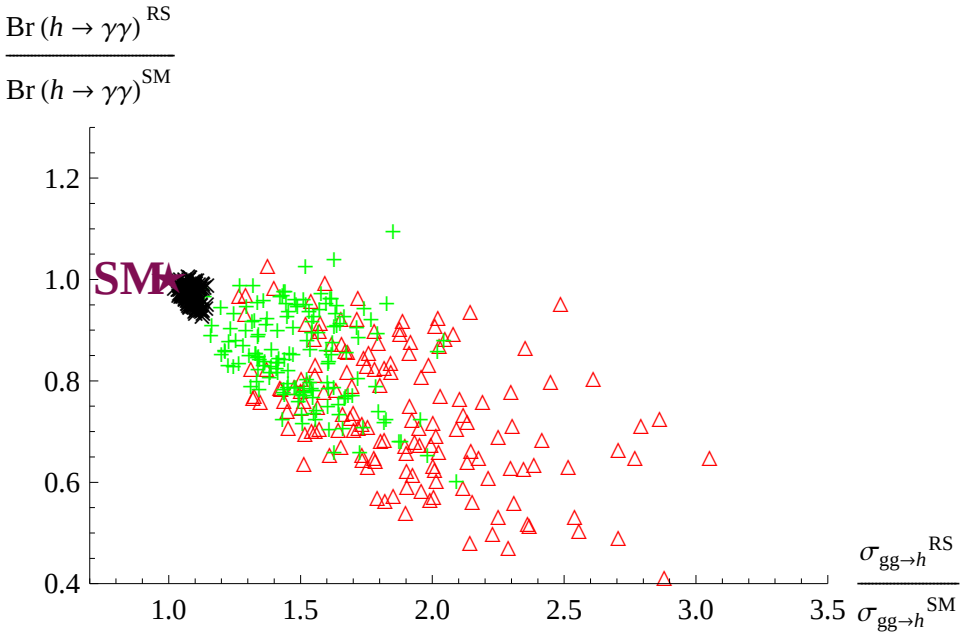

Figure 5.2: Scattered plot of $\frac{\sigma^{RS}_{gg\to h}}{\sigma^{SM}_{gg\to h}}$ and $\frac{\mathrm{Br}(h\to\gamma\gamma)^{RS}}{\mathrm{Br}(h\to\gamma\gamma)^{SM}}$, for bulk Higgs with vector-like Yukawa couplings ($Y_1 = Y_2$). The dimensionless 5D Yukawa couplings are varied between $Y \in [0.3, 3]$ and $m_h = 120$ GeV. The black "$\times$" corresponds to the KK scale $R'^{-1} = 5$ TeV, green "+" to $R'^{-1} = 2$ TeV, and red "$\triangle$" to $R'^{-1} = 1.5$ TeV. The SM value is marked by the star.

physics contribution to $\sigma(gg \to h)$ and $\mathrm{Br}(h \to \gamma\gamma)$ are correlated: an increase in $\sigma(gg \to h)$ is accompanied by a decrease in $\mathrm{Br}(h \to \gamma\gamma)$. Before proceeding further let us stop and see whether we can understand these results intuitively. First let us focus on the enhancement of the Higgs production due to gluon fusion. As we argued in the sections 5.3.1 these effects come mainly from the modification of the top Yukawa coupling and from the loop with KK fermions. As was shown in [11] top Yukawa coupling is reduced compared to the SM value, so naively one should expect the reduction of the Higgs production. But let us now look on the contribution of

the KK modes. One can see from (Eq. 5.29) that this contribution is proportional to $\mathrm{Tr}(Y_u Y_u^\dagger + Y_d Y_d^\dagger)$ which is always positive, so the sign of this contribution is fixed. Also the typical size of this term will be roughly equal to $N^2 \bar{Y}^2$ where N is number of SM families and $\bar{Y}$ is an average size of the Yukawa couplings, so adding both up and down quark KK towers will lead to an overall enhancement factor of 18.[6] Therefore KK fermions give a large positive contribution to $\sigma(gg \to h)$. Reduction of the $\mathrm{Br}(h \to \gamma\gamma)$ can be understood from the fact that in the SM the dominant contribution comes from the loop with $W^\pm$, and the fermion contribution has an opposite sign, thus enhancement of the fermion contributions effectively decreases the overall coupling.

This implication is two-fold. First, it means that even with a KK scale out of the reach of the LHC ($\gtrsim$ 5 TeV), we can still probe the framework of warped extra dimension by precision measurements of various Higgs production and decay processes. Second, by comparing our result with that of [63], we can see that $\sigma(gg \to h)$ can be used to distinguish between RS with bulk Higgs and holographic PNGB Higgs model (or gauge-Higgs unification). In the latter model, a reduction is usually expected, which can be contrasted with our results for bulk Higgs. Note that the difference in these two models comes from the extra symmetry in PNGB

[6] One can see that for sufficiently large Yukawa couplings our expansion in powers of $YY^\dagger v^2 R'^2$ might become ill defined, and also contribution of the higher order loops with KK fermions and Higgs might become important, so the one loop result becomes not reliable if the new physics contribution is much larger than that of the SM. At the same time we would like to note that our result even for the large 5D Yukawa couplings will give a typical size of the expected correction to the SM coupling.

Higgs, which constrains the Higgs interactions (see discussion in [64, 65]).

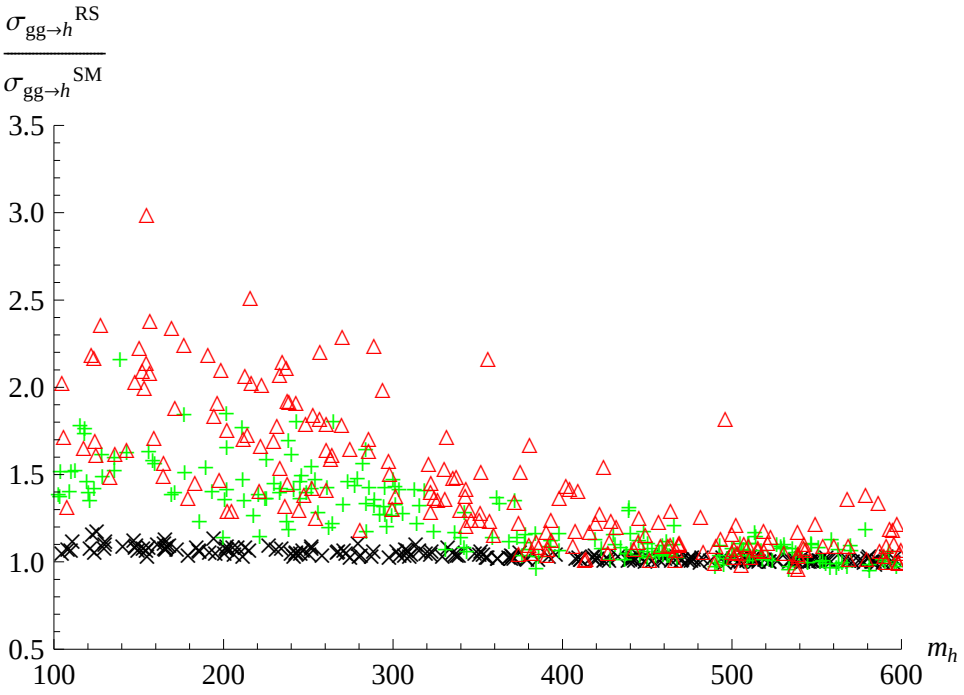

Figure 5.3: Dependence of $\frac{\sigma^{RS}_{gg\to h}}{\sigma^{SM}_{gg\to h}}$ on the Higgs mass for different values of R'^{-1} in bulk Higgs scenario with vector-like Yukawa couplings ($Y_1 = Y_2$). The dimensionless 5D Yukawa couplings are varied between $Y \in [0.3, 3]$. The black "$\times$" corresponds to KK scale $R'^{-1} = 5$ TeV, green "+" to $R'^{-1} = 2$ TeV, and red "$\triangle$" to $R'^{-1} = 1.5$ TeV.

To study the dependence of new physics contributions on the Higgs boson mass, we plot in Fig. 5.3 the ratio $\frac{\sigma^{RS}_{gg\to h}}{\sigma^{SM}_{gg\to h}}$ vs. m_h for various KK scales. We can see that the new physics contribution decreases as m_h increase from 100 to ~ 360 GeV. This can be understood from the fact that in SM, the form factor for the top quark attains its largest value when $m_h \approx 2m_t$. Since in RS with bulk Higgs, the top quark Yukawa coupling is reduced compared to that of SM, there is a larger negative new physics contribution to hgg coupling when $m_h \approx 2m_t$, leading to a

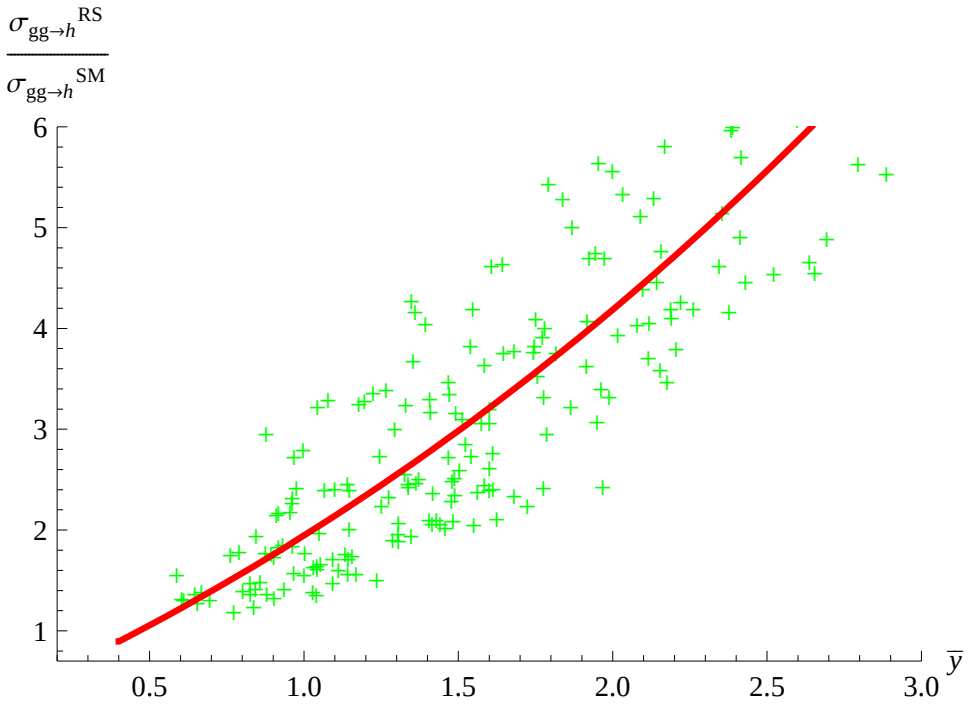

Figure 5.4: Dependence of $\frac{\sigma_{gg\to h}^{RS}}{\sigma_{gg\to h}^{SM}}$ on the average size of dimensionless 5D Yukawa couplings $\bar{Y}$, for the Higgs mass $m_h = 120$ GeV and KK scale $R'^{-1} = 2$ TeV.

smaller total new physics contribution.

In Fig. 5.4, we plot the dependence of the ratio $\frac{\sigma_{gg\to h}^{RS}}{\sigma_{gg\to h}^{SM}}$ on the average size of the 5D Yukawa couplings. We can see quite clearly that the size of new physics contribution increases as the 5D Yukawa couplings increases. This is expected from the fact that KK fermion contributions are proportional to $\mathrm{Tr}(Y_u Y_u^\dagger + Y_d Y_d^\dagger)$. In the framework of flavor anarchy, the 5D Yukawa couplings are order one. We can see from Fig. 5.4 that for order one Yukawa couplings, we have sizable new physics contributions to $\sigma(gg \to h)$.

So far we have been assuming that the Higgs is the bulk field and 5D Yukawa

couplings are vector-like i.e.

$$\mathcal{L} = Y_1 \bar{Q}^u_L U_R H + Y_2 \bar{U}_L Q^u_R H \quad \text{with } Y_1 = Y_2. \tag{5.33}$$

In the case where the Higgs is a 5D bulk field this condition of $Y_1 = Y_2$ is forced by the 5D Lorentz symmetry. But the Higgs can be brane localized or even a bulk Higgs might have brane localized couplings and these couplings do not have to respect 5D bulk Lorentz symmetry. So generally speaking $Y_1 \neq Y_2$, and they could be independent of each other. Let us see how this might modify our results. The first thing to notice is that the contribution of the tower of KK modes now has the following structure $Y_1 Y_2^\dagger$. Before proceeding further we immediately see that the overall sign of the contribution is not fixed any more! So we cannot predict in generic RS model the sign of the effect: whether it is enhancement or suppression for both hgg and $h\gamma\gamma$ couplings. This is shown in Fig. 5.5. We can see that the size of new physics contribution is generically large for moderate KK scale, but now its sign can be both positive and negative.

5.5 Summary

We summarize the results presented in this chapter. We calculated the corrections to the hgg and $h\gamma\gamma$ couplings in RS at one loop order. We have found that the dominant new physics contribution to these coupling comes from the towers of KK fermions running inside the triangle diagrams, and the KK towers of the light fermions do contribute significantly to these couplings, contrary to the models with Higgs being a PNGB boson where this contribution is sub-leading. We have

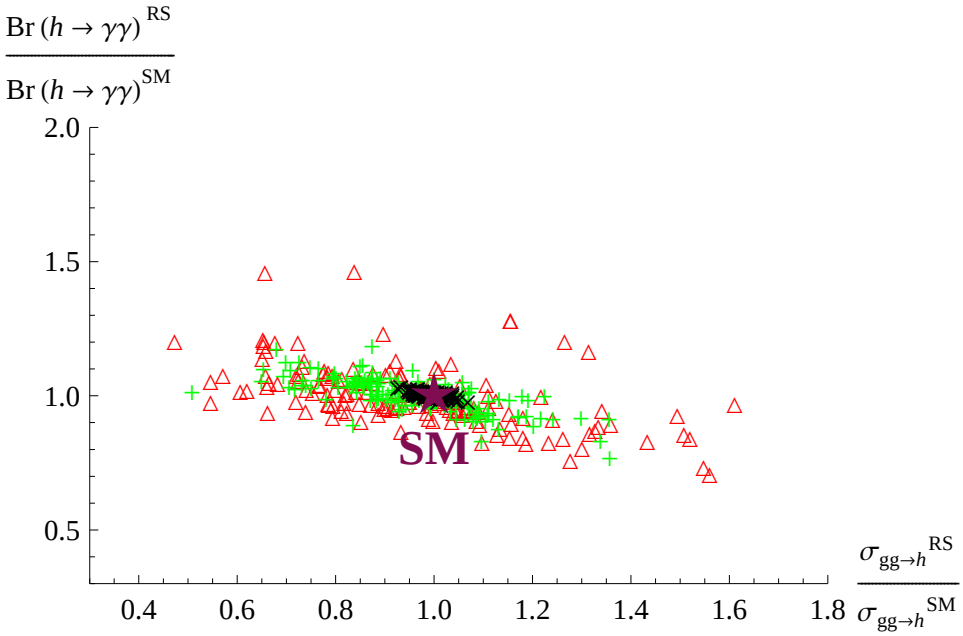

Figure 5.5: Scattered plot for the modification of $\frac{\mathrm{Br}(h\to\gamma\gamma)^{RS}}{\mathrm{Br}(h\to\gamma\gamma)^{RS}}$ and $\frac{\sigma^{RS}_{gg\to h}}{\sigma^{SM}_{gg\to h}}$ for brane Higgs with Y_1 independent of Y_2, where 5D Yukawa couplings are varied between $Y \in [0.3, 3]$ and $m_h = 120$ GeV. The black "$\times$" corresponds to the KK scale $R'^{-1} = 5$ TeV, green "+" to the $R'^{-1} = 2$ TeV, and red "$\triangle$" to the $R'^{-1} = 1.5$ TeV. The SM value is marked by the star.

shown that in the models with the Higgs in the bulk and Yukawa couplings being vectorlike ($Y_1 = Y_2$), hgg coupling becomes enhanced and $h\gamma\gamma$ coupling suppressed compared to that of SM, even though the top Yukawa coupling is suppressed compared to the SM value. This naively counterintuitive result is explained by the fact that the contribution of the KK towers of all SM fermions is so strong that it overcomes the effect from suppression of the top Yukawa coupling. Modification of the Higgs production cross-section remains significant even for a KK scale far from LHC accessibility. Specifically, we can get order one corrections even with lightest

KK modes above 5 TeV. For the generic models with Higgs on the brane or bulk Higgs with brane Yukawa couplings the sign of the effect remains unpredictable. We might have enhancement as well as suppression, but the parametric size of the effect remains the same. The total effect comes from collective contributions of the KK partners of all generations. Therefore, the size of these new physics contributions is large, even if the KK fermions are heavy. This shows us that in the absence of new resonances an analysis of the Higgs couplings might become a very important tool in understanding the structure of BSM physics.

Chapter 6

Conclusions and Outlook

In this thesis, I first demonstrated that warped extra dimension is a very attractive and robust framework that addresses the Planck-weak hierarchy problem. The beauty of warped extra dimension resides in its geometric approach, which leads to an effective cutoff scale that depends on the location along the extra dimension. Therefore, the mass of the Higgs boson, which resides near the IR brane, gets protected from disastrous large UV contribution. Moreover, by putting SM fields in the bulk, we can easily explain the hierarchy of fermion masses and mixing angles with order one 5D parameters. The new physics contributions to FCNC are protected by the RS-GIM mechanism.

With the starting of the LHC, more and more attention has been put into collider study of various BSM models. In this thesis, I mainly discussed two types of collider signatures of the warped extra dimension models. In chapter 4, I discussed the collider signals for coset gauge bosons in warped/composite PGB Higgs model. I reviewed the basic features of the warped/composite PGB Higgs model, including its motivation to solve the little hierarchy problem and the existence of the coset gauge bosons. Various properties of the coset gauge bosons, including their couplings and masses, are discussed using the two-site approach. It was argued that the general pattern of coset gauge boson couplings is fairly model independent and mainly

determined by their quantum numbers and composite nature. Specifically, the coset gauge bosons couple strongly with one third generation SM fermion and one KK fermion, and the couplings to two SM fermions are weak. A collider study of these new gauge bosons (W_C) is carried out in detail, focusing on the associated production with lightest top KK state ($t^{(1)}$) $pp \to W_C t^{(1)}$, and the decay channel $W_C \to t^{(1)} b$. Various decay channels for $t^{(1)}$ are included in the study. Our analysis shows that a 3σ reach at the LHC for coset gauge bosons with mass ~ 2 (2.6) TeV would require a luminosity of ~ 100 (1000) fb^{-1}. On the other hand, the coset gauge bosons are generically heavier than the usual KK gauge bosons, leading to an indirect bound on their masses to be at least ~ 3 TeV. Therefore, an upgrade of the LHC is needed to test this framework in detail.

In chapter 5, I gave a detailed analysis of the Higgs boson coupling with massless gauge bosons in warped extra dimensions. The motivation for this study is the following. To solve the Planck-weak hierarchy problem, we need to place the Higgs near the IR brane. But various KK modes are also localized towards the IR brane, thus leading to large couplings between the Higgs boson and KK states. These large couplings naturally lead to significant corrections to the properties of the Higgs boson. Based on this argument, a study of Higgs boson couplings to SM states can be a very powerful tool to shed light on the underlying structure of warped extra dimensions. We carried out a detailed calculation for the couplings hgg and $h\gamma\gamma$, leading to analytical formulas for the result of the full KK fermion sum. We found that the KK partners of $1^{\text{st}}/2^{\text{nd}}$ generation fermions give sizable new physics contributions even for moderately high KK scale. In addition, for bulk Higgs models

with vector-like Yukawa couplings, the new physics contribution to hgg coupling is always positive, while that to $h\gamma\gamma$ coupling is negative. From our numerical analysis, we found that order one new physics contribution can be obtained with KK scale ~ 5 TeV. This indicates that a careful measurement of Higgs production and decay can probe the structure of warped extra dimensions even if the KK resonances are too heavy to be produced directly at the LHC.

Armed with these studies, along with collider studies of other KK states, we hope to discover warped extra dimension in the near future!

Appendix A

Gauge Fixing and KK Decomposition for Gauge Bosons in the Bulk

In this appendix, we illustrate the details of gauge fixing and KK decomposition for bulk gauge fields. The action of the bulk gauge fields is given by Eq. (3.2). To eliminate the cross term, we can choose the following gauge fixing term

$$S_{GF} = \int d^4x dz - \frac{1}{2\xi g_5^2}\frac{1}{kz}\left[\partial_\mu A^\mu - \xi kz \partial_z\left(\frac{A_5}{kz}\right)\right]^2. \tag{A.1}$$

Add this gauge fixing term we get

$$\begin{aligned} S_{gauge+GF} = \int d^4x dz \Big\{ &\frac{1}{2g_5^2}\frac{1}{kz}A_\mu\left[\eta^{\mu\nu}\partial^2 - \left(1-\frac{1}{\xi}\right)\partial^\mu\partial^\nu\right]A_\nu \\ -\frac{1}{2g_5^2}\eta^{\mu\nu}A_\nu\partial_z\left[\frac{1}{kz}(\partial_z A_\mu)\right] &+ \frac{1}{2g_5^2}\frac{1}{kz}(\partial_\mu A_5)^2 + \frac{\xi}{2g_5^2}\frac{A_5}{kz}\partial_z\left[kz\partial_z\left(\frac{A_5}{kz}\right)\right]\Big\} \end{aligned} \tag{A.2}$$

We can do the following KK decomposition

$$A_\mu(x,z) = A_\mu^{(n)}(x) f_A^{(n)}(z) \tag{A.3}$$

$$A_5(x,z) = A_5^{(n)}(x) \tilde{f}_A^{(n)}(z) \tag{A.4}$$

These wavefunctions satisfy the following equation of motion:

$$\left(\frac{d^2}{dz^2} - \frac{1}{z}\frac{d}{dz} + m_n^2\right) f_A^{(n)}(z) = 0, \tag{A.5}$$

$$\left(\frac{d^2}{dz^2} - \frac{1}{z}\frac{d}{dz} + \frac{1}{z^2} + m_n^2\right) \tilde{f}_A^{(n)}(z) = 0. \tag{A.6}$$

Note that if we take derivative on Eq. (A.5), we get

$$\left(\frac{d^3}{dz^3} + \frac{1}{z^2}\frac{d}{dz} - \frac{1}{z}\frac{d^2}{dz^2} + m_n^2\frac{d}{dz}\right) f_A^{(n)}(z) = 0. \tag{A.7}$$

From this equation, it is easy to see that $\tilde{f}_A^{(n)}(z) = C\partial_z f_A^{(n)}(z)$ is a solution to the equation of motion. The orthonormality condition on wavefunctions give us

$$\int dz \frac{1}{kz} f_A^{(n)}(z) f_A^{(m)}(z) = \delta_{mn}, \tag{A.8}$$

$$\int dz \frac{1}{kz} \tilde{f}_A^{(n)}(z) \tilde{f}_A^{(m)}(z) = \delta_{mn}. \tag{A.9}$$

The second orthonormality condition tells us that $\tilde{f}_A^{(n)}(z) = \partial_z f_A^{(n)}(z)/m_n$, this can be seen as follows

$$\int \frac{dz}{kz} \frac{\partial_z f_A^{(n)} \partial_z f_A^{(m)}}{m_n m_m} = \int \frac{dz}{kz} \left[-\frac{\partial_z^2 f_A^{(n)} f_A^{(m)}}{m_n m_m} + \frac{1}{z} \frac{\partial_z f_A^{(n)} f_A^{(m)}}{m_n m_m} \right] = \delta_{mn}, \tag{A.10}$$

where we used the equation of motion in the second equality. Therefore, we showed that the wavefunctions of the A_5 field is related to that of A_μ fields. There are two independent solutions for $f_A^{(n)}(z)$. Following [52], we define basis functions C and S which are even/odd at UV brane:

$$C_A(1, m_n) = 1, \quad \partial_z C_A(1, m_n) = 0, \tag{A.11}$$

$$S_A(1, m_n) = 0, \quad \partial_z S_A(1, m_n) = m_n. \tag{A.12}$$

These basis functions for gauge bosons are given by

$$C_A(z, m_n) = \frac{\pi m_n}{2} z \left[J_1(m_n z) Y_0(m_n R) - J_0(m_n R) Y_1(m_n z) \right], \tag{A.13}$$

$$S_A(z, m_n) = \frac{\pi m_n}{2} z \left[J_1(m_n R) Y_1(m_n z) - J_1(m_n z) Y_1(m_n R) \right].$$

These basis functions are like cosine and sine in flat extra dimension.

Appendix B

$SO(5)$ generators and group algebras

The commutation relations of $SO(5)$ generators are given by

$$
\begin{aligned}
&[T_L^a, T_L^b] = i\epsilon^{abc} T_L^c, \quad [T_R^a, T_R^b] = i\epsilon^{abc} T_R^c, \quad [T_L^a, T_R^b] = 0 \\
&[T^{\hat{a}}, T^{\hat{b}}] = \frac{i}{2}\epsilon^{abc}(T_L^c + T_R^c), \quad [T^{\hat{a}}, T^{\hat{4}}] = \frac{i}{2}(T_L^a - T_R^a) \\
&[T_{L,R}^a, T^{\hat{b}}] = \frac{i}{2}(\epsilon^{abc} T^{\hat{c}} \pm \delta^{ab} T^{\hat{4}}), \quad [T_{L,R}^a, T^{\hat{4}}] = \mp\frac{i}{2} T^{\hat{a}}
\end{aligned}
\tag{B.1}
$$

For **5** representation, the generators are

$$
\begin{aligned}
T_{L,R}^1 &= \frac{-i}{2}\begin{pmatrix} 0 & 0 & 0 & \pm 1 & 0 \\ 0 & 0 & 1 & 0 & 0 \\ 0 & -1 & 0 & 0 & 0 \\ \mp 1 & 0 & 0 & 0 & 0 \\ 0 & 0 & 0 & 0 & 0 \end{pmatrix}, \quad T_{L,R}^2 = \frac{-i}{2}\begin{pmatrix} 0 & 0 & -1 & 0 & 0 \\ 0 & 0 & 0 & \pm 1 & 0 \\ 1 & 0 & 0 & 0 & 0 \\ 0 & \mp 1 & 0 & 0 & 0 \\ 0 & 0 & 0 & 0 & 0 \end{pmatrix} \\
T_{L,R}^3 &= \frac{-i}{2}\begin{pmatrix} 0 & 1 & 0 & 0 & 0 \\ -1 & 0 & 0 & 0 & 0 \\ 0 & 0 & 0 & \pm 1 & 0 \\ 0 & 0 & \mp 1 & 0 & 0 \\ 0 & 0 & 0 & 0 & 0 \end{pmatrix}, \quad T^{\hat{1}} = \frac{-i}{\sqrt{2}}\begin{pmatrix} 0 & 0 & 0 & 0 & 1 \\ 0 & 0 & 0 & 0 & 0 \\ 0 & 0 & 0 & 0 & 0 \\ 0 & 0 & 0 & 0 & 0 \\ -1 & 0 & 0 & 0 & 0 \end{pmatrix} \\
T^{\hat{2}} &= \frac{-i}{\sqrt{2}}\begin{pmatrix} 0 & 0 & 0 & 0 & 0 \\ 0 & 0 & 0 & 0 & 1 \\ 0 & 0 & 0 & 0 & 0 \\ 0 & 0 & 0 & 0 & 0 \\ 0 & -1 & 0 & 0 & 0 \end{pmatrix}, \quad T^{\hat{3}} = \frac{-i}{\sqrt{2}}\begin{pmatrix} 0 & 0 & 0 & 0 & 0 \\ 0 & 0 & 0 & 0 & 0 \\ 0 & 0 & 0 & 0 & 1 \\ 0 & 0 & 0 & 0 & 0 \\ 0 & 0 & -1 & 0 & 0 \end{pmatrix} \\
T^{\hat{4}} &= \frac{-i}{\sqrt{2}}\begin{pmatrix} 0 & 0 & 0 & 0 & 0 \\ 0 & 0 & 0 & 0 & 0 \\ 0 & 0 & 0 & 0 & 0 \\ 0 & 0 & 0 & 0 & 1 \\ 0 & 0 & 0 & -1 & 0 \end{pmatrix}
\end{aligned}
\tag{B.2}
$$

Appendix C

KK Decomposition and Spectral Functions of Gauge Bosons and Fermions

In this appendix, we review the KK decomposition and spectral functions of gauge bosons and fermions in the model [35]. First, we recall the base functions for gauge bosons (see Eq. (A.13)). These base functions are like cosine and sine in flat extra dimension. $C_A(z, m_n)$ has "+" boundary condition on the UV brane and $S_A(z, m_n)$ has "−" boundary condition on the UV brane. They both solve the equations of motion for gauge boson wavefunctions with vanishing Higgs vev. Then the wavefunctions of gauge fields with vanishing Higgs vev are easy to write down in terms of these base functions

$$f_n^{a_L}(z, 0) = C_{a_L,n} C_A(z, m_n) \tag{C.1}$$

$$f_n^{\hat{a}}(z, 0) = C_{\hat{a},n} S_A(z, m_n) \tag{C.2}$$

$$f_n^{Y}(z, 0) = C_{Y,n} C_A(z, m_n) \tag{C.3}$$

$$f_n^{a_R}(z, 0) = C_{a_R,n} S_A(z, m_n) \tag{C.4}$$

The wavefunctions in the presence of background $\langle A_z^{\hat{4}} \rangle$ can be obtained by using Eq. (4.27). For simplicity, we define

$$\theta_G(z) = \frac{v(z^2 - R^2)}{\sqrt{2} f_h (z_\pi^2 - R'^2)} \tag{C.5}$$

Then $\Omega(z,v) = e^{-i\sqrt{2}\theta_G(z)T^{\hat{4}}}$. Use the representation of $SO(5)$ generators in Appendix B, we obtain

$$
\begin{aligned}
f^{1_L}(v) &= \frac{1}{2}(1+\cos\theta_G)C_{1_L}C_A(z) + \frac{1}{2}(1-\cos\theta_G)C_{1_R}S_A(z) \\
&+ \frac{\sqrt{2}}{2}\sin\theta_G C_{\hat{1}}S_A(z) \\
f^{2_L}(v) &= \frac{1}{2}(1+\cos\theta_G)C_{2_L}C_A(z) + \frac{1}{2}(1-\cos\theta_G)C_{2_R}S_A(z) + \frac{\sqrt{2}}{2}\sin\theta_G C_{\hat{2}}S_A(z) \\
f^{3_L}(v) &= \frac{1}{2}(1+\cos\theta_G)C_{3_L}C_A(z) + \frac{1}{2}(1-\cos\theta_G)[c_\phi C_{3_R}S_A(z) + s_\phi C_Y C_A(z)] \\
&+ \frac{\sqrt{2}}{2}\sin\theta_G C_{\hat{3}}S_A(z) \\
f^{1_R}(v) &= \frac{1}{2}(1-\cos\theta_G)C_{1_L}C_A(z) + \frac{1}{2}(1+\cos\theta_G)C_{1_R}S_A(z) - \frac{\sqrt{2}}{2}\sin\theta_G C_{\hat{1}}S_A(z) \\
f^{2_R}(v) &= \frac{1}{2}(1-\cos\theta_G)C_{2_L}C_A(z) + \frac{1}{2}(1+\cos\theta_G)C_{2_R}S_A(z) - \frac{\sqrt{2}}{2}\sin\theta_G C_{\hat{2}}S_A(z) \\
f^{3_R}(v) &= \frac{1}{2}(1-\cos\theta_G)C_{3_L}C_A(z) + \frac{1}{2}(1+\cos\theta_G)\left[c_\phi C_{3_R}S_A(z) + s_\phi C_Y C_A(z)\right] \\
&- \frac{\sqrt{2}}{2}\sin\theta_G C_{\hat{3}}S_A(z) \\
f^{\hat{1}}(v) &= \cos\theta_G C_{\hat{1}}S_A(z) + \sin\theta_G\frac{1}{\sqrt{2}}\left[C_{1_R}S_A(z) - C_{1_L}C_A(z)\right] \\
f^{\hat{2}}(v) &= \cos\theta_G C_{\hat{2}}S_A(z) + \sin\theta_G\frac{1}{\sqrt{2}}\left[C_{2_R}S_A(z) - C_{2_L}C_A(z)\right] \\
f^{\hat{3}}(v) &= \cos\theta_G C_{\hat{3}}S_A(z) + \sin\theta_G\frac{1}{\sqrt{2}}\left[c_\phi C_{3_R}S_A(z) + s_\phi C_Y C_A(z) - C_{3_L}C_A(z)\right] \\
f^{\hat{4}}(v) &= C_{\hat{4}}S_A(z) \\
f^{X}(v) &= c_\phi C_Y C_A(z) - s_\phi C_{3_R}S_A(z)
\end{aligned}
\tag{C.6}
$$

where the dependence on z and KK number n is not shown explicitly. The boundary conditions of $f^{a,\hat{a}}(v,z)$ at $z = R'$ set the eigenvalues m_n. We can separate the gauge bosons in three sectors: (i) $a = 1_L, 1_R, \hat{1}, 2_L, 2_R, \hat{2}$, these gauge bosons correspond to $W^\pm$ and their KK modes and coset W_C gauge boson. (ii) $a = 3_L, 3_R, \hat{3}, X$, these correspond to neutral gauge bosons (Z, γ and coset Z_C gauge boson). (iii) $a = \hat{4}$,

corresponds to the gauge boson partner of physical Higgs boson. We now study these sectors.

- (i) $W^{\pm}$ sector. The boundary conditions on the IR brane are

$$\partial_z f_{i_L}(z_\pi, v) = 0 \tag{C.7}$$

$$\partial_z f_{i_R}(z_\pi, v) = 0 \tag{C.8}$$

$$f_{\hat{i}}(z_\pi, v) = 0 \tag{C.9}$$

where $i = 1, 2$. These boundary conditions give us

$$\begin{aligned} & C_{i_L}\left[C_A(R') - \sin\theta_G C_A(z_\pi)\theta'_G + \cos\theta_G C'_A(R')\right] \\ + \; & C_{i_R}\left[S'_A(R') + \sin\theta_G S_A(R')\theta'_G - \cos\theta_G S'_A(R')\right] \\ + \; & C_{\hat{i}}\left[\sqrt{2}\cos\theta_G\theta'_G S_A(R') + \sqrt{2}\sin\theta_G S'_A(R')\right] = 0 \end{aligned} \tag{C.10}$$

$$\begin{aligned} & C_{i_L}\left[C'_A(R') + \sin\theta_G C_A(R')\theta'_G - \cos\theta_G C'_A(R')\right] \\ + \; & C_{i_R}\left[S'_A(R') - \sin\theta_G S_A(R')\theta'_G + \cos\theta_G S'_A(R')\right] \\ - \; & C_{\hat{i}}\left[\sqrt{2}\cos\theta_G\theta'_G S_A(R') + \sqrt{2}\sin\theta_G S'_A(R')\right] = 0 \end{aligned} \tag{C.11}$$

$$\cos\theta_G C_{\hat{i}} S_A(R') + \sin\theta_G \frac{1}{\sqrt{2}}\left[C_{i_R} S_A(R') - C_{i_L} C_A(R')\right] = 0 \tag{C.12}$$

where all functions are evaluated at $z = R'$. These are linear algebraic equations for the coefficients $C_{i_L, i_R, \hat{i}}$. To have a solution on the coefficients $C_{i_L, i_R, \hat{i}}$, we need to require the determinant to be zero. It gives us

$$C_A(R')S'_A(R')\sin^2\theta_G + (2 - \sin^2\theta_G)C'_A(R')S_A(R') = 0 \tag{C.13}$$

which can be further simplified to

$$1 + F_W(m_n^2)\sin^2\left(\frac{v}{\sqrt{2}f_h}\right) = 0 \tag{C.14}$$
$$F_W(m^2) \equiv \frac{mR'}{2C'(R',m)S(R',m)}$$

Here we defined the form factor of W bosons $F_W(m^2)$. Now we can see that the spectral function of W boson is

$$\rho_W(m) = 1 + F_W(m^2)\sin^2\left(\frac{v}{\sqrt{2}f_h}\right) \tag{C.15}$$

- (ii) Z, γ sector. The boundary conditions on the IR brane are

$$\partial_z f_{3_L}(z_\pi, v) = 0 \tag{C.16}$$

$$\partial_z[c_\phi f_{3_R}(z_\pi, v) - s_\phi f_X(z_\pi, v)] = 0 \tag{C.17}$$

$$\partial_z[s_\phi f_{3_R}(z_\pi, v) + c_\phi f_X(z_\pi, v)] = 0 \tag{C.18}$$

$$f_{\hat{3}}(z_\pi, v) = 0 \tag{C.19}$$

These boundary conditions give us

$$C_{3_L}\left[C'_A(R') - \sin\theta_G C_A(R')\theta'_G + \cos\theta_G C'_A(R')\right] \tag{C.20}$$
$$+ \quad C_{3_R} c_\phi \left[S'_A(R') + \sin\theta_G S(R')\theta'_G - \cos\theta_G S'_A(R')\right]$$
$$+ \quad C_Y s_\phi \left[C'_A(R') + \sin\theta_G C_A(R')\theta'_G - \cos\theta_G C'_A(R')\right]$$
$$+ \quad \sqrt{2} C_{\hat{3}} \left[\sin\theta_G S'_A(R') + \cos\theta_G S_A(R')\theta'_G\right] = 0$$

$$C_{3_L} c_\phi [C'_A(R') - \cos\theta_G C'_A(R') + \sin\theta_G C_A(R')\theta'_G] \tag{C.21}$$
$$+ \quad C_{3_R}[(1+s_\phi^2)S'_A(R') + c_\phi^2 \cos\theta_G S'_A(R') - c_\phi^2 \sin\theta_G S_A(R')\theta'_G]$$
$$+ \quad C_Y s_\phi c_\phi [-C'_A(R') - \sin\theta_G C_A(R')\theta'_G + \cos\theta_G C'_A(R')]$$
$$- \quad C_{\hat{3}}\sqrt{2} c_\phi [\sin\theta_G S'_A(R') + \cos\theta_G S_A(R')\theta'_G] = 0$$

$$C_{3_L} s_\phi [C'_A(R') - \cos\theta_G C'_A(R') + \sin\theta_G C_A(R')\theta'_G] \tag{C.22}$$
$$+ \quad C_{3_R} s_\phi c_\phi [-S'_A(R') + \cos\theta_G S'_A(R') - \sin\theta_G S_A(R')\theta'_G]$$
$$+ \quad C_Y [(1+c_\phi^2)C'_A(R') + s_\phi^2 \cos\theta_G C'_A(R') - s_\phi^2 \sin\theta_G C_A(R')\theta'_G]$$
$$- \quad C_{\hat{3}}\sqrt{2} s_\phi [\sin\theta_G S'_A(R') + \cos\theta_G S_A(R')\theta'_G] = 0$$

$$C_{3_L}[-\sin\theta_G C_A(R')] + C_{3_R}[c_\phi \sin\theta_G S_A(R')] \tag{C.23}$$
$$+ \quad C_Y [s_\phi \sin\theta_G C_A(R')] + C_{\hat{3}}[\sqrt{2}\cos\theta_G S_A(R')] = 0$$

By requiring the determinant is zero, we get

$$C'_A(R')S'_A(R')\Big\{2C'_A(R')S_A(R') \tag{C.24}$$
$$+ \quad \sin^2\theta_G(1+s_\phi^2)[C'_A(R')S_A(R') - C_A(R')S'_A(R')]\Big\} = 0$$

$C'_A(R') = 0$ gives the spectrum of KK photon and $S'_A(R') = 0$ gives the spectrum of KK W_{3_R}. Note that their spectrum does not depend on the Higgs vev thus does not contribute to the CW potential. With some simplification we can get the spectral function for Z boson

$$\rho_Z(m) = 1 + F_Z(m^2)\sin^2\left(\frac{v}{\sqrt{2}f_h}\right) \tag{C.25}$$

with the Z boson form factor

$$F_Z(m^2) = \frac{(1+s_\phi^2)mR'}{2C'(R',m)S(R',m)} \tag{C.26}$$

- (iii) $A^{\hat{4}}$ sector. The gauge transformation $\Omega(z,v)$ does not change the wave-function of $A^{\hat{4}}$. Therefore

$$f_n^{\hat{4}}(z,v) = f_n^{\hat{4}}(z,0) = C_{\hat{4},n}S_A(z,m_n) \tag{C.27}$$

Its spectrum is determined by $S_A(R',m_n) = 0$. Since the spectral function does not depend on the Higgs vev, it will not contribute to the Higgs potential.

For the fermionic section, we define the following base function

$$\tilde{S}_M^F(z,m_n) = \frac{\pi m_n}{2}z^\alpha[J_\alpha(m_n)Y_\alpha(m_nz) - Y_\alpha(m_n)J_\alpha(m_nz)] \tag{C.28}$$
$$S_{\pm M}^F = z^{2\pm M}\tilde{S}_{\pm M}^F \tag{C.29}$$
$$\dot{S}_{\pm M}^F = \mp\frac{z^{2\pm M}}{m_n}\partial_z\tilde{S}_{\pm M}^F \tag{C.30}$$

with $\alpha = 1/2 + c$ and $M = -c$. $S_{\pm M}$ and $\dot{S}_{\pm M}$ satisfy Dirichlet and Neunman boundary conditions respectively at the UV brane. We can do the following KK decomposition for fermionic wavefunctions with vanishing Higgs vev

$$F^{\Psi}_{1L}(z,0) = \begin{pmatrix} C_1 S^F_{M_1} \\ C_2 S^F_{M_1} \\ C_3 \dot{S}^F_{-M_1} \\ C_4 \dot{S}^F_{-M_1} \\ C_5 S^F_{M_1} \end{pmatrix}, \; F^{\Psi}_{2R}(z,0) = \begin{pmatrix} C_6 S^F_{-M_2} \\ C_7 S^F_{-M_2} \\ C_8 S^F_{-M_2} \\ C_9 \dot{S}^F_{-M_2} \\ C_{10} \dot{S}^F_{M_2} \end{pmatrix}, \; F^{\Psi}_{3R}(z,0) = \begin{pmatrix} C_{11} S^F_{-M_3} \\ C_{12} S^F_{-M_3} \\ C_{13} S^F_{-M_3} \\ C_{14} S^F_{-M_3} \\ C_{15} S^F_{-M_3} \\ C_{16} S^F_{-M_3} \\ C_{17} S^F_{-M_3} \\ C_{18} S^F_{-M_3} \\ C_{19} S^F_{-M_3} \\ C_{20} \dot{S}^F_{M_3} \end{pmatrix} \quad \text{(C.31)}$$

As before, the wavefunctions with non-vanishing Higgs vev is given by doing gauge transformation Eq. (4.29). The boundary terms in Eq. (4.25) give twisted boundary conditions for fermions at the IR brane

$$\begin{aligned} \chi_{1R} + M_{B_2}\chi_{3R} &= 0, \qquad \tilde{t}_{1R} + M_{B_2}\tilde{t}_{3R} = 0, \qquad t_{1R} + M_{B_2} t_{3R} = 0 \quad \text{(C.32)} \\ b_{1R} + M_{B_2} b_{3R} &= 0, \qquad \hat{t}_{1R} + M_{B_1}\hat{t}_{2R} = 0, \qquad \chi_{3L} - M_{B_2}\chi_{1L} = 0 \\ \tilde{t}_{3L} - M_{B_2}\tilde{t}_{1L} &= 0, \qquad t_{3L} - M_{B_2} t_{1L} = 0, \qquad b_{3L} - M_{B_2} b_{1L} = 0, \\ \hat{t}_{2L} - M_{B_1}\hat{t}_{1L} &= 0 \end{aligned}$$

The rest of the boundary conditions are not changed

$$(\chi_{2L}, \hat{t}_{2L}, t_{2L}, b_{2L}) = 0 \quad \text{(C.33)}$$

$$(\Xi'_{3L}, T'_{3L}, B'_{3L}, \Xi_{3L}, T_{3L}, B_{3L}) = 0 \quad \text{(C.34)}$$

This boundary conditions set the mass spectra for fermions. The calculation for fermionic spectral function is similar to the case of gauge boson. We do not carry out the calculation here but present the fermionic form factors and spectral functions

here for reference (for more detailed calculation, see [35]). The fermionic form factors are

$$F_b(m^2) = -\frac{M_{B_2}^2 S_{-c_1}^{F\prime}}{2S_{c_3}^F(M_{B_2}^2 S_{-c_3}^F S_{-c_1}^{F\prime} + S_{-c_1}^F S_{-c_3}^{F\prime})} \tag{C.35}$$

$$F_{t_1}(m^2) = \frac{F_1(m^2)}{F_0(m^2)} \tag{C.36}$$

$$F_{t_2}(m^2) = \frac{F_2(m^2)}{F_0(m^2)} \tag{C.37}$$

$$\begin{aligned} F_1(m^2) &= kz\Big\{M_{B_2}^2 S_{c_2}^F S_{-c_3}^F S_{-c_2}^{F\prime} + M_{B_1}^2[2M_{B_2}^2 S_{c_1}^F S_{-c_3}^F S_{-c_1}^{F\prime} \\ &+ S_{-c_3}^{F\prime} + 2S_{c_1}^F S_{-c_1}^F S_{-c_3}^{F\prime} - S_{c_2}^F S_{-c_2}^F S_{-c_3}^{F\prime}]\Big\} \end{aligned} \tag{C.38}$$

$$F_2(m^2) = -(kz)M_{B_1}^2 S_{-c_3}^{F\prime} \tag{C.39}$$

$$\begin{aligned} F_0(m^2) &= 2\Big\{M_{B_1}^2 S_{c_1}^F(-1 + S_{c_2}^F S_{-c_2}^F)(M_{B_2}^2 S_{-c_3}^F S_{-c_1}^{F\prime} kz + S_{-c_1}^F S_{-c_3}^{F\prime} kz) \\ &+ S_{c_2}^F S_{-c_2}^{F\prime} kz\left[M_{B_2}^2(-1 + S_{c_1}^F S_{-c_1}^F)S_{-c_3}^F - \frac{1}{m^2} S_{-c_1}^F S_{c_1}^{F\prime} S_{-c_3}^{F\prime}\right]\Big\} \end{aligned} \tag{C.40}$$

The fermionic spectral functions are given by

$$\rho_b(m) = 1 + F_b(m^2)\sin^2\left(\frac{v}{\sqrt{2}f_h}\right), \tag{C.41}$$

$$\rho_t(m) = 1 + F_{t_1}(m^2)\sin^2\left(\frac{v}{\sqrt{2}f_h}\right) + F_{t_2}(m^2)\sin^4\left(\frac{v}{\sqrt{2}f_h}\right). \tag{C.42}$$

Appendix D

Suppression of $Z_c b_L \bar{b}_L$ coupling

In chapter 4 we commented that the couplings of the SM b quark to the coset Z_C gauge boson are strongly suppressed compared to the their naive estimates. In this appendix we will explain the origin of this suppression. From isospin quantum numbers of the coset gauge bosons $(T_L^3, T_R^3) = (\pm\frac{1}{2}, \pm\frac{1}{2})$, we see that to get coupling between coset gauge boson and SM fermion we need odd number of Higgs vev insertions. In this section we will study only the effects coming from one Higgs insertion because the diagrams with three Higgs insertions will be suppressed due to the additional powers of the $\theta_H^2 \equiv \left(\frac{v}{\sqrt{2}f_h}\right)^2$. The dominant contribution to the $Z_C b_L \bar{b}_L$ is shown on the Fig. D.1. If we only consider individual contributions coming from these mixings, then the naive estimate of the $Z_C b_L \bar{b}_L$ coupling will be (we ignore the difference between θ_H and $\sin\theta_H$)

$$\sim g_* \left(\frac{1}{2} - c_1\right) \theta_H. \tag{D.1}$$

However, to get a more precise estimate, first let us look at the diagram (1) of Fig. D.1. In this case intermediate gauge boson can be either $W_L^{3,\mathrm{KK}}$ or $W_R^{3,\mathrm{KK}}$ (they are the heavy gauge bosons of the generators T_L^3 and T_R^3 in two-site language). To analyze the coupling $hZ_{C,\mu}W_{L,R}^{3,\mathrm{KK},\mu}$ we will use two-site approach, one can see that this coupling arises from the covariant derivative of the ϕ field $|D_\mu\phi|^2$ (see Eq. (4.6)). Performing commutation relations one can show that the couplings of Z_C to $W_L^{3,\mathrm{KK}}$

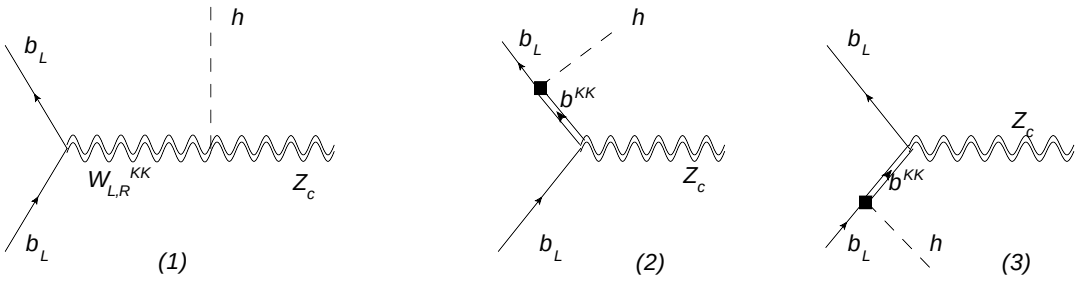

Figure D.1: Diagrams contributing to the $Z_c\bar{b}b$ at $\frac{v}{f_h}$ order

and $W_R^{3,\mathrm{KK}}$ have opposite signs, so the effective coupling of Z_C to the SM fermions coming from diagram(1) of Fig. D.1 is proportional to $(T_L^3 - T_R^3)$ of the b_L field. But we know that to overcome the constraint from the shift in $Z\bar{b}_L b_L$ coupling, b_L should be in such representation of $SU(2)_L \times SU(2)_R$ to have $T_L^3 = T_R^3$ [43]. This means that in realistic models of PGB Higgs, contribution to $Z_c b_L \bar{b}_L$ coupling from diagram (1) of Fig. D.1 is zero.

Now let us look on the diagrams (2) and (3) of Fig.D.1. Note that h and Z_C are accompanied by the generators T_c^4 and T_c^3 of $SO(5)$ respectively. Therefore in this case coupling of the Z_C to the SM b_L is proportional to

$$\bar{b}_L \left\{T_c^3, T_c^4\right\} b_L. \tag{D.2}$$

But one can see that in our model SM b_L lives mostly in the **5** of the SO(5), then one can check by direct calculation that

$$\xi_b^\dagger \cdot A^\dagger \cdot \left\{T_c^3, T_c^4\right\} \cdot A \cdot \xi_b = 0 \tag{D.3}$$

where $\xi_b^T = (0, 0, 0, \psi_b, 0)$. This concludes our analysis of the suppression of the $Z_C b_L \bar{b}_L$ couplings.

Appendix E

KK sum rules for hgg coupling

In this section we will present a way of efficiently performing KK sums for the fermions (such as Eq. (5.24)). Let us look at the equations of motions for the fermions in the absence of the Higgs vev. In the absence of the Higgs vev we can always choose a basis where 5D bulk masses are diagonal, and so we can ignore all the mixings. Let us concentrate on the KK decomposition of the $SU(2)_L$ doublet $Q_{L,R}$ with boundary conditions $(\pm,\pm)$. The equations of motion of the KK wavefunctions are

$$-m_n q_L^{(n)} - \partial_z q_R^{(n)} + \frac{c_q+2}{z} q_R^{(n)} = 0, \tag{E.1}$$

$$-m_n^* q_R^{(n)} + \partial_z q_L^{(n)} + \frac{c_q-2}{z} q_L^{(n)} = 0. \tag{E.2}$$

We take the first equation and rewrite it as:

$$-m_n q_L^{(n)} - z^{c_q+2}\partial_z \left(q_R^{(n)}\ z^{-c_q-2} \right) = 0. \tag{E.3}$$

We now multiply by z^{-c_q-2} and integrate between R and z_1:

$$\begin{aligned} -m_n \int_R^{z_1} dz z^{-c_q-2} q_L^{(n)}(z) &= q_R^{(n)}\ z^{-c_q-2} \Big|_R^{z_1}, \\ \int_R^{z_1} dz z^{-c-2} q_L^{(n)}(z) &= -\frac{1}{m_n} q_R^{(n)}(z_1)\ z_1^{-c-2}. \end{aligned} \tag{E.4}$$

We now use the completeness relation

$$\sum_{n=0}^{\infty} q_L^{(n)}(z_2) q_L^{(n)}(z) = \frac{z^4}{R^4}\delta(z_2 - z) \tag{E.5}$$

$$\Rightarrow \quad \sum_{n=1}^{\infty} q_L^{(n)}(z_2) q_L^{(n)}(z) = \frac{z^4}{R^4}\delta(z_2 - z) - q_L^0(z_2) q_L^0(z). \tag{E.6}$$

Based on (Eq E.4) we will get

$$-\int_R^{z_1} dz\ z^{-c_q-2} \sum_{n=1}^{\infty} q_L^{(n)}(z_2) q_L^{(n)}(z) = z_1^{-c_q-2} \sum_{n=1}^{\infty} \frac{q_R^{(n)}(z_1) q_L^{(n)}(z_2)}{m_n}, \tag{E.7}$$

where we have explicitly extracted the zero mode contribution from the sum. Let us note that

$$q_L^0(z) = N_L z^{2-c_q} \quad \text{with} \quad N_L = \sqrt{\frac{1-2c_q}{\epsilon^{2c_q-1}-1}} R^{c_q-5/2}, \tag{E.8}$$

and where we have defined the warp factor $\epsilon = \frac{R}{R'} \sim 10^{-16}$.

Now we can finally write:

$$\begin{aligned} \sum_{n=1}^{\infty} \frac{q_R^{(n)}(z_1) q_L^{(n)}(z_2)}{m_n} &= -z_1^{c+2} \int_R^{z_1} dz\ z^{-c-2} \Big(\frac{z^4}{R^4}\delta(z_2 - z) - q_L^0(z_2) q_L^0(z) \Big) \\ &= \frac{z_1^{2+c_q} z_2^{2-c_q}}{R^4} \left[-\theta(z_1 - z_2) + \frac{\left(\frac{z_1}{R}\right)^{1-2c} - 1}{\left(\frac{R'}{R}\right)^{1-2c} - 1} \right]. \end{aligned} \tag{E.9}$$

Similarly we can calculate the sum for the other three possible boundary conditions :

$$\begin{aligned} \psi_L(+,+): &\ \sum \frac{q_R^{(n)}(z_1) q_L^{(n)}(z_2)}{m_n} = \frac{z_1^{2+c} z_2^{2-c}}{R^4} \left[-\theta(z_1 - z_2) + \frac{\left(\frac{z_1}{R}\right)^{1-2c} - 1}{\left(\frac{R'}{R}\right)^{1-2c} - 1} \right], \\ \psi_L(+,-): &\ \sum \frac{q_R^{(n)}(z_1) q_L^{(n)}(z_2)}{m_n} = -\frac{z_1^{2+c} z_2^{2-c}}{R^4} \theta(z_1 - z_2), \\ \psi_L(-,+): &\ \sum \frac{q_R^{(n)}(z_1) q_L^{(n)}(z_2)}{m_n} = \frac{z_2^{2-c} z_1^{2+c}}{R^4} \theta(z_2 - z_1), \\ \psi_L(-,-): &\ \sum \frac{q_R^{(n)}(z_1) q_L^{(n)}(z_2)}{m_n} = \frac{z_1^{2+c} z_2^{2-c}}{R^4} \left[\theta(z_2 - z_1) - \frac{\left(\frac{z_2}{R}\right)^{1+2c} - 1}{\left(\frac{R'}{R}\right)^{1+2c} - 1} \right] \end{aligned} \tag{E.10}$$

Using these relations we can now perform all the necessary sums to calculate the KK fermion contribution to hgg coupling.

Appendix F

Gauge boson couplings and contribution to $h\gamma\gamma$ coupling

In this section just for the sake of the completion we present analysis for the modification of the gauge boson coupling to the Higgs boson, and their contribution to the $h\gamma\gamma$ coupling. We start from the modification of the Higgs vev

$$v_{SM}^2 \approx \tilde{v}^2 - \frac{\tilde{v}^4 R'^2}{8R}\left(g_{5D}^2 + \tilde{g}_{5D}^2\right), \tag{F.1}$$

where $v_{SM} = 246$ GeV, $\tilde{g}_{5D}$ is five dimensional gauge coupling of the custodial $SU(2)_R$, so

$$\tilde{v} \approx v_{SM}\left(1 + \frac{R'^2 v_{SM}^2}{16R}(g_{5D}^2 + \tilde{g}_{5D}^2)\right). \tag{F.2}$$

This effect will lead to the overall modification of the SM hgg and $h\gamma\gamma$ coupling by the factor $1 - \frac{R'^2 v_{SM}^2}{16R}(g_{5D}^2 + \tilde{g}_{5D}^2) \approx 0.95$ for $(R'^{-1} = 1500\,\text{TeV}, g_{5D} = \tilde{g}_{5D})$.

F.1 Couplings of $W^{\pm}$ to Higgs in RS

To calculate modification of the $h\gamma\gamma$ coupling we also have to calculate contribution coming from the W boson. From the Lagrangian (see [29])

$$\mathcal{L} = \frac{g^2}{2}\left(\left(\frac{h+\tilde{v}}{\sqrt{2}}\right)^2 - \frac{R'^2(g_{5D}^2 + \tilde{g}_{5D}^2)}{4R}\left(\frac{h+\tilde{v}}{\sqrt{2}}\right)^4\right) W_\mu^+ W^{-\mu}, \tag{F.3}$$

one can immediately deduce coupling between Higgs and W.

$$\begin{aligned}\mathcal{L} &= C_{hww}\, h W_\mu^+ W^{-\mu},\\ C_{hww} &= \frac{g^2\tilde{v}}{2}\left[1 - \frac{R'^2(g_{5D}^2 + \tilde{g}_{5D}^2)\tilde{v}^2}{4R}\right].\end{aligned} \tag{F.4}$$

F.2 Contribution of the KK tower of $W_\pm$ to the $h\gamma\gamma$

In this subsection we derive the contribution of the $W_\pm$ KK modes to the $h\gamma\gamma$ coupling (we will closely follow discussion presented in [14]). First let us denote by M^2 the mass squared matrix of the charged gauge bosons, then the coupling to the Higgs boson will be given by the matrix

$$C = \frac{\partial M^2}{\partial \tilde{v}},$$

rotating back to the basis where mass matrix M^2 is diagonal we will get

$$C_{diag} = U \frac{\partial M^2}{\partial \tilde{v}} U^\dagger, \tag{F.5}$$

where U is a unitary matrix that diagonalizes M. We can parameterize the contribution of the gauge boson KK modes to the $h\gamma\gamma$ coupling in the following way:

$$\sum_{n\geq 0} \frac{C^n_{diag}}{2M_n^2} A_1(\tau_n) = \frac{C_{hww}}{2M_w^2} A_1(\tau_w) + \sum_{n>0} \frac{C^n_{diag}}{2M_n^2} A_1(\tau_n), \tag{F.6}$$

where $A_1(\tau)$ is the form factor for vector bosons in the loop [67] ($\tau = m_h^2/4M_n^2$)

$$A_1(\tau) = -[2\tau^2 + 3\tau + 3(2\tau - 1)f(\tau)]\tau^{-2}, \tag{F.7}$$

where $f(\tau)$ is given by Eq. (5.3). For KK gauge bosons $\tau_n \to 0$, and $A_1(\tau_n) \approx -7$, so we get

$$\frac{C_{hww}}{2M_w^2} A_1(\tau_w) - 7 \sum_{n>0} \frac{C^n_{diag}}{2M_n^2} \;=\; \frac{C_{hww}}{2M_w^2} (A_1(\tau_w) + 7) - 7 \sum_{n\geq 0} \frac{C^n_{diag}}{2M_n^2}\,. \tag{F.8}$$

To evaluate $\sum_{n\geq 0} \frac{C^n_{diag}}{2M_n^2}$ we can use the following trick [68]

$$\sum_{n\geq 0} \frac{C^n_{diag}}{M_n^2} = \mathrm{Tr}\left[\left(M^2_{diag}\right)^{-1} C\right] = \mathrm{Tr}\left[\frac{\partial M^2}{\partial \tilde{v}} \left(M^2\right)^{-1}\right] = \frac{\partial}{\partial \tilde{v}} \ln\left(\mathrm{Det} M^2\right). \tag{F.9}$$

Let us see how the determinant of the gauge boson mass matrix depends on $\tilde{v}$. For simplicity we assume that the Higgs is localized on the IR brane. We denote by $f_{(i)}, \tilde{f}_{(j)}$ values of the profiles on the IR brane for KK modes of $SU(2)_L$ and $SU(2)_R$ gauge bosons respectively. Then the mass matrix will look like:

$$M^2 = \begin{pmatrix} g_{5D}^2 f_{(0)}^2 \frac{\tilde{v}^2}{4} & f_{(0)} f_{(1)} g_{5D}^2 \frac{\tilde{v}^2}{4} & f_{(0)} \tilde{f}_{(1)} g_{5D} \tilde{g}_{5D} \frac{\tilde{v}^4}{2} & \cdots \\ g_{5D}^2 f_{(0)} f_{(1)} \frac{\tilde{v}^2}{4} & M_1^2 + {f_{(1)}}^2 g_{5D}^2 \frac{\tilde{v}^2}{4} & f_{(1)} \tilde{f}_{(1)} g_{5D} \tilde{g}_{5D} \frac{\tilde{v}^2}{4} & \cdots \\ g_{5D} \tilde{g}_{5D} f_{(0)} \tilde{f}_{(1)} \frac{\tilde{v}^2}{4} & f_{(1)} \tilde{f}_{(1)} g_{5D} \tilde{g}_{5D} \frac{\tilde{v}^2}{4} & \tilde{M}_1^2 + \tilde{f}_{(1)}^2 \tilde{g}_{5D}^2 \frac{\tilde{v}^2}{4} & \cdots \\ \vdots & \vdots & \vdots & \ddots \end{pmatrix}. \quad \text{(F.10)}$$

One can see from the structure of the matrix that the determinant is equal to

$$\mathrm{Det} M^2 = g_{5D}^2 f_{(0)}^2 \frac{\tilde{v}^2}{4} \prod_{i,j} M_i^2 \tilde{M}_j^2. \quad \text{(F.11)}$$

We have checked that for generic bulk Higgs $\mathrm{Det} M^2 \propto \tilde{v}^2 + O(\tilde{v}^6)$, one can calculate it using mixed position momentum propagators. So the results presented in this section are approximately independent of the Higgs localization. Now we can proceed to the evaluation of the sum in Eq. (F.8) and substituting result for the determinant we get

$$\sum_{n \geq 0} \frac{C_{diag}^n}{2M_n^2} A_1(\tau_n) \quad = \quad \frac{C_{hww}}{2M_w^2} (A_1(\tau_w) + 7) - \frac{7}{\tilde{v}}. \quad \text{(F.12)}$$

Appendix G

Review of Higgs Flavor violation

In this appendix we present general formulas for the misalignment between SM fermion masses and Higgs Yukawa couplings in RS(see for details[11]). We define the following quantity to parameterize the misalignment

$$\hat{\Delta} = \hat{m} - \tilde{v}\hat{y}, \tag{G.1}$$

where $\hat{m}, \hat{y}$ are mass matrix and Yukawa couplings of the SM fermions. Then it can be split into two parts

$$\hat{\Delta} = \hat{\Delta}_1 + \hat{\Delta}_2, \tag{G.2}$$

where $\hat{\Delta}_1$ is the main contribution for the light generations and $\hat{\Delta}_2$ becomes important only for the third generation of quarks. Then calculations show that $\hat{\Delta}_1$ for the up type quarks is equal to

$$\hat{\Delta}_1^u = \frac{\tilde{v}\sqrt{2}}{3}\left(\frac{\tilde{v}^2 R'^2}{2}\right)\hat{F}(c_q)\left[Y_u Y_u^\dagger Y_u + Y_d Y_d^\dagger Y_u\right]\hat{F}(-c_u) \tag{G.3}$$

[1] where c_u, c_q are bulk mass parameters for the multiplets containing zero modes of the SM right-handed and left-handed up quarks respectively. $\hat{F}(c)$ is a diagonal matrix with elements given by the profiles of the corresponding quarks respectively

$$F(c) \equiv \sqrt{\frac{1-2c}{1-\left(\frac{R}{R'}\right)^{1-2c}}}. \tag{G.4}$$

[1] We assume here that Yukawa couplings are vectorlike $Y_2 = Y_1$

One can get these expressions by evaluating the sum (Eq. 5.19) directly using the rules of (Eq. E.10) or by solving for the exact wavefunctions profiles as described in [11]. For the other contribution $\hat{\Delta}_2$ we will get the following expression

$$\hat{\Delta}_2^u = R'^2 \left[\hat{m}_u \left(\hat{m}_u^\dagger \hat{K}(c_q) + \hat{K}(-c_u) \hat{m}_u^\dagger \right) m_u + \hat{m}_d \hat{\tilde{K}}(-c_d) \hat{m}_d^\dagger \hat{m}_u \right] \tag{G.5}$$

where

$$\begin{aligned} \tilde{K}(c) &\equiv \frac{1 - \left(\frac{R'}{R}\right)^{2c-1}}{1-2c} \frac{1 - \left(\frac{R'}{R}\right)^{-2c-1}}{1+2c}, \\ K(c) &\equiv \frac{1}{1-2c} \Big[- \frac{1}{\left(\frac{R}{R'}\right)^{2c-1} - 1} + \frac{\left(\frac{R}{R'}\right)^{2c-1} - \left(\frac{R}{R'}\right)^2}{\left(\left(\frac{R}{R'}\right)^{2c-1} - 1\right)(3-2c)} \\ &+ \frac{\left(\frac{R}{R'}\right)^{1-2c} - \left(\frac{R}{R'}\right)^2}{(1+2c)\left(\left(\frac{R}{R'}\right)^{2c-1} - 1\right)} \Big]. \end{aligned} \tag{G.6}$$

$$\tag{G.7}$$

Note that subdominant contribution Δ_2 is only important for the third generation, and in the text we denote $\Delta_2^{t,b}$ to be equal to $(\hat{\Delta}_2^{u,d})_{33}$.

Bibliography

[1] L. Susskind, Phys. Rev. D **20**, 2619 (1979).

[2] L. Randall and R. Sundrum, Phys. Rev. Lett. **83**, 3370 (1999) [arXiv:hep-ph/9905221]; L. Randall and R. Sundrum, Phys. Rev. Lett. **83**, 4690 (1999) [arXiv:hep-th/9906064].

[3] K. Agashe, A. Belyaev, T. Krupovnickas, G. Perez and J. Virzi, Phys. Rev. D **77**, 015003 (2008) [arXiv:hep-ph/0612015]; B. Lillie, L. Randall and L. T. Wang, JHEP **0709**, 074 (2007) [arXiv:hep-ph/0701166]; B. Lillie, J. Shu and T. M. P. Tait, Phys. Rev. D **76**, 115016 (2007) [arXiv:0706.3960 [hep-ph]]; A. Djouadi, G. Moreau and R. K. Singh, Nucl. Phys. B **797**, 1 (2008) [arXiv:0706.4191 [hep-ph]]; M. Guchait, F. Mahmoudi and K. Sridhar, Phys. Lett. B **666**, 347 (2008) [arXiv:0710.2234 [hep-ph]]; U. Baur and L. H. Orr, Phys. Rev. D **76**, 094012 (2007) [arXiv:0707.2066 [hep-ph]] and Phys. Rev. D **77**, 114001 (2008) [arXiv:0803.1160 [hep-ph]].

[4] K. Agashe *et al.*, Phys. Rev. D **76**, 115015 (2007) [arXiv:0709.0007 [hep-ph]]; K. Agashe, S. Gopalakrishna, T. Han, G-Y. Huang and A. Soni, Phys. Rev. D **80**, 075007 (2009) [arXiv:0810.1497 [hep-ph]].

[5] R. Contino, Y. Nomura and A. Pomarol, Nucl. Phys. B **671**, 148 (2003) [arXiv:hep-ph/0306259].

[6] K. Agashe, R. Contino and A. Pomarol, Nucl. Phys. B **719**, 165 (2005) [arXiv:hep-ph/0412089].

[7] R. Contino, L. Da Rold and A. Pomarol, Phys. Rev. D **75**, 055014 (2007) [arXiv:hep-ph/0612048].

[8] M. Carena, A. D. Medina, B. Panes, N. R. Shah and C. E. M. Wagner, Phys. Rev. D **77**, 076003 (2008) [arXiv:0712.0095 [hep-ph]]. R. Contino and G. Servant, JHEP **0806**, 026 (2008) [arXiv:0801.1679 [hep-ph]]; J. Mrazek and A. Wulzer, arXiv:0909.3977 [hep-ph]; for a general analysis of LHC signals of such top quark "partners", see J. A. Aguilar-Saavedra, JHEP **0911**, 030 (2009) [arXiv:0907.3155 [hep-ph]].

[9] K. Agashe, A. Azatov, T. Han, Y. Li, Z. G. Si and L. Zhu, arXiv:0911.0059 [hep-ph].

[10] K. Agashe and R. Contino, Phys. Rev. D **80**, 075016 (2009) [arXiv:0906.1542 [hep-ph]].

[11] A. Azatov, M. Toharia and L. Zhu, Phys. Rev. D **80**, 035016 (2009) [arXiv:0906.1990 [hep-ph]].

[12] B. Duling, arXiv:0912.4208 [hep-ph].

[13] S. Casagrande, F. Goertz, U. Haisch, M. Neubert and T. Pfoh, arXiv:1005.4315 [hep-ph].

[14] C. Bouchart and G. Moreau, Phys. Rev. D **80**, 095022 (2009) [arXiv:0909.4812 [hep-ph]].

[15] G. Cacciapaglia, A. Deandrea and J. Llodra-Perez, JHEP **0906**, 054 (2009) [arXiv:0901.0927 [hep-ph]].

[16] A. Azatov, M. Toharia and L. Zhu, arXiv:1006.5939 [hep-ph].

[17] M. E. Peskin and D. V. Schroeder, "An Introduction To Quantum Field Theory," *Reading, USA: Addison-Wesley (1995) 842 p*

[18] T. P. Cheng and L. F. Li, "Gauge theory of elementary particle physics: Problems and solutions," *Oxford, UK: Clarendon (2000) 306 p*

[19] J. F. Donoghue, E. Golowich and B. R. Holstein, "Dynamics Of The Standard Model," Camb. Monogr. Part. Phys. Nucl. Phys. Cosmol. **2**, 1 (1992).

[20] V. M. Abazov *et al.* [The D0 Collaboration], arXiv:1005.2757 [hep-ex].

[21] S. P. Martin, arXiv:hep-ph/9709356.

[22] P. Sikivie, "An Introduction To Technicolor."

[23] M. Schmaltz and D. Tucker-Smith, Ann. Rev. Nucl. Part. Sci. **55**, 229 (2005) [arXiv:hep-ph/0502182].

[24] R. Sundrum, arXiv:hep-th/0508134.

[25] W. D. Goldberger and M. B. Wise, Phys. Rev. Lett. **83**, 4922 (1999) [arXiv:hep-ph/9907447]; W. D. Goldberger and M. B. Wise, Phys. Lett. B **475**, 275 (2000) [arXiv:hep-ph/9911457].

[26] S. Chang, J. Hisano, H. Nakano, N. Okada and M. Yamaguchi, Phys. Rev. D **62**, 084025 (2000) [arXiv:hep-ph/9912498]; T. Gherghetta and A. Pomarol, Nucl. Phys. B **586**, 141 (2000) [arXiv:hep-ph/0003129].

[27] L. Randall and M. D. Schwartz, JHEP **0111**, 003 (2001) [arXiv:hep-th/0108114].

[28] K. Agashe, G. Perez and A. Soni, Phys. Rev. D **71**, 016002 (2005) [arXiv:hep-ph/0408134].

[29] K. Agashe, A. Delgado, M. J. May and R. Sundrum, JHEP **0308**, 050 (2003) [arXiv:hep-ph/0308036].

[30] K. Agashe, M. Papucci, G. Perez and D. Pirjol, [arXiv:hep-ph/0509117].

[31] S. J. Huber and Q. Shafi, Phys. Lett. B **498**, 256 (2001) [arXiv:hep-ph/0010195].

[32] H. Davoudiasl, S. Gopalakrishna, E. Ponton and J. Santiago, arXiv:0908.1968 [hep-ph].

[33] See, for example, M. Carena, E. Ponton, J. Santiago and C. E. M. Wagner, Nucl. Phys. B **759**, 202 (2006) [arXiv:hep-ph/0607106] and Phys. Rev. D **76**, 035006 (2007) [arXiv:hep-ph/0701055]

[34] R. Contino, T. Kramer, M. Son and R. Sundrum, JHEP **0705**, 074 (2007) [arXiv:hep-ph/0612180].

[35] A. D. Medina, N. R. Shah and C. E. M. Wagner, Phys. Rev. D **76**, 095010 (2007) [arXiv:0706.1281 [hep-ph]].

[36] M. Serone, arXiv:0909.5619 [hep-ph].

[37] Y. Hosotani, Phys. Lett. B **126**, 309 (1983) and Phys. Lett. B **129**, 193 (1983).

[38] Y. Hosotani, K. Oda, T. Ohnuma and Y. Sakamura, Phys. Rev. D **78**, 096002 (2008) [Erratum-ibid. D **79**, 079902 (2009)] [arXiv:0806.0480 [hep-ph]].

[39] J. M. Maldacena, Adv. Theor. Math. Phys. **2**, 231 (1998) [Int. J. Theor. Phys. **38**, 1113 (1999)] [arXiv:hep-th/9711200]; S. S. Gubser, I. R. Klebanov and A. M. Polyakov, Phys. Lett. B **428**, 105 (1998) [arXiv:hep-th/9802109]; E. Witten, Adv. Theor. Math. Phys. **2**, 253 (1998) [arXiv:hep-th/9802150].

[40] H. Georgi and D. B. Kaplan, Phys. Lett. B **136**, 183 (1984); B **145**, 216 (1984); D. B. Kaplan, H. Georgi and S. Dimopoulos, Phys. Lett. B **136**, 187 (1984); H. Georgi, D. B. Kaplan and P. Galison, Phys. Lett. B **143**, 152 (1984); M. J. Dugan, H. Georgi and D. B. Kaplan, Nucl. Phys. B **254**, 299 (1985).

[41] N. Arkani-Hamed, M. Porrati and L. Randall, JHEP **0108**, 017 (2001) [arXiv:hep-th/0012148]; R. Rattazzi and A. Zaffaroni, JHEP **0104**, 021 (2001) [arXiv:hep-th/0012248].

[42] M. V. Chizhov and G. Dvali, arXiv:0908.0924 [hep-ph].

[43] K. Agashe, R. Contino, L. Da Rold and A. Pomarol, Phys. Lett. B **641** (2006) 62 [arXiv:hep-ph/0605341].

[44] S. J. Huber, Nucl. Phys. B **666**, 269 (2003) [arXiv:hep-ph/0303183]; S. Casagrande, F. Goertz, U. Haisch, M. Neubert and T. Pfoh, JHEP **0810**, 094 (2008) [arXiv:0807.4937 [hep-ph]]; M. Blanke, A. J. Buras, B. Duling, S. Gori and A. Weiler, JHEP **0903**, 001 (2009) [arXiv:0809.1073 [hep-ph]]; M. Blanke, A. J. Buras, B. Duling, K. Gemmler and S. Gori, JHEP **0903**, 108 (2009) [arXiv:0812.3803 [hep-ph]]; M. E. Albrecht, M. Blanke, A. J. Buras, B. Duling and K. Gemmler, arXiv:0903.2415 [hep-ph]; A. J. Buras, B. Duling and S. Gori, JHEP **0909**, 076 (2009) [arXiv:0905.2318 [hep-ph]].

[45] C. Csaki, A. Falkowski and A. Weiler, JHEP **0809**, 008 (2008) [arXiv:0804.1954 [hep-ph]].

[46] K. Agashe, arXiv:0902.2400 [hep-ph].

[47] O. Gedalia, G. Isidori and G. Perez, arXiv:0905.3264 [hep-ph].

[48] A. L. Fitzpatrick, G. Perez and L. Randall, arXiv:0710.1869 [hep-ph]; M. C. Chen and H. B. Yu, Phys. Lett. B **672**, 253 (2009) [arXiv:0804.2503 [hep-ph]]; G. Perez and L. Randall, JHEP **0901**, 077 (2009) [arXiv:0805.4652 [hep-ph]]; C. Csaki, C. Delaunay, C. Grojean and Y. Grossman, JHEP **0810**, 055 (2008) [arXiv:0806.0356 [hep-ph]]; J. Santiago, JHEP **0812**, 046 (2008) [arXiv:0806.1230 [hep-ph]]; C. Csaki, A. Falkowski and A. Weiler, arXiv:0806.3757 [hep-ph]; C. Csaki, G. Perez, Z. Surujon and A. Weiler, arXiv:0907.0474 [hep-ph]; M. C. Chen, K. T. Mahanthappa and F. Yu, arXiv:0909.5472 [hep-ph].

[49] H. Davoudiasl, J. L. Hewett and T. G. Rizzo, Phys. Rev. D **68**, 045002 (2003) [arXiv:hep-ph/0212279]; M. Carena, E. Ponton, T. M. P. Tait and C. E. M. Wagner, Phys. Rev. D **67**, 096006 (2003) [arXiv:hep-ph/0212307]; M. S. Carena, A. Delgado, E. Ponton, T. M. P. Tait and C. E. M. Wagner, Phys. Rev. D **68**, 035010 (2003) [arXiv:hep-ph/0305188]; M. S. Carena, A. Delgado, E. Ponton, T. M. P. Tait and C. E. M. Wagner, Phys. Rev. D **71**, 015010 (2005) [arXiv:hep-ph/0410344].

[50] P. McGuirk, G. Shiu and K. M. Zurek, JHEP **0803**, 012 (2008) [arXiv:0712.2264 [hep-ph]]; G. Shiu, B. Underwood, K. M. Zurek and D. G. E. Walker, Phys. Rev. Lett. **100**, 031601 (2008) [arXiv:0705.4097 [hep-ph]]; A. Falkowski and M. Perez-Victoria, arXiv:0806.1737 [hep-ph]; B. Batell, T. Gherghetta and D. Sword, arXiv:0808.3977 [hep-ph]; A. Delgado and D. Diego, Phys. Rev. D **80**, 024030 (2009) [arXiv:0905.1095 [hep-ph]]; S. Mert Aybat and J. Santiago, arXiv:0905.3032 [hep-ph].

[51] private communication with A. Falkowski and M. Son.

[52] A. Falkowski, Phys. Rev. D **75**, 025017 (2007) [arXiv:hep-ph/0610336].

[53] T. E. W. Group [CDF Collaboration and D0 Collaboration], arXiv:0908.2171 [hep-ex].

[54] K. Agashe, A. Azatov and L. Zhu, Phys. Rev. D **79**, 056006 (2009) [arXiv:0810.1016 [hep-ph]].

[55] T. Han, H. E. Logan and L. T. Wang, JHEP **0601**, 099 (2006) [arXiv:hep-ph/0506313].

[56] J. Pumplin, D. R. Stump, J. Huston, H. L. Lai, P. M. Nadolsky and W. K. Tung, JHEP **0207**, 012 (2002) [arXiv:hep-ph/0201195].

[57] G. L. Bayatian *et al.* [CMS Collaboration], J. Phys. G **34**, 995 (2007). G. Aad *et al.* [The ATLAS Collaboration], arXiv:0901.0512 [hep-ex].

[58] V. M. Abazov *et al.* [D0 Collaboration], Phys. Rev. Lett. **99**, 191802 (2007) [arXiv:hep-ex/0702005].

[59] T. Han, H. E. Logan, B. McElrath and L. T. Wang, Phys. Rev. D **67**, 095004 (2003) [arXiv:hep-ph/0301040].

[60] W. Y. Keung and G. Senjanovic, Phys. Rev. Lett. **50**, 1427 (1983).

[61] A. Djouadi and G. Moreau, Phys. Lett. B **660**, 67 (2008) [arXiv:0707.3800 [hep-ph]].

[62] B. Lillie, JHEP **0602**, 019 (2006) [arXiv:hep-ph/0505074].

[63] A. Falkowski, Phys. Rev. D **77**, 055018 (2008) [arXiv:0711.0828 [hep-ph]].

[64] G. F. Giudice, C. Grojean, A. Pomarol and R. Rattazzi, JHEP **0706**, 045 (2007) [arXiv:hep-ph/0703164].

[65] I. Low, R. Rattazzi and A. Vichi, JHEP **1004**, 126 (2010) [arXiv:0907.5413 [hep-ph]].

[66] A. Pierce, J. Thaler and L. T. Wang, JHEP **0705**, 070 (2007) [arXiv:hep-ph/0609049].

[67] J. Gunion, H. Haber, G. Kane, S Dawson "The Higgs Hunter's Guide" 2000, Westview Press.

[68] J. R. Ellis, M. K. Gaillard and D. V. Nanopoulos, Nucl. Phys. B **106**, 292 (1976).

[69] G. Cacciapaglia, C. Csaki, G. Marandella and J. Terning, JHEP **0702**, 036 (2007), [arXiv:hep-ph/0611358]; H. Davoudiasl, B. Lillie and T. G. Rizzo, JHEP **0608**, 042 (2006), [arXiv:hep-ph/0508279].